

**UNCLASSIFIED**

**AD 409 551**

**DEFENSE DOCUMENTATION CENTER**

**FOR**

**SCIENTIFIC AND TECHNICAL INFORMATION**

**CAMERON STATION, ALEXANDRIA, VIRGINIA**



**UNCLASSIFIED**

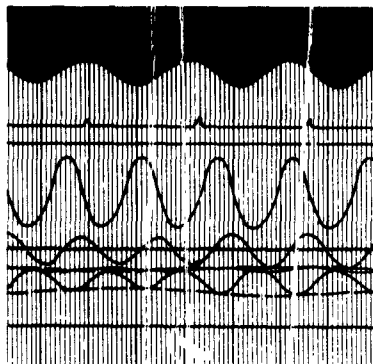
NOTICE: When government or other drawings, specifications or other data are used for any purpose other than in connection with a definitely related government procurement operation, the U. S. Government thereby incurs no responsibility, nor any obligation whatsoever; and the fact that the Government may have formulated, furnished, or in any way supplied the said drawings, specifications, or other data is not to be regarded by implication or otherwise as in any manner licensing the holder or any other person or corporation, or conveying any rights or permission to manufacture, use or sell any patented invention that may in any way be related thereto.

CATALOGED BY DDC 409551

AS AD No. \_\_\_\_\_

409 551

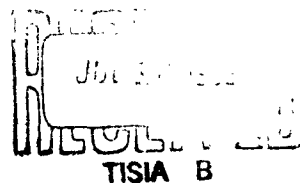
GD/C-63-032



# FLAPPED HYDROFOILS IN WAVES, SUBCAVITATING FLOW

TECHNICAL REPORT

MAY 1963



## GD

GENERAL DYNAMICS | CONVAIR

Post Office Box 1953, San Diego 12, California

FOR ERRATA

AD 409 551

THE FOLLOWING PAGES ARE CHANGES

TO BASIC DOCUMENT

AD 409551

409 551

GENERAL DYNAMICS

GENERAL DYNAMICS | CONVAIR

Enclosed is General Dynamics/Convair Report  
GDC-63-032, and a correction sheet, Figure 17,  
for GDC Report ZH-153, "Flapped Hydrofoils in  
Smooth Water, Subcavitating Flow" by C. E. Jones, Jr.  
November 1961



**GDC-63-032**

**FLAPPED HYDROFOILS IN WAVES,  
SUBCAVITATING FLOW**

**Prepared by  
A. C. Conolly**

**May 1963**

**Contract Nonr-3180(00)  
Task No. NR062-252**

## ABSTRACT

This report presents tank test data for a rectangular flapped hydrofoil mounted to the carriage by a single strut. Tests were carried out separately with flaps oscillating in smooth water, flaps fixed in regular waves, and then various combinations of conditions with flaps oscillating in regular waves. The separate effects of flap and wave on the force and moment coefficients for the hydrofoil were obtained, and compared with the results when both flap and wave were cycled together.

# CONTENTS

1. INTRODUCTION . . . . .	1
2. MODEL DESCRIPTION AND INSTRUMENTATION . . . . .	3
2.1 Model Description . . . . .	3
2.2 Instrumentation . . . . .	3
3. TEST PROCEDURE . . . . .	5
4. METHOD OF ANALYSIS . . . . .	7
4.1 Tests in Smooth Water With Flaps Cycled at Various Frequencies . . . . .	7
4.2 Tests in Regular Waves With Flaps Fixed — Head and Following Seas . . . . .	8
4.3 Tests in Regular Waves With Flaps Cycling — Head and Following Seas . . . . .	10
4.4 Data Analysis on Time Basis . . . . .	11
5. DISCUSSION OF RESULTS . . . . .	13
5.1 General . . . . .	13
5.2 Flaps Cycling in Smooth Water . . . . .	13
5.3 Flaps Fixed in Regular Waves . . . . .	16
5.4 Flaps Cycling in Regular Waves . . . . .	19
5.5 Time History Analysis to Isolate Effects of Flap Motions From Effects of Wave Motions . . . . .	22
5.6 Comparisons With Reference 1 Smooth Water Tests . . . . .	24
5.7 Comparisons With Reference 4 . . . . .	25
5.8 One-Half Cycle Tests in Smooth Water . . . . .	27
6. RELIABILITY AND ACCURACY OF DATA . . . . .	29
7. CONCLUSIONS . . . . .	31
8. REFERENCES . . . . .	33
9. NOMENCLATURE . . . . .	35
DISTRIBUTION LIST . . . . .	129

# T A B L E S

1. Summary of Approximate Test Variables . . . . .	14
2. Flap Configuration 1; $c_f/c = 0.3$ , $b_f/b = 0.6$ ; Tests in Smooth Water, Flaps Oscillating, Static $h/c = 1.0$ . . . . .	39
3. Flap Configuration 2; $c_f/c = 0.3$ , $b_f/b = 0.8$ ; Tests in Smooth Water, Flaps Oscillating, Static $h/c = 1.0$ . . . . .	40
4. Flap Configuration 3; $c_f/c = 0.2$ , $b_f/b = 0.6$ ; Tests in Smooth Water, Flaps Oscillating, Static $h/c = 1.0$ . . . . .	41
5. Flap Configuration 4; $c_f/c = 0.2$ , $b_f/b = 0.8$ ; Tests in Smooth Water, Flaps Oscillating, Static $h/c = 1.0$ . . . . .	42
6. Flap Configuration 1; $c_f/c = 0.3$ ; $b_f/b = 0.6$ ; Tests in Regular Head Seas, Flaps Fixed, Static $h/c = 1.0$ . . . . .	43
7. Flap Configuration 2; $c_f/c = 0.3$ , $b_f/b = 0.8$ ; Tests in Regular Head Seas, Flaps Fixed, Static $h/c = 1.0$ . . . . .	44
8. Flap Configuration 3; $c_f/c = 0.2$ , $b_f/b = 0.6$ ; Tests in Regular Head Seas, Flaps Fixed, Static $h/c = 1.0$ . . . . .	45
9. Flap Configuration 4; $c_f/c = 0.2$ , $b_f/b = 0.8$ ; Tests in Regular Head Seas, Flaps Fixed, Static $h/c = 1.0$ . . . . .	46
10. Flap Configuration 1; $c_f/c = 0.3$ , $b_f/b = 0.6$ ; Tests in Following Seas, Flaps Fixed . . . . .	47
11. Flap Configuration 2; $c_f/c = 0.3$ , $b_f/b = 0.8$ ; Tests in Following Seas, Flaps Fixed . . . . .	48
12. Flap Configuration 3; $c_f/c = 0.2$ , $b_f/b = 0.6$ ; Tests in Following Seas, Flaps Fixed . . . . .	49
13. Flap Configuration 4; $c_f/c = 0.2$ ; $b_f/b = 0.8$ ; Tests in Following Seas, Flaps Fixed . . . . .	50
14. Flap Configuration 1; $c_f/c = 0.3$ , $b_f/b = 0.6$ ; Tests in Regular Head and Following Seas, Flaps Oscillating; Static $h/c = 1.0$ , $\alpha = 5^\circ$ . . . . .	51
15. Flap Configuration 2; $c_f/c = 0.3$ , $b_f/b = 0.8$ ; Tests in Regular Head and Following Seas, Flaps Oscillating; Static $h/c = 1.0$ , $\alpha = 5^\circ$ . . . . .	53

16.	Flap Configuration 3; $c_f/c = 0.2$ , $b_f/b = 0.6$ ; Tests in Regular Head and Following Seas, Flaps Oscillating; Static $h/c = 1.0$ , $\alpha = 5^\circ$ . . . . .	55
17.	Flap Configuration 4; $c_f/c = 0.2$ , $b_f/b = 0.8$ ; Tests in Regular Head and Following Seas, Flaps Oscillating; Static $h/c = 1.0$ , $\alpha = 5^\circ$ . . . . .	57

## ILLUSTRATIONS

1.	Model with Flap Configuration $c_f/c = 0.2$ , $b_f/b = 0.6$ . . . . .	59
2.	Schematic Drawing of Model and Balances . . . . .	60
3.	Lift Frequency Response, Flaps Oscillating, Smooth Water, Flap Configurations 1 and 2 . . . . .	61
4.	Lift Frequency Response, Flaps Oscillating, Smooth Water, Flap Configurations 3 and 4 . . . . .	62
5.	Drag Frequency Response, Flaps Oscillating, Smooth Water, Flap Configurations 1 and 2 . . . . .	63
6.	Drag Frequency Response, Flaps Oscillating, Smooth Water, Flap Configurations 3 and 4 . . . . .	64
7.	Pitching Moment Frequency Response, Flaps Oscillating, Smooth Water, Flap Configurations 1 and 2 . . . . .	65
8.	Pitching Moment Frequency Response, Flaps Oscillating, Smooth Water, Flap Configurations 3 and 4 . . . . .	66
9.	Lift Frequency Response, Head Seas, Flaps Fixed, Flap Configurations 1 and 2 . . . . .	67
10.	Lift Frequency Response, Head Seas, Flaps Fixed, Flap Configurations 3 and 4 . . . . .	68
11.	Drag Frequency Response, Head Seas, Flaps Fixed, Flap Configurations 1 and 2 . . . . .	69
12.	Drag Frequency Response, Head Seas, Flaps Fixed, Flap Configurations 3 and 4 . . . . .	70
13.	Pitching Moment Frequency Response, Head Seas, Flaps Fixed, Flap Configurations 1 and 2 . . . . .	71
14.	Pitching Moment Frequency Response, Head Seas, Flaps Fixed, Flap Configurations 3 and 4 . . . . .	72

15.	Lift Frequency Response, Following Seas, Flaps Fixed, Flap Configurations 1 and 2 . . . . .	73
16.	Lift Frequency Response, Following Seas, Flaps Fixed, Flap Configurations 3 and 4 . . . . .	74
17.	Drag Frequency Response, Following Seas, Flaps Fixed, Flap Configurations 1 and 2 . . . . .	75
18.	Drag Frequency Response, Following Seas, Flaps Fixed, Flap Configurations 3 and 4 . . . . .	76
19.	Pitching Moment Frequency Response, Following Seas, Flaps Fixed, Flap Configurations 1 and 2 . . . . .	77
20.	Pitching Moment Frequency Response, Following Seas, Flaps Fixed, Flap Configurations 3 and 4 . . . . .	78
21.	Mean Values of Force Coefficients, Flaps Cycling in Smooth Water, Flap Configuration 1 . . . . .	79
22.	Mean Values of Force Coefficients, Flaps Cycling in Smooth Water, Flap Configuration 2 . . . . .	80
23.	Mean Values of Force Coefficients, Flaps Cycling in Smooth Water, Flap Configuration 3 . . . . .	81
24.	Mean Values of Force Coefficients, Flaps Cycling in Smooth Water, Flap Configuration 4 . . . . .	82
25.	Mean Pitching Moment Coefficients, Flaps Cycling in Smooth Water, All Flap Configurations . . . . .	83
26.	Mean Values of Force Coefficients, Flaps Fixed in Waves, Flap Configuration 1 . . . . .	84
27.	Mean Values of Force Coefficients, Flaps Fixed in Waves, Flap Configuration 2 . . . . .	85
28.	Mean Values of Force Coefficients, Flaps Fixed in Waves, Flap Configuration 3 . . . . .	86
29.	Mean Values of Force Coefficients, Flaps Fixed in Waves, Flap Configuration 4 . . . . .	87
30.	Mean Pitching Moment Coefficients, Flaps Fixed in Waves, All Flap Configurations . . . . .	88
31.	Mean Values of Lift Coefficients, Flaps Cycling in Waves, All Flap Configurations . . . . .	89
32.	Mean Values of Drag Coefficients, Flaps Cycling in Waves, All Flap Configurations . . . . .	90

33.	Mean Values of Pitching Moment Coefficients, Flaps Cycling in Waves, All Flap Configurations .....	91
34.	Maximum and Minimum $C_L$ Vs. Phase of Flap to Wave — Flap Configuration 1 .....	92
35.	Maximum and Minimum $C_L$ Vs. Phase of Flap to Wave — Flap Configuration 2 .....	93
36.	Maximum and Minimum $C_L$ Vs. Phase of Flap to Wave — Flap Configuration 3 .....	94
37.	Maximum and Minimum $C_L$ Vs. Phase of Flap to Wave — Flap Configuration 4 .....	95
38.	Maximum and Minimum $C_D$ Vs. Phase of Flap to Wave — Flap Configuration 1 .....	96
39.	Maximum and Minimum $C_D$ Vs. Phase of Flap to Wave — Flap Configuration 2 .....	97
40.	Maximum and Minimum $C_D$ Vs. Phase of Flap to Wave — Flap Configuration 3 .....	98
41.	Maximum and Minimum $C_D$ Vs. Phase of Flap to Wave — Flap Configuration 4 .....	99
42.	Maximum — $C_M$ Vs. Phase of Flap to Wave — All Flap Configurations, Head Sea .....	100
43.	Maximum — $C_M$ Vs. Phase of Flap to Wave — All Flap Configurations, Following Sea .....	101
44.	$C_L$ Time History, Following Sea, Flap Configuration 1, Run 13191 .....	102
45.	$C_D$ Time History, Following Sea, Flap Configuration 1, Run 13191 .....	102
46.	$C_M$ Time History, Following Sea, Flap Configuration 1, Run 13191 .....	103
47.	$C_L$ Time History, Comparison of Flap and Wave Effects, Flap Configuration 1, Run 13191 .....	103
48.	$C_L$ Time History, Head Sea, Flap Configuration 1, Run 13157 .....	104
49.	$C_D$ Time History, Head Sea, Flap Configuration 1, Run 13157 .....	104
50.	$C_M$ Time History, Head Sea, Flap Configuration 1, Run 13157 .....	105

51.	$C_L$ and $C_D$ Time History, Head Sea, Flap Configuration 1, Run 13154, Flap Lag $\pi$ Rads .....	105
52.	$C_L$ and $C_D$ Time History, Head Sea, Flap Configuration 1, Run 13154, in Phase .....	106
53.	$C_M$ Time History, Head Sea, Flap Configuration 1, Run 13154 .....	106
54.	Maximum Lift Frequency Response, Flaps Oscillating in Waves, All Flap Configurations .....	107
55.	Flap and Wave Effectiveness, Summary Sheet, All Flap Configurations .....	108
56.	$C_{L_{AV}}$ Vs. $\sqrt{\nu\omega_f}$ or $\nu$ or $\omega_f$ All Flap Configurations, All Tests $\alpha = 5^\circ$ , $\delta_f = 0^\circ$ .....	109
57.	$C_{D_{AV}}$ Vs. $\sqrt{\nu\omega_f}$ or $\nu$ or $\omega_f$ All Flap Configurations, All Tests $\alpha = 5^\circ$ , $\delta_f = 0^\circ$ .....	110
58.	$C_{L_{AV}}$ Vs. $\alpha$ , Flaps Fixed in Waves, and Smooth Water (Ref. 1) .....	111
59.	$C_{D_{AV}}$ Vs. $\alpha$ , Flaps Fixed in Waves, and Smooth Water (Ref. 1) .....	112
60.	Effect of Depth on Average $C_L$ Flaps Fixed in Waves, Following Sea .....	113
61.	Oscillatory Lift and Drag Parameters Vs. Wave Length and Height, Flaps Fixed in Waves, Following Sea, Flap Configuration 1 .....	114
62.	Phase Relationships, Flaps Cycling in Waves, Head Sea, Flap Configuration 1 .....	115
63.	Phase Relationships, Flaps Cycling in Waves, Head Sea, Flap Configuration 2 .....	116
64.	Phase Relationships, Flaps Cycling in Waves, Head Sea, Flap Configuration 3 .....	117
65.	Phase Relationships, Flaps Cycling in Waves, Head Sea, Flap Configuration 4 .....	118
66.	Phase Relationships, Flaps Cycling in Waves, Following Sea, Flap Configuration 2 .....	119
67.	Typical Oscillograph Record, Flaps Cycling in Waves, Following Sea, Run 13191 .....	120

68.	Sudden Flap Deflection, Time History of Force and Moment Build-up, Flap Configuration 1, Flap Rate 1.6 CPS . . . . .	120
69.	Sudden Flap Deflection, Time History of Force and Moment Build-up, Flap Configuration 1, Flap Rates 3.0, 5.2 CPS . . . . .	121
70.	Sudden Flap Deflection, Time History of Force and Moment Build-up, Flap Configuration 1, Flap Rate 6.5 CPS . . . . .	122
71.	Sudden Flap Deflection, Time History of Force and Moment Build-up, Flap Configuration 2, Flap Rate 1.6 CPS . . . . .	122
72.	Sudden Flap Deflection, Time History of Force and Moment Build-up, Flap Configuration 2, Flap Rates 3.0, 5.2 CPS . . . . .	123
73.	Sudden Flap Deflection, Time History of Force and Moment Build-up, Flap Configuration 2, Flap Rate 6.5 CPS . . . . .	124
74.	Sudden Flap Deflection, Time History of Force and Moment Build-up, Flap Configuration 3, Flap Rates 3.0, 5.2 CPS . . . . .	125
75.	Sudden Flap Deflection, Time History of Force and Moment Build-up, Flap Configuration 3, Flap Rate 6.3 CPS . . . . .	126
76.	Sudden Flap Deflection, Time History of Force and Moment Build-up, Flap Configuration 4, Flap Rates 3.0, 5.2 CPS . . . . .	127
77.	Sudden Flap Deflection, Time History of Force and Moment Build-up, Flap Configuration 4, Flap Rate 6.3 CPS . . . . .	128

# 1 | INTRODUCTION

The purpose of the test program described in this report was to experimentally determine the effects of wave and flap motions and possible intermittent ventilation on hydrofoil forces and moments. In order to do this, the program was divided into four test phases:

- a. Tests in smooth water with flaps cycled at various frequencies.
- b. Tests in regular waves with flaps fixed, running in both head and following seas.
- c. Tests in regular waves with flaps cycled at various frequencies, in both head and following seas.
- d. Tests with flaps driven through a  $1/2$  cycle at high frequency in smooth water, to determine the effect of sudden flap deflections on the hydrofoil forces and moments.

By comparison of the results of a, b and c it was possible to isolate and evaluate the force and moment variations caused by wave action and the variations caused by flap motion. The individual wave profiles were measured and correlated with the hydrofoil forces and moments.

The hydrofoil tested had an NACA 16-309 section and was capable of being fitted with four different flap sizes. It was the same hydrofoil model used in the tests reported in Reference 1. The measurements obtained during unsteady flow conditions were therefore compared with the results given in Reference 1.

Data is presented in coefficient form (in both tables and graphs) in this report. In certain cases time histories have been produced to bring out salient points and to show the effect of having two forcing functions (wave and flap) of different frequencies.

## 2 | MODEL DESCRIPTION AND INSTRUMENTATION

### 2.1 MODEL DESCRIPTION

The model used in this test program was the same as that used in tests reported in Reference 1; consequently, only a brief description will be given here. It exhibited a span of 24 inches, a chord of 4.0 inches, and a rectangular planform with a NACA 16-309 section. The model was fitted with simple flaps as follows:

<u>Flap Configuration</u>	<u><math>c_f/c</math></u>	<u><math>b_f/b</math></u>
1	0.3	0.6
2	0.3	0.8
3	0.2	0.6
4	0.2	0.8

The single center strut was enclosed in a double ogive fairing which did not touch the foil or strut, and thus strut drag was eliminated from the test results.

Figure 1 shows the model with Flap Configuration No. 3. Figure 2 is a schematic drawing of the model and balances, and also shows the method of flap cycling.

The strain gages were waterproofed with Dijell wax, which was melted first and then brushed on. The gages were then coated with Ten-X waterproofing compound for mechanical protection.

### 2.2 INSTRUMENTATION

Forces were measured by means of strain gage balances mounted at the top of the strut (Figure 1). Data was recorded on a Consolidated Electrodynamics

Corp. (CEC) oscillograph, Type 5-114-P3-26. The circuit incorporated a CEC 3-kc amplifier with an output calibration circuit, and a variable attenuation and galvanometer damping circuit. This enabled amplifier output to be maintained within 1%.

Model velocity was obtained from a carriage-mounted photocell, whose signal on the oscillograph trace was deflected by interrupters placed every five feet along the carriage rails.

Wave contours were measured during each test by a sonic-type wave recorder developed and constructed by the University of Minnesota-St. Anthony Falls Hydraulics Laboratory (Reference 3). The wave recorder was mounted on the carriage to measure wave amplitudes at the foil 1/4-chord point.

Flap position was recorded continuously by a strain gage balance connected to the flap bell-crank. No readings were taken of flap forces and moments.

A 16-mm Eyemo motion picture camera was mounted on the carriage to document possible intermittent cavitation or ventilation on the foil and strut.

### 3 | TEST PROCEDURE

The test program was conducted in the 300-foot General Dynamics/Convair hydrodynamics towing tank (Reference 2). The model was tested at constant velocities between 18 and 32 ft/sec. approximately. It was run at fixed depths (1/4-chord point to smooth water level) of between 3 and 5 inches, and with fixed wing angles of attack between -5 and +10 deg. Flap oscillation frequencies which were constant for any given run, varied between 0.5 and 7.0 cycles per second. Regular waves from the paddle-type wavemaker, again constant for any run, were varied between 2 inches and 4 inches in height, and between 3.5 and 8.25 ft. in length (i.e., 20:1 to 24:1 approx.)

Flap angles were varied through the range -8 to +8 degrees during cycling tests, between -5 and +10 degrees for flaps fixed in wave tests, and between 0 and +16 degrees for 1/2 cycle tests. Positive values denote flaps deflected downward.

The procedure when testing with flaps cycling in waves was to choose a flap frequency, wave size and model velocity such that the frequency of encounter with a wave was almost the same as the frequency of oscillation of the flap. Usually, two runs were carried out under identical conditions in order to get instantaneous phase relationships between flap down and wave peak between  $\pi$  radians lag, progressing through the "in-phase" condition to  $\pi$  radians lead.

## 4 | METHOD OF ANALYSIS

### 4.1 TESTS IN SMOOTH WATER WITH FLAPS CYCLED AT VARIOUS FREQUENCIES

The purpose of this part of the program was to determine the frequency response of the system by sinusoidally moving the flaps.

Data from tests covered in Reference 1, with flap cycling frequencies of 0.50 to 1.66 cycles per second, were combined with more recent data with flap cycling frequencies between 3.0 and 7.0 cycles per second.

Average values of maximum and minimum trace readings for lift, drag, pitching moment and flap deflection were read from the oscillograph traces. The force and moment equations were programmed into the IBM 704 computer and  $C_L$ ,  $C_D$ , and  $C_M$  for the foil were read out.

The lift, drag, and moment traces were read at close intervals (i.e., as time histories) throughout the force cycles in order to determine the true maximum and minimum values of drag. Maximum and minimum drag could not be determined from inspection of the oscillograph traces because of the effects of balance interactions.

Phase relationships of the force coefficients were read as lead (positive) or lag (negative) in radians of the maximum values to the maximum flap down position. They were obtained by measuring from the oscillograph trace the time distance between the flap down and the force peak, and arithmetically solving for  $\phi$  by the equation

$$\frac{\phi}{2\pi} = \frac{t}{T_1} ,$$

where  $T_1$  was the time distance from flap down to the next flap down (flap cycling period). If the force peak occurred later than maximum flap down position it was defined as lagging.

The frequency of flap oscillation was obtained from the oscillograph trace by measuring the time interval between successive peaks. Then

$$\omega_f = \frac{2\pi}{T_1} \text{ rads/sec.}$$

Force coefficient and flap amplitudes were defined as  $1/2$  (max. value - min. value). There was a tendency for the flapping mechanism to deflect slightly under heavy load, thus causing slight indentations in the sine traces of the almost simple harmonic motion of the flaps. However, the frequency of oscillation held very steady and was easily read from the traces.

#### 4.2 TESTS IN REGULAR WAVES WITH FLAPS FIXED — HEAD AND FOLLOWING SEAS

The data was analyzed in the same manner as for flaps cycling in smooth water (described previously). Phase relationships of the force coefficients were read as lead, or lag, of the maximum values to the wave peak. Waves varied in size slightly during the course of each run, and thus average values of amplitude and phase angles were read from the oscillograph traces.

The frequency of wave encounter was obtained from the oscillograph trace by measuring the time interval between successive peaks,  $T_2$  then,

$$\nu = \frac{2\pi}{T_2} \text{ rads/sec.}$$

Force coefficient and wave amplitudes were defined as  $1/2$  (max. value - min. value). Wave length was determined by solving the following simultaneous equations: The frequency of wave encounter

$$\nu = \frac{2\pi}{\lambda_K} \left( U_\infty \pm V_\omega \right), \quad (1)$$

where (+) indicates head seas and (-) indicates following seas.

The velocity of a trochoidal wave

$$V_{\omega} = \sqrt{\frac{g \cdot \lambda_K}{2\pi}} \quad (2)$$

a. Head Sea Case

From Equation (1)

$$V_{\omega} = \left( \frac{\nu \lambda_K}{2\pi} - U_{\infty} \right)$$

Wave length

$$\begin{aligned} \lambda_K &= \frac{2\pi V_{\omega}^2}{g} \\ &= \frac{2\pi}{g} \left( \frac{\nu \lambda_K}{2\pi} - U_{\infty} \right)^2 \end{aligned}$$

$$\lambda_K = \frac{2\pi}{g} \left( \frac{\nu^2 \lambda_K^2}{4\pi^2} + U_{\infty}^2 - \frac{U_{\infty} \nu \lambda_K}{\pi} \right)$$

$$= \frac{\nu^2 \lambda_K^2}{2\pi g} + \frac{2\pi U_{\infty}^2}{g} - \frac{2U_{\infty} \nu \lambda_K}{g}$$

$$\therefore \frac{\nu^2 \lambda_K^2}{2\pi g} - \left( \frac{2U_{\infty} \nu}{g} + 1 \right) \lambda_K + \frac{2\pi U_{\infty}^2}{g} = 0$$

$$\therefore \lambda_K = \left\{ \frac{\pi g \left( \frac{2U_{\infty} \nu}{g} + 1 \right)}{\nu^2} \right\} \pm \left\{ \frac{\pi g \sqrt{\left( \frac{2U_{\infty} \nu}{g} + 1 \right)^2 - \frac{4\nu^2 U_{\infty}^2}{g^2}}}{\nu^2} \right\}$$

b. Following Sea Case

From Equation (1)

$$\begin{aligned}V_{\omega} &= \left( U_{\infty} - \frac{\nu \lambda_K}{2\pi} \right) \\ \lambda_K &= \frac{2\pi V_{\omega}^2}{g} \\ &= \frac{2\pi}{g} \left( U_{\infty} - \frac{\nu \lambda_K}{2\pi} \right)^2 \\ &= \frac{2\pi}{g} \left( U_{\infty}^2 + \frac{\nu^2 \lambda_K^2}{4\pi^2} - \frac{U_{\infty} \nu \lambda_K}{\pi} \right)\end{aligned}$$

Consequently, the expression for wavelength is the same for both head and following seas. Take second term in equation at the bottom of page 9 as positive for head seas and negative for following seas.

4.3 TESTS IN REGULAR WAVES WITH FLAPS  
CYCLING — HEAD AND FOLLOWING SEAS

Data was read from the oscillograph traces in exactly the same way as for the two previous cases. Phase relationships of the force coefficients were read as lead or lag of the maximum values to the wave peak. But in addition there was (at any time during a run) an instantaneous phase relationship between the flap position and the wave. This was defined as a lead if the maximum flap-down position occurred  $\pi$  radians or less ahead of the wave peak. In order to obtain the phase in radians, the reference was taken as the encounter period of the wave in seconds — the same as for the force coefficient phase angles.

Because of the varying phase relationship between the flap and the wave, it was not possible to average the waves to take account of variations in wave size, and all values had to be read as close as possible to the times at which flap-wave phases were equal to  $+\pi$ ,  $+\pi/2$ ,  $0$ ,  $-\pi/2$  and  $-\pi$ . This meant that the results

for flaps cycling in waves could not be so accurate as for flaps fixed in waves. However, errors caused by this source were very much diminished by the fact that the flap is by far the more powerful forcing function.

Wave lengths were again calculated as for the flaps fixed in waves case.

#### 4.4 DATA ANALYSIS ON TIME BASIS

The purpose of this part of the analysis was to get force and moment coefficients from 1) Steady-state data, flaps fixed in smooth water; 2) Data for flaps fixed in waves; and 3) Data for flaps cycling in smooth water. These three sets of data were added together in a time history and compared with the measured total as given by tests with flaps cycling in waves.

Because of the difference in frequency of the two forcing functions (wave and flap), there will be a "beating" of the resultant force and moment coefficients; i. e., the amplitudes of the oscillations will rise and fall periodically over a number of oscillations. The period of this "beating" will be of longer time duration as the frequencies of the two forcing functions come closer together. This effect was clearly observed on the oscillograph traces. See Figure 67 for a typical record, and Figures 34 through 37 for plots of the envelopes of  $C_L$  with flap phase.

$$\text{At any time from } t = 0 \quad \left\{ \begin{array}{l} \text{Wave amplitude } A_{K_t} = A_K \times \sin \nu_t. \\ \text{Flap Deflection} \quad = \delta_{f_t} = \delta_f \times \sin (\omega_f t + \phi_1). \end{array} \right.$$

Adding wave and flap effects

$$\Delta C_{L(t)} = \left( \frac{C_L}{A_K} \right)_{\nu} \times A_K \times \sin \left[ \nu_t + \phi_{L_1} \right] + \left( \frac{C_L}{\delta_f} \right)_{\omega_f} \times \delta_f \times \sin \left[ \left( \omega_f t + \phi_1 \right) + \phi_{L_2} \right].$$

Similar expressions can be derived for  $\Delta C_{D(t)}$  and  $\Delta C_{M(t)}$ . Values of force and moment amplitude ratio and phase relationships are read from Figures 3 through 20.

## 5 | DISCUSSION OF TEST RESULTS

### 5.1 GENERAL

The results of the tests are presented in coefficient form in Tables 2 through 17.  $C_L$  and  $C_D$  were obtained normal and parallel to the water surface respectively, and  $C_M$  was measured at the 1/4-chord point. Total drag measurements were not corrected for interference effects due to the presence of the center strut, as this was found to be very small. (See Figure 25 of Reference 1.)

There was no evidence of cavitation or ventilation in any of the tests. The approximate test variables for which data has been obtained are summarized in Table 1. Not all combinations of the variables were tested; consequently, Table 1 must be read in conjunction with Tables 2 through 17.

### 5.2 FLAPS CYCLING IN SMOOTH WATER

Graphs have been plotted of

$\frac{\Delta C_{L2}}{\Delta \delta_f}$  and  $\phi_{L2}$  ( the phase of maximum  $C_L$  to the flap-down position) against a base of flap cycling frequency in radians/sec. Similar graphs have been plotted for

$$\frac{\Delta C_{D2}}{\Delta \delta_f} \text{ and } \frac{\Delta C_{M2}}{\Delta \delta_f} .$$

Figures 3 through 8 show these graphs for all four flap configurations.

Table 1. Summary of Approximate Test Variables

Type of Test	Flaps Cycling in Smooth Water	Flaps Fixed in Waves		Flaps Cycling in Waves		Flaps Deflected 1/2 Cycle
		Head Sea	Following Sea	Head Sea	Following Sea	
Flap Configuration	1, 2, 3, 4	1, 2, 3, 4	1, 2, 3, 4	1, 2, 3, 4	1, 2, 3, 4	1, 2, 3, 4
Depth of 1/4-Chord (Inches)	4	4	3, 4, 5	4	4	4
Wave Height - Trough to Crest (Inches)	-	4	2, 3, 4	2, 4	2, 4	-
Wavelength (Ft.)	-	8	3.5 to 8.25	3.5 to 8.25	3.5 to 8.25	-
Angle of Attack of Foil (Degrees)	0, +5	-5, 0, +5, +10	+5	+5	+5	+5
Flap Angle (Degrees)	0 ± 8	-5, 0 +5, +10	+10	0 ± 8	0 ± 8	0 to +16
Velocity (Ft./Sec.)	30	18-32	18-32	20, 30	20, 30	30
Flap Frequency (Cycles/Sec.)	.5 to 7.0	-	-	2.0 to 7.5	2.0 to 7.5	1.6 to 6.5

It will be noted that

$$\frac{\Delta C_{L2}}{\Delta \delta_f}$$

tends to increase with increase of flap cycling frequency, and this may mean that there is no flow separation at the higher frequencies. However, this possibility was not investigated.

With regard to

$$\frac{\Delta C_{D2}}{\Delta \delta_f},$$

it will be noted that the flap cycling tests of Reference 1 (with the lowest cycling rates) were performed at foil angle of attack of zero degrees, whereas the later cycling tests at higher cycling rates were done at angle of attack of +5 degrees. Now the  $C_D \sim \alpha$  curves for flaps fixed in smooth water are "trough" shaped with minimums for the different flap angles occurring at approximately  $\alpha = 0^\circ$ . At  $\alpha = 5^\circ$ ,  $C_D$  increases progressively when  $\delta_f$  is moved from negative, through zero, to positive. However, at  $\alpha = 0^\circ$ ,  $C_D$  may be greater at  $\delta_f = -5^\circ$ , for example, than it is at  $\delta_f = 0^\circ$ . This is probably the cause of the scatter in the tests points for

$$\frac{\Delta C_{D2}}{\Delta \delta_f}$$

and drag phase angle at the lowest flap frequencies.

Force and moment phase lag increases with increase of cycling frequency, and would probably reach a value of  $\pi$  at very high frequencies.

Average values of  $C_{L2}$ ,  $C_{D2}$  and  $C_{M2}$  were plotted against cycling frequency (Figures 21 through 25) and were found to be close (within limits of experimental error) to the steady-state values for  $\alpha = 5^\circ$ . However, at  $\alpha = 0^\circ$  values of  $C_{D2}$  tended to be negative. No explanation is offered for this, but the data was carefully checked and is felt to be good. Negative drags did not occur in any other test.

### 5.3 FLAPS FIXED IN REGULAR WAVES

Graphs have been plotted of the non-dimensional coefficient

$$\frac{\Delta C_{L1}}{A_K} \left( \frac{C}{2} \right)$$

and the phase of maximum  $C_L$  to the wave peak, against a base of frequency of wave encounter in radians/sec. Similar graphs have been plotted for

$$\frac{\Delta C_{D1}}{A_K} \left( \frac{C}{2} \right)$$

and

$$\frac{\Delta C_{M1}}{A_K} \left( \frac{C}{2} \right)$$

These are shown in Figures 9 through 20 for all 4 flap configurations, and for both head and following sea conditions.

It was observed that there was a pronounced difference in the phase relationships between head and following seas. Because of the orbital velocity of the wave, the maximum lift occurs approximately  $\pi/2$  radians ahead of the wave peak in a head sea, and approximately  $\pi/2$  radians after the wave peak in a following sea. This is because of the change of effective angle of attack on the foil as it passes through the waves.

The frequency of wave encounter was defined as

$$\nu = \frac{2\pi}{\lambda_K} \left( U_\infty \pm V_\omega \right) \text{ radians/sec.}$$

The positive sign is taken with head seas, and the negative sign with following seas. Other experimenters, notably those discussed in Reference 5, have used a non-dimensional reduced frequency, which is useful where comparisons have to be made.

This is defined as:

$$\begin{aligned}\text{Reduced frequency} &= \frac{\nu c}{2U_{\infty}}, \\ &= \frac{c}{2U_{\infty}} \times \frac{2\pi}{\lambda_K} (U_{\infty} \pm v_{\omega}), \\ &= \frac{c\pi}{U_{\infty}\lambda_K} (U_{\infty} \pm v_{\omega}).\end{aligned}$$

For head sea tests with flaps fixed, the same wave was used throughout, and therefore the reduced frequency remained almost the same even though the velocity changed. Consequently, it was not possible to use this form for graphical presentation of the results.

The oscillatory lift parameter decreases slowly with increase of  $\nu$  for all four flap configurations in a head sea, and increases slowly for all configurations in a following sea. This is in agreement with Reference 4, Page 10, where it is noted that the unsteady lift effects are decreased in head seas with increasing velocity for the same range of wave conditions.

In general, it appears that the angle of attack of the foil, and flap angle, have little effect on the oscillatory lift coefficient in waves. (See Figures 9, 10, 15, 16.) Head sea tests were carried out at  $\alpha = -5^\circ, 0^\circ, 5^\circ, 10^\circ$ , and  $\delta_f = -5^\circ, 0^\circ, 5^\circ, 10^\circ$ , whereas following sea tests were all carried out at  $\alpha = 5^\circ$  and  $\delta_f = 10^\circ$ .

The oscillatory drag parameter decreases slowly with increase of  $\nu$  for all four flap configurations in a head sea, but is almost constant for all configurations in a following sea.

Drag is out of phase with lift in head seas. It has been suggested that this may be caused by leading edge suction. If the suction force increases with increase of instantaneous angle of attack in head seas as the foil approaches the

wave peak. then it would be expected to increase commensurately with increase of lift. This suction force would therefore act in complete opposition to the drag because of lift, and would tend to shift the phase angle of the drag relative to the wave.

In Reference 6, J. M. Wetzell gives another explanation of how lift and drag become out of phase, and also how it is possible for even negative drags to occur. To quote Reference 6, with explanations for Reference 4 that are applicable to this present report: "The lift and drag were measured perpendicular and parallel to the still water surface. As the instantaneous angle of attack was increased (up-wash) by the orbital velocity of the wave, the true lift and drag with respect to the instantaneous velocity vector also increased. However, the resultant force vector tilted forward, thereby increasing the measured lift and decreasing the measured drag. A downwash effect would decrease the measured lift and increase the measured drag. Thus, for quasi-steady conditions the lift and drag should be out of phase about 180 degrees, measurements in head seas (Figures 6 and 10 of Reference 4) indicate about 230 degrees. It may also be possible to obtain negative drags if the instantaneous angle of attack is sufficient to tilt the force vector forward of the vertical for part of the cycle, and if the steady drag is low. It should be mentioned that the drag reduction in an upwash can be expected only in a wetted, non-separated flow." These remarks are directly applicable to this present report, as flow was fully wetted, and lift and drag were also measured perpendicular and parallel to the water surface. In these tests lift and drag were out of phase in head seas by about 220 degrees.

There is considerable scatter in the test points for the oscillatory pitching moment parameter plotted against frequency of wave encounter in head seas, but there appears to be very little change in this parameter as frequency is increased (Figures 13, 14). In a following sea the oscillatory pitching moment parameter increases with increase of frequency for all four flap configurations (Figures 19, 20). The pitching moment oscillograph traces follow the lift traces

closely, and the maximum and minimum pitching moments occur at nearly the same phase angles as the lift maximum and minimums. In head seas the pitching moment leads the lift slightly, and in following seas it lags slightly.

Figures 26, 27, 28 and 29 show mean values of force coefficients for tests with flaps fixed in waves, for both head and following seas. Results indicate that within the range of frequencies tested there is slight decrease in both lift and drag as frequency of encounter increases. This is true for all positions of the wing and flap settings, and for all flap configurations, but particularly for Configurations 3 and 4.

Figure 30 shows mean values of pitching moment coefficient for all flap configurations in both head and following seas. Within the limits of experimental error there is very little change of mean pitching moment coefficients from the steady-state values of Reference 1.

#### 5.4 FLAPS CYCLING IN REGULAR WAVES

The plotting of data from these tests is complicated because there are two forcing functions (flap and wave) of different frequencies. The forces and moments not only have phase relationships with the wave, but different phase relationships with the flap. Actually, all measured phases (which are instantaneous in this case) have been referred to the wave as the basic forcing function. The oscillatory force and moment coefficients would vary with both frequency of wave encounter and frequency of flap oscillation, as well as with the phase relationship of the flap to the wave. Consequently, the best way to analyze this data is in terms of continuous time histories (described in Paragraph 5.5). However, to cover all of the data in this way would be exceedingly lengthy and time consuming, and there are various other ways to plot in order to summarize and bring out the salient points. Figures 31, 32 and 33 present plots of average  $C_L$ ,  $C_D$  and  $C_M$  respectively, against a combined frequency of flap and wave in radians per second. In general, there is a slight falling off in  $C_L$  as frequency increases,  $C_D$  remains sensibly constant and  $C_M$  becomes slightly more

negative. The points for head and following seas fall very close to the same curves.

In Figures 34 through 37 instantaneous maximum and minimum lift coefficients have been plotted against the phase of the flap to the wave, for all flap configurations in head and following seas. The curves are really envelopes of the  $\Delta C_L$  and show the harmonic "beating" of  $\Delta C_L$  with change of phase between the two forcing functions. This effect can also be seen in the representative oscillograph trace in Figure 67, where there is a large frequency difference between the flap cycle and the wave cycle. It will be noted that in head seas  $\Delta C_L$  is a maximum where the flap-down position leads the wave peak by  $\pi/2$  radians, and that in following seas  $\Delta C_L$  is a maximum where the flap lags the wave by  $\pi/2$ . This would be expected since these are the points where there is maximum disturbance input.

Figures 38, 39, 40, and 41 present curves of instantaneous maximum and minimum drag coefficients plotted against the phase of the flap to the wave, for all flap configurations in head and following seas. These curves do not exhibit so clearly as those of lift coefficient the change of drag with phase change between the forcing functions. Figures 42 and 43 show that there is little change of maximum instantaneous  $C_M$  when plotted against the phase of the flap to the wave, in head or following seas.

Figure 54 is a summary plot that was prepared of an oscillatory lift parameter against frequency in radians per second. With this plot it is possible to compare on one sheet the tests with flaps cycling in waves, flaps cycling in smooth water and flaps fixed in waves for all four flap configurations in both head and following seas:

- a. For flaps cycling in waves, the oscillatory lift parameter was taken as

$$\frac{(\Delta C_{L3})^2}{A_K \cdot \delta_f} \times \frac{C}{2} ,$$

which brings in the effects of both flap and wave, and the frequency factor was taken as  $\sqrt{\nu \cdot \omega_f}$  radians/sec.

b. For flaps cycling in smooth water, and flaps fixed in waves, a combined oscillatory lift parameter was taken as

$$\frac{(\Delta C_{L_1} + \Delta C_{L_2})^2}{A_K \cdot \delta_f} \times \frac{C}{2},$$

which was again plotted against the combined frequency factor  $\sqrt{\nu \cdot \omega_f}$  radians/sec.

Values of  $\Delta C_{L_3}$  were read from the Summary Tables 14, 15, 16, and 17 as maximum values, at maximum flap down leading the wave peak by  $\pi/2$  radians for head seas, and lagging by  $\pi/2$  radians in following seas.

Figures 54 shows that for each flap configuration the oscillatory lift parameters for the different cases fall on the same curve for both head and following seas. Thus, the separate effects of flap and wave can be evaluated and then added together vectorially to give the combined effects with both flap and wave acting together.

Figure 55 is a summary diagram of flap and wave effectiveness in lift for all flap configurations in both head and following seas. It can be seen that for all flap configurations except No. 3 the flap is a very much more powerful forcing function than the wave and could easily cancel changes in  $C_L$  caused by running through waves. Both Figures 54 and 55 show that much more flap effectiveness is derived from increase of flap chord than from increase of flap span. Phase relationships for flaps cycling in waves are presented in Figures 62 through 66. For Flap Configurations 1 and 2 in head seas, Figures 62 and 63 show that drag lags lift and that pitching moment lags drag fairly consistently by about 20 degrees each for all phase relationships between flap and wave. As the phase of flap to wave progresses from lag to lead, the phases of lift, drag and pitching moment become more leading. However, when the flap is in phase

with the wave, forces and moments are all lagging the wave. At a higher frequency of wave encounter and flap oscillation all forces and moments are more lagging to the wave than at a lower frequency. Considering Figures 64 and 65, for Flap Configurations 3 and 4 in head seas, roughly the same conclusions apply, but there is much more scatter in the data.

In following seas, the scatter was very bad, and made graph plotting impossible except for Flap Configuration 2 which had the largest flap. Figure 66 shows that Flap Configuration 2 in a following sea exhibited approximately the same characteristics as in a head sea.

#### 5.5 TIME HISTORY ANALYSIS TO ISOLATE EFFECTS OF FLAP MOTIONS FROM EFFECTS OF WAVE MOTIONS

All comparisons were made with Flap Configuration No. 1 ( $c_f/c = .3$ ,  $b_f/b = .6$ ), but a variety of conditions was chosen to show that the method works for head and following seas, and for different instantaneous phase relationships between flap and wave. The results are shown in Figures 44 through 53.

Figures 44, 45 and 46 present lift, drag and pitching moment variation respectively, for Test Run 13191 through two complete cycles starting with  $\pi/2$  radians flap lag and finishing with flap and wave in phase. The wave frequency of encounter was 4.72 cycles/sec. The wave height (trough to crest) was 1.73 inches and its length, 3.66 ft. The flap frequency was 6.30 cycles/sec. This was a following sea case.

$C_L$  variation with flaps cycling in waves agrees very closely with  $C_L$  obtained by adding 1) components caused by flaps fixed in calm water (Reference 1), 2) components caused by flaps cycling in smooth water, and 3) components caused by flaps fixed in waves. Agreement is found in amplitude of oscillation, period and reduction in amplitude (i.e., beating) on going from flap "lag" to "in phase" conditions.

With  $C_D$  it was found that there was good agreement in amplitude variation and period of oscillation, but the actual values of  $C_D$  obtained by adding up separate components were an almost constant amount less than the values for flaps cycling in waves. This appears to be the result of an increase in the basic  $C_D$  of the foil in going from steady to unsteady flow conditions. The same remarks apply to  $C_M$ , which was an almost constant amount more positive when made up of component parts.

Figure 47 shows the separate components of  $\Delta C_L$  resulting from flap and  $\Delta C_L$  caused by the wave for Run No. 13191. It can be seen that the flap is a very much more powerful forcing function than the wave, and could easily cancel out the variations of  $C_L$  caused by the wave.

Figures 48, 49 and 50 present lift, drag and pitching moment variation respectively for Run No. 13157 at  $\pi/2$  radians flap lead. Only one oscillation has been plotted since the two forcing functions were very nearly of the same frequency, and "beating" would be evident over a larger number of waves. The wave frequency of encounter was 3.42 cycles/sec. The wave height (trough to crest) was 3.77 inches and its length, 8.31 ft. The flap frequency was 3.22 cycles/sec. This was a head sea case.

There was good agreement for both lift and drag, but pitching moment was more positive by an almost constant amount when made up of component parts. Figures 51 and 53 present lift, drag and pitching moment variation for Test Run 13154, with flap lagging the wave by  $\pi$  radians. Figure 52 and 53 present lift, drag and pitching moment variation for the same run, but with flap and wave in phase. The wave frequency of encounter was 7.88 cycles/sec. The wave height (trough to crest) was 1.51 inches and its length, 3.65 ft. The flap frequency was 7.35 cycles/sec. This again was a head sea case.

There was very close agreement in  $C_L$  variation for both flap and wave, "out-of-phase" and "in-phase," and not much change in the actual values.  $C_D$  again was a constant amount low when made up of component parts, for both

out-of-phase and in-phase conditions.  $C_M$  showed very good agreement, both for actual values and for dimensions of the wave form.

It is felt that this detailed plotting of a small part of the experimental data obtained in the test program shows fairly conclusively that it is possible to isolate and evaluate the effects of flap motions from the effects of wave motion when running with flaps cycling in waves — if test results from flaps cycling in smooth water and flaps fixed in waves are available separately. It also shows that if a complicated wave of several superimposed sine waves is built up, it should be possible to obtain flap motions that would give a constant running  $C_L$ . This information would be useful to the hydrofoil boat designer but will require further analysis.

#### 5.6 COMPARISONS WITH REFERENCE 1 SMOOTH WATER TESTS

Some of the figures that show comparisons with Reference 1 (flaps fixed in smooth water) were discussed previously in this section of the report. These are the plots of average force and moment coefficients against frequency of disturbance in radians per second (Figures 21 through 33). In general, these average force and moment coefficients show very good agreement, within the limits of experimental error, with the steady-state values. Sometimes average lift and drag coefficients are a little lower than steady state, and average pitching moment coefficients tend to be a little more negative. Figures 56 and 57 summarize some of this data for average force coefficients. Figure 56 shows average values of lift coefficients for all four flap configurations at a constant angle of attack of  $5^\circ$ , and for flaps cycling in waves, flaps cycling in smooth water, and flaps fixed in waves (plotted against frequency in radians per second). The steady-state value of  $C_L$  is 0.34. Figure 57 shows average values of drag coefficients at constant  $\alpha = 5^\circ$ . The steady-state value of  $C_D$  is 0.024. No particular trends are discernable from the curves, but it appears that there is not much change in the force coefficients from the steady-state value within the range of frequencies tested.

For the tests of flaps fixed in waves there was sufficient coverage of angle of attack to plot  $C_L$  vs.  $\alpha$  and  $C_D$  vs.  $\alpha$ . These are compared with the steady-state curves from Reference 1, at a flap deflection of 10 degrees down in Figures 58 and 59. Two wave cases were evaluated: one where the wave encounter rate was 3 waves per second, and the other at 5 waves per second. Test points were plotted for head and following seas. The average force coefficients for flaps fixed in waves fall slightly below the steady-state curves, but are of the same form, and the lift curve slopes are the same. There is very little difference between the encounter rates of 3 or 5 waves per second, and these differences can probably be attributed to experimental scatter.

5.6.1 THE EFFECT OF DEPTH — In all of the tests described in this report the static depth of the 1/4-chord point of the foil was held steady at 1 chord, with the exception of tests with flaps fixed in waves in a following sea. Figure 60 presents values of the average lift coefficient plotted against the non-dimensional static depth of the foil ( $h/c$ ) for all four flap configurations at  $\alpha = 5^\circ$  and  $\delta_f = 10^\circ$ . As  $h/c$  drops from 1.25 to 0.75 the average  $C_L$  falls about 10% for all four flap configurations. It is not possible to exactly compare this data with Figure 18 of Reference 1, because the Reference 1 plot is for Flap Configuration 2 only, at  $\alpha = 2^\circ$  and foil submergences ( $h/c$ ) between 0.5 and 1.0. However, considering this case with a flap deflection of  $10^\circ$  down, as  $h/c$  drops from 1.0 to 0.5 the  $C_L$  falls about 11%. Therefore, the foils running in waves exhibit approximately the same reduction in average lift on approaching the mean water surface as in the steady-state conditions.

## 5.7 COMPARISONS WITH REFERENCE 4

In Reference 4 (hydrofoils in regular waves tests) oscillatory lift parameter was plotted against wave length in feet, and oscillatory drag parameter against wave height. The plotting of the lift parameter against wave length had a theoretical basis, but the plotting of the drag parameter against wave height was arbitrarily adopted, since this parameter had little dependence on wave length.

In this report the only data obtained at a sufficiently large number of wave sizes was for flaps fixed in waves in a following sea. From Reference 4:

$$\begin{aligned}\text{Oscillatory lift parameter} &= \frac{L_m}{ab\rho V^2} \quad (\text{Reference 4 symbols}), \\ &= \frac{\Delta C_L \rho V^2 bc}{2A_K \cdot c\rho V^2} \quad (\text{symbols used in this report}), \text{ and} \\ &= \frac{\Delta C_L}{A_K} \left( \frac{b}{2} \right).\end{aligned}$$

Similarly, oscillatory drag parameter

$$= \frac{\Delta C_D}{A_K} \left( \frac{b}{2} \right).$$

Figure 61 presents plots of

$$\left( \frac{\Delta C_{L1}}{A_K} \right) \frac{b}{2}$$

against wave length  $\lambda_K$  feet, and

$$\left( \frac{\Delta C_{D1}}{A_K} \right) \frac{b}{2}$$

against wave height in feet (trough to crest), for Flap Configuration 1 at two speeds: 21 and 30 feet per second, and  $\alpha = 5^\circ$ ,  $\delta_f = 10^\circ$ . As in Reference 4, the oscillatory lift parameter is fairly constant, falling slowly with increase of wave length. The actual values are lower, since the 16-309 is a low-lift, high-speed section when compared with the Wright 1903 tested in Reference 4. The oscillatory drag parameter falls with increase of wave-height; this is in opposition to Figure 10 of Reference 4. However, the drag change with wave is greater at the lower speed, which agrees with Reference 4.

## 5.8 ONE-HALF CYCLE TESTS IN SMOOTH WATER

Figures 68 through 76 present results of tests in which the flaps were driven through one-half of one cycle at various frequencies to determine the effect of sudden flap deflections on the hydrofoil forces and moments. Figure 77 presents a case where the flaps were driven through one complete cycle at 6.3 cycles/sec. These tests simulate sudden control motions which may occur during the operation of a full-scale hydrofoil vehicle.

It is noted from the curves that there is always considerable over-swing of  $C_L$  and  $C_M$ , and to a much lesser extent of  $C_D$ . The maximum  $C_L$  usually occurs just before the maximum flap-down position, and the maximum  $C_D$  and  $C_M$  just after maximum flap down.  $C_M$  in particular does not become steady until about 100% of the flap deflection time has elapsed, after the flap is fully down. The overswing in  $C_M$  may be up to 100% of the change resulting from steady flap deflection.

Except for the very low cycling rate of 1.6 cycles/sec., phase relationships between the flap, and the hydrofoil forces and moments, do not seem to be much affected by flap cycling rate within the range of frequencies tested. In the case where the flap was moved through one complete cycle (see Figure 77 for results on Flap Configuration 4), the peak values of  $C_L$ ,  $C_D$  and  $C_M$  all occurred after the flap was in the full down position. As the flap returned to its original neutral position,  $C_L$  and  $C_D$  returned smoothly to their original values without over-swing, but with  $C_M$  there was again some overswing.

## 6 | RELIABILITY AND ACCURACY OF DATA

In general, the accuracy of the test points can be taken as  $\pm 5\%$ . However, the accuracy of faired curves may be considerably better. The maximum frequency of the transient loads and moments obtained in waves was approximately 7 cycles/sec. The natural frequency of the complete model system was about 10 times this value; consequently, the force and moment variations could be read with good accuracy. Waves sometimes varied slightly both in height and length during any one run; therefore, the data had to be averaged over three or more waves.

Because the flap and its drive mechanism deflected slightly under very heavy loads, the flap deflection trace departed slightly at such times from a pure sinusoidal form. However, its frequency did not appear to vary. Flaps cycling in wave tests gave oscillograph traces which were essentially transitory in nature because of the different frequencies of the flap and the wave; consequently, this data is probably less accurate than that obtained from the other tests. It was read later, however, with the experience gained from reading all the earlier data, and so this may have increased its accuracy somewhat. Also, the flap was the stronger forcing function, and the flap trace was of more constant form than the wave trace — giving greater overall accuracy.

Of all the traces, the pitching moment was the worst one from the standpoint of harmonic distortion, especially with long waves in following seas. The lift trace exhibited good sinusoidal form (as did the wave), but the drag trace was masked by gage interactions. (See paragraph 4.1, Section 4.)

On page 11 of Reference 4 it is stated that an investigation was made of the wave profile used as the forcing function in the experiments. A harmonic analysis was made of several typical wave forms and a distortion of about 8 to 12% was found in most cases. In Reference 4 a harmonic analysis was also made on the lift traces.

No harmonic analysis was made on any of the data in this report. Consequently, the values presented for lift, drag and pitching moment represent peak-to-peak measurements taken directly from the records, rather than the maximum amplitude of the fundamental. Average values are  $\left( \frac{\text{Max. Value} + \text{Min. Value}}{2} \right)$

In measuring phase angles it was found to be more difficult to measure drag phase angles in following seas than in head seas because the peak position fluctuated between waves. Therefore, it was rather difficult to select an average value. Also, the peaks were not sharply defined, but spanned a considerable length on the trace, and the midpoint fluctuated on each peak. In general, all phase angles were found to be difficult to measure accurately because the peaks were often not too clearly defined, and in flaps cycling in waves tests, phase relationships were transitory. This is illustrated in Figure 67, which presents a typical oscillograph record for flaps cycling in waves in a following sea. Note that the wave trace is inverted in Figure 67. This is a case where the flap frequency is considerably different from the wave frequency, and in three complete wave cycles the phase of the flap to the wave has changed from "in phase" to " $\pi$  lag" and back again to "in phase".

## 7 | CONCLUSIONS

a. The oscillatory lift coefficients and the oscillatory drag coefficients are not apparently affected by flap deflection or angle of attack within the range -5 degrees to +10 degrees.

b. The average values of lift, drag and pitching moment coefficients in unsteady flow do not vary much from the equivalent steady-state conditions.

c. It is possible to isolate and evaluate the separate effects of flap and wave motion, and then add these vectorially to get the combined effects of flap and wave acting together.

d. For the range of flap sizes and waves tested, the flap is by far the more powerful forcing function. Increase of flap chord has more effect than increase of flap span.

e. Flap 1/2-cycle tests show overswing of the force and moment coefficients, with center of pressure still moving up to 100% of the flap movement time beyond flap steady. There are varying phase relationships between force and moment coefficients and the flap.

f. No cavitation or intermittent ventilation was observed at any time.

## 8 | REFERENCES

1. Convair Report No. GDC-ZH-153, Flapped Hydrofoils in Smooth Water — Subcavitating Flow, C. E. Jones, Jr., November 1961.
2. Convair Report No. ZH-114, General Dynamics/Convair Hydrodynamics Laboratory.
3. St. Anthony Falls Hydraulic Laboratory (University of Minnesota) Memorandum No. M-74, The Sonic Surface-Wave Transducer, J. M. Killen, February 1959.
4. St. Anthony Falls Hydraulic Laboratory Project Report No. 64, Lift and Drag on Surface-Piercing Dihedral Hydrofoils in Regular Waves, J. M. Wetzel and F. R. Schiebe, September 1960.
5. St. Anthony Falls Hydraulic Laboratory Technical Paper No. 37-B, Longitudinal Motions and Stability of Two Hydrofoil Systems Free to Heave and Pitch in Regular Waves, J. M. Wetzel and W. H. Maxwell, December 1961.
6. Letter from J. M. Wetzel, Research Fellow, St. Anthony Falls Hydraulic Laboratory, to C. E. Jones, dated 12 April 1962.

### ASSOCIATED REPORTS:

7. D. T. M. B. Report No. 1140, Experimental and Theoretical Studies of Hydrofoil Configurations in Regular Waves, P. Leehey and J. M. Steele, Jr., October 1957.
8. Work Sponsored by O.N.R., Contract No. N62-558-2236, On Oscillating Hydrofoils, Part I; S. Schuster and H. Schwanecke; December 1960, Part II; S. Schuster and H. Schwanecke; June 1962.
9. National Luchtvaartlab, Amsterdam Reports F-101, F-102, F-103, F-104; Experimental Determination of the Aerodynamic Coefficients of an Oscillating Wing in Incompressible, 2-Dimensional Flow; H. Greidanus and B. D. Van Vooren; 1952.

10. NACA Report No. 1108, Experimental Aerodynamic Derivatives of a Sinusoidally Oscillating Airfoil in 2-Dimensional Flow; R. L. Halfman, 1952.
11. NACA Technical Note No. 1372, Some Considerations on an Airfoil in an Oscillating Stream; J. M. Greenberg, 1947.
12. Dent. Luftfahrt-Forsch UM 1207, Results of Wind Tunnel Tests for the Determination of the Moments of the Aerodynamic Forces on an Oscillating Control Surface; F. Walter and W. Heger; 1944.
13. Journal of Aeronautical Sciences, 16; Readers Forum, p.511; "Oscillating Aileron"; 1949.
14. Journal of Aeronautical Sciences, 15, p.565-568, 1948; Journal of Aeronautical Sciences Errata, 16, Oscillating Flap, p.442-443, 1949.

## 9 | NOMENCLATURE

$U_{\infty}$	Model Velocity (Ft. /Sec. ).
$\alpha$	Foil Angle of Attack (Degrees).
$\delta_f$	Flap Angle (Degrees).
$\delta_f \tau$	Flap Angle (Radians).
$\Delta \delta_f$	Flap, 1/2 Amplitude of Oscillation (Radians).
$A_K$	Wave, 1/2 Amplitude (Ft. )
$\lambda_K$	Wave Length (Ft. )
$\nu$	Frequency of Wave Encounter (Rad. /Sec. ).
$V_{\omega}$	Wave Velocity (Ft. /Sec. ).
$\omega_f$	Frequency of Flap Oscillation (Rad. /Sec. ).
$c$	Hydrofoil Chord (Ft. ).
$b$	Hydrofoil Span (Ft. ).
$c_f$	Flap Chord (Ft. ).
$b_f$	Flap Span (Ft. ).
$h$	Depth of Foil 1/4-Chord Pt. (Ft. ).
$H_0$	Depth of Foil 1/4-Chord Pt. (In. ).
$L$	Foil Lift Normal to Water Surface (Lb. ).
$D$	Foil Drag Parallel to Water Surface (Lb. ).
$P. M.$	Pitching Moment About Foil, 1/4-Chord Point, Positive Leading Edge Up (Lb. /Ft. )

$\rho$	Water Density (Slugs/Ft. <sup>3</sup> ).
$C_{L_1}$	Average Lift Coefficient, Flaps Fixed in Waves = $\frac{L}{1/2\rho U_\infty^2 cb.}$
$C_{D_1}$	Average Drag Coefficient, Flaps Fixed in Waves = $\frac{D}{1/2\rho U_\infty^2 cb.}$
$C_{M_1}$	Average Pitching Moment Coefficient, Flaps Fixed in Waves = $\frac{P. M.}{1/2\rho U_\infty^2 c^2b.}$
$C_{L_2}$	Average Lift Coefficient, Flaps Cycling in Smooth Water.
$C_{D_2}$	Average Drag Coefficient, Flaps Cycling in Smooth Water.
$C_{M_2}$	Average Pitching Moment Coefficient, Flaps Cycling in Smooth Water.
$C_{L_3}$	Average Lift Coefficient, Flaps Cycling in Waves.
$C_{D_3}$	Average Drag Coefficient, Flaps Cycling in Waves.
$C_{M_3}$	Average Pitching Moment Coefficient, Flaps Cycling in Waves.
$\Delta C_{L_1}$	1/2 Amplitude of $C_{L_1}$ Fluctuation, Flaps Fixed in Waves.
$\Delta C_{D_1}$	1/2 Amplitude of $C_{D_1}$ Fluctuation, Flaps Fixed in Waves.
$\Delta C_{M_1}$	1/2 Amplitude of $C_{M_1}$ Fluctuation, Flaps Fixed in Waves.
$\Delta C_{L_2}$	1/2 Amplitude of $C_{L_2}$ Fluctuation, Flaps Cycling in Smooth Water.
$\Delta C_{D_2}$	1/2 Amplitude of $C_{D_2}$ Fluctuation, Flaps Cycling in Smooth Water.
$\Delta C_{M_2}$	1/2 Amplitude of $C_{M_2}$ Fluctuation, Flaps Cycling in Smooth Water.
$\Delta C_{L_3}$	1/2 Amplitude of $C_{L_3}$ Fluctuation, Flaps Cycling in Waves.

$\Delta C_{D3}$	1/2 Amplitude of $C_{D3}$ Fluctuation, Flaps Cycling in Waves.
$\Delta C_{M3}$	1/2 Amplitude of $C_{M3}$ Fluctuation, Flaps Cycling in Waves.
$\phi_{L1}$	Phase Lag or Lead Angle of Max. $C_{L1}$ to Wave Peak (Radians).
$\phi_{D1}$	Phase (negative lag) or (positive lead) Angle of Max. $C_{D1}$ to Wave Peak (Radians).
$\phi_{M1}$	Phase (negative lag) or (positive lead) Angle of Max. $C_{M1}$ to Wave Peak (Radians).
$\phi_{L2}$	Phase (negative lag) or (positive lead) Angle of Max. $C_{L2}$ to Max. Flap Down (Radians).
$\phi_{D2}$	Phase (negative lag) or (positive lead) Angle of Max. $C_{D2}$ to Max. Flap Down (Radians).
$\phi_{M2}$	Phase (negative lag) or (positive lead) Angle of Max. $C_{M2}$ to Max. Flap Down (Radians).
$\phi_{L3}$	Phase (negative lag) or (positive lead) Angle of Max. $C_{L3}$ to Wave Peak (Radians).
$\phi_{D3}$	Phase (negative lag) or (positive lead) Angle of Max. $C_{D3}$ to Wave Peak (Radians).
$\phi_{M3}$	Phase (negative lag) or (positive lead) Angle of Max. $C_{M3}$ to Wave Peak (Radians).
$\phi_f$	Phase (negative lag) or (positive lead) Angle of Max. Flap Down to Wave Peak (Radians).
$\phi_1$	Instantaneous Phase of Flap to Wave, Referenced to Flap Frequency, and Measured at $t = 0$ .
$t$	Time on Oscillograph Trace from Start of Time History (Seconds).
$\left( \frac{C_L}{A_K} \right)_\nu$	Lift Amplitude Ratio, Flaps Fixed in Waves.
$\left( \frac{C_D}{A_K} \right)_\nu$	Drag Amplitude Ratio, Flaps Fixed in Waves.

$$\left( \frac{C_M}{A_K} \right)_\nu$$

**P. M. Amplitude Ratio, Flaps Fixed in Waves.**

$$\left( \frac{C_L}{\delta_f} \right)_{\omega_f}$$

**Lift Amplitude Ratio, Flaps Cycling in Smooth Water.**

$$\left( \frac{C_D}{\delta_f} \right)_{\omega_f}$$

**Drag Amplitude Ratio, Flaps Cycling in Smooth Water.**

$$\left( \frac{C_M}{\delta_f} \right)_{\omega_f}$$

**P. M. Amplitude Ratio, Flaps Cycling in Smooth Water.**

Table 2. Flap Configuration 1;  $c_f/c = 0.3, b_f/b = 0.6$ ; Tests in Smooth Water, Flaps Oscillating, Static  $h/c = 1.0$

Run No.	$U_\infty$ Ft./Sec.	$\Delta\delta_f$ Rad.	$\omega_f$ Rad./Sec.	$C_{L2}$	$C_{D2}$	$C_{M2}$	$\frac{\Delta C_{L2}}{\Delta\delta_f}$	$\phi_{L2}$ Rad.	$\frac{\Delta C_{D2}}{\Delta\delta_f}$	$\phi_{D2}$ Rad.	$\frac{\Delta C_{M2}}{\Delta\delta_f}$	$\phi_{M2}$ Rad.	$\alpha^\circ$
13128	29.40	.1466	13.95	0.32	0.0282	-0.046	0.955	-.134	0.0689	-0.403	0.259	-0.376	5
13130	28.70	.1449	28.53	0.34	0.0240	-0.056	1.173	-.441	0.0821	-0.523	0.386	-0.688	5
13132	29.85	.1452	33.49	0.34	0.0238	-0.060	1.102	-.478	0.0751	-0.683	0.413	-1.127	5
11359	30.30	.1374	4.99	0.06	0.0030	-0.079	0.873	0	0.0073	0	0.342	0	0
11355	31.25	.1352	3.48	0.07	-0.0005	-0.068	0.814	0	0.0059	+0.487	0.325	0	0
11349	30.08	.1431	8.10	0.08	0.0014	-0.077	0.804	-.081	0.0444	+1.135	0.328	-0.081	0
11326	30.77	.1256	8.32	0.17	0.0039	-0.099	0.796	0	0.0163	+0.666	0.330	+0.374	0
11322	30.77	.1108	3.51	0.16	0.0036	-0.088	0.722	0	0.0226	+0.457	0.289	0	0
11317	31.25	.1248	5.19	0.15	0.0041	-0.109	0.681	-.171	0.0132	-0.748	0.353	-0.239	0

Table 3. Flap Configuration  $2c_f/c = 0.3$ ,  $b_f/b = 0.8$ ; Tests in Smooth Water, Flaps Oscillating, Static  $h/c = 1.6$

Run No.	$U_\infty$ Ft./Sec.	$\Delta\delta_f$ Rad.	$\omega_f$ Rad./Sec.	$C_{L2}$	$C_{D2}$	$C_{M2}$	$\frac{\Delta C_{L2}}{\Delta\delta_f}$	$\phi_{L2}$ Rad.	$\frac{\Delta C_{D2}}{\Delta\delta_f}$	$\phi_{D2}$ Rad.	$\frac{\Delta C_{M2}}{\Delta\delta_f}$	$\phi_{M2}$ Rad.	$\alpha^\circ$
13232	28.10	.1632	17.34	0.30	0.0245	-0.030	1.195	-.259	0.0705	0	0.334	-0.190	5
13234	27.70	.1579	31.92	0.30	0.0245	-0.039	1.470	-.317	0.0766	-.253	0.481	-0.952	5
13236	27.40	.1579	41.59	0.29	0.0240	-0.037	1.654	-.620	0.0735	-.413	0.441	-1.530	5
11270	30.76	.1152	8.67	0.06	-0.0012	-0.084	1.215	0	0.1180	+.607	0.443	0	0
11263	29.20	.1099	3.44	0.07	0.0053	-0.072	1.365	0	0.0746	+.275	0.464	+.0.275	0
11257	31.25	.1326	5.32	0.07	-0.0053	-0.084	1.131	+.186	0.0837	0	0.430	+.0.160	0
11309	31.50	.1396	5.11	0.17	0.0022	-0.109	1.218	+.179	0.0057	+.245	0.358	+.0.204	0
11305	29.85	.1222	3.51	0.17	0.0001	-0.115	0.982	0	0.0074	+.562	0.385	+.0.070	0
11301	29.85	.1396	8.38	0.17	-0.0039	-0.118	0.931	+.335	0.0473	+.503	0.358	+.0.251	0

Table 4. Flap Configuration 3;  $c_f/c = 0.2$ ,  $b_f/b = 0.6$ ; Tests in Smooth Water, Flaps Oscillating, Static  $h/c = 1.0$

Run No.	$U_\infty$ Ft./Sec.	$\Delta\delta_f$ Rad.	$\omega_f$ Rad./Sec.	$C_{L2}$	$C_{D2}$	$C_{M2}$	$\frac{\Delta C_{L2}}{\Delta\delta_f}$	$\phi_{L2}$ Rad.	$\frac{\Delta C_{D2}}{\Delta\delta_f}$	$\phi_{D2}$ Rad.	$\frac{\Delta C_{M2}}{\Delta\delta_f}$	$\phi_{M2}$ Rad.	$\alpha^\circ$
12859	30.30	.1304	20.92	0.310	0.0227	-0.044	0.615	-.383	0.0346	-0.745	0.238	-1.065	5
12861	30.80	.1300	31.60	0.310	0.0227	-0.041	0.692	-.330	0.0338	-0.826	0.269	-1.289	5
12863	31.30	.1287	39.52	0.310	0.0248	-0.036	0.698	-.445	0.0372	-1.134	0.132	-1.417	5
11552	32.26	.0925	8.06	0.035	0.0004	-0.069	0.595	-.201	0.0346	+0.161	0.308	0	0
11544	31.25	.1283	4.78	0.035	0.0014	-0.070	0.429	-.144	0.0207	+0.119	0.218	0	0
11572	31.75	.1475	3.21	0.070	0.0031	-0.097	0.339	0	0.0115	+0.546	0.207	0	0
11568	30.77	.1475	3.22	0.050	0.0023	-0.061	0.203	0	0.0047	+0.371	0.125	0	0
11566	32.79	.1457	4.76	0.080	0.0007	-0.093	0.412	0	0.0045	+0.476	0.209	0	0
11560	32.79	.1492	7.95	0.080	0.0003	-0.092	0.335	-.238	0.0174	+0.318	0.191	0	0

Table 5. Flap Configuration 4;  $c_f/c = 0.2$ ,  $b_f/b = 0.8$ ; Tests in Smooth Water, Flaps Oscillating, Static  $h/c = 1.0$

Run No.	$U_\infty$ Ft./Sec.	$\Delta\delta_f$ Rad.	$\omega_f$ Rad./Sec.	$C_{L2}$	$C_{D2}$	$C_{M2}$	$\frac{\Delta C_{L2}}{\Delta\delta_f}$	$\phi_{L2}$ Rad.	$\frac{\Delta C_{D2}}{\Delta\delta_f}$	$\phi_{D2}$ Rad.	$\frac{\Delta C_{M2}}{\Delta\delta_f}$	$\phi_{M2}$ Rad.	$\alpha^\circ$
12911	33.70	.1300	29.47	0.30	0.0235	-0.053	0.923	-.364	0.0438	-.728	0.331	-0.910	5
12913	34.85	.1309	32.23	0.29	0.0224	-0.048	0.840	-.324	0.0397	-.809	0.336	-0.971	5
12915	35.40	.1300	41.91	0.30	0.0212	-0.040	1.000	-.586	0.0415	-.753	0.215	-1.422	5
11491	31.25	.1012	9.82	0.025	-0.0008	-0.048	0.642	-.393	0.0553	+.196	0.346	-0.393	0
11487	28.99	.0777	3.73	0.020	0.0021	-0.064	0.901	0	0.0766	0	0.541	0	0
11481	29.41	.0899	5.76	0.030	0.0004	-0.049	0.667	-.230	0.0300	+.288	0.445	-0.173	0
11520	32.26	.1230	4.80	0.075	-0.0026	-0.070	0.610	-.239	0.0358	+.240	0.317	-0.384	0
11512	29.41	.1335	8.06	0.070	-0.0069	-0.086	0.524	-.177	0.0479	+.403	0.281	-0.177	0

Table 6. Flap Configuration 1;  $c_f/c = 0.3$ ,  $b_f/b = 0.6$ ; Tests in Regular Head Seas,  
Flaps Fixed, Static  $h/c = 1.0$

Run No.	$\lambda_K$ Ft.	$\alpha$ Deg.	$\delta_f$ Deg.	$U_\infty$ Ft./Sec.	$\nu$ Rad./Sec.	$C_{L1}$	$C_{D1}$	$C_{M1}$	$\frac{\Delta C_{L1}}{A_K} \frac{c}{2}$ Rad.	$\phi_{L1}$ Rad.	$\frac{\Delta C_{D1}}{A_K} \frac{c}{2}$ Rad.	$\phi_{D1}$ Rad.	$\frac{\Delta C_{M1}}{A_K} \frac{c}{2}$ Rad.	$\phi_{M1}$ Rad.
12162	8.04	5	-5	21.74	22.02	.230	.0136	-.00545	.0874	1.277	.00101	-2.33	-.00510	0.793
12164	8.23	5	-5	31.75	29.20	.228	.0157	+.00105	.0674	1.314	.00137	-3.22	-.00758	0.759
12166	7.80	5	0	21.51	22.40	.335	.0201	-.0103	.0840	1.411	.00169	-1.61	-.00758	1.030
12168	7.56	5	0	29.85	29.20	.340	.0201	-.0073	.0750	1.110	.00069	-1.05	-.00308	0.730
12156	7.84	5	5	22.73	23.30	.388	.0273	-.0389	.0734	1.584	.00267	-2.47	-.00162	1.281
12158	7.99	5	5	30.77	29.20	.393	.0285	-.0496	.0476	1.080	.00128	-2.63	-.00696	0.818
12160	8.01	5	10	31.75	29.90	.443	.0397	-.0629	.0504	0.927	.00126	-2.09	-.00642	0.419
12136	7.96	5	10	22.47	22.80	.305	.0474	-.0559	.0806	1.140	.00300	-1.09	-.00372	0.958
12120	8.03	0	10	31.25	29.45	.209	.0232	-.0844	.0816	1.355	.00270	-0.88	-.00836	0.795
12118	8.28	0	10	22.47	22.00	.202	.0262	-.0821	.0958	1.188	.00395	-0.88	-.00491	1.188
12132	7.94	10	10	25.31	25.10	.693	.0793	-.0609	.0870	1.004	.00118	-2.89	-.00706	0.276
12130	7.82	10	10	20.62	21.65	.659	.0803	-.0701	.0820	0.909	.00349	-1.30	-.01010	0.693
12126	8.11	-5	10	30.30	28.50	.062	.0271	-.0890	.0772	1.710	.00901*	-0.14	-.00406	1.197
12124	7.99	-5	10	18.51	19.60	-.080	.0320	-.0893	.1122	1.823	.01016*	-0.39	-.00646	1.333

\* Wild Points.

Table 7. Flap Configuration 2;  $c_f/c = 0.3$ ,  $b/b_f = 0.8$ : Tests in Regular Head Seas,  
Flaps Fixed, Static  $h/c = 1.0$

Run No.	$\lambda_K$ Ft.	$A_K$ Ft.	$\alpha$ Deg.	$\delta_f$ Deg.	$U_\infty$ Ft./Sec.	$\nu$ Rad./Sec.	$C_{L1}$	$C_{D1}$	$CM_1$	$\frac{\Delta C_{L1}}{A_K} \frac{c}{2}$ Rad.	$\frac{\phi_{L1}}{2}$ Rad.	$\frac{\Delta C_{D1}}{A_K} \frac{c}{2}$ Rad.	$\frac{\phi_{D1}}{2}$ Rad.	$\frac{\Delta CM_1}{A_K} \frac{c}{2}$	$\phi_{M1}$ Rad.
12050	8.21	.211	5	10	20.80	20.93	.509	.0369	-.04331	.1024	1.298	.00438	-1.15	-.00548	1.005
12054	8.10	.203	5	10	31.25	29.22	.519	.0472	-.05975	.0518	1.023	.00193	-1.81	-.01030	0.701
12056	8.06	.174	5	-5	20.40	20.93	.244	.0179	-.01089	.1014	1.298	.00103	-1.19	-.00800	0.963
12058	8.20	.190	5	-5	31.70	29.22	.242	.0186	-.01154	.0696	1.110	.00155	-2.40	-.00542	0.643
12062	7.86	.203	5	0	21.70	22.43	.393	.0282	-.04954	.0738	1.480	.00145	-1.41	-.00648	1.077
12064	8.20	.192	5	0	31.70	29.22	.368	.0239	-.01709	.0688	1.052	.00115	+0.76	-.00822	0.438
12066	7.71	.193	5	5	22.20	23.25	.436	.0370	-.05379	.0876	1.349	.00321	-1.33	-.00482	1.023
12068	7.99	.187	5	5	30.80	29.22	.427	.0306	-.05660	.0538	1.227	.00098	-2.40	-.00892	0.877
12108	8.12	.191	-5	10	20.20	20.61	-.075	.0299	-.06988	.1012	1.546	.01024*	-0.80	-.01024	1.113
12100	7.87	.206	-5	10	30.30	29.22	-.074	.0356	-.12230	.0664	1.812	.00742*	-0.88	-.00712	1.344
12046	8.16	.194	0	10	21.70	21.68	.258	.0240	-.08060	.1106	1.019	.00221	-0.65	-.00508	0.759
12048	8.34	.203	0	10	32.30	29.22	.279	.0156	-.04761	.0676	0.935	.00213	-1.05	-.00536	0.643
12102	7.86	.188	10	10	21.70	22.43	.704	.0839	-.03893	.1084	0.942	.00415	-1.79	+.00380*	0.718
12104	8.02	.192	10	10	25.00	24.63	.747	.0951	-.06361	.0976	1.010	.00625	-1.97	-.00728	0.616

\* Wild points.

Table 8. Flap Configuration 3;  $c_f/c = 0.2$ ,  $b_f/b = 0.6$ ; Tests in Regular Head Seas, Flaps Fixed, Static  $h/c = 1.0$

Run No.	$\lambda_K$ Ft.	$\alpha_K$ Ft.	$\alpha$ Deg.	$\delta_f$ Deg.	$U_\infty$ Ft./Sec.	$\nu$ Rad./Sec.	$C_{L1}$	$C_{D1}$	$C_{M1}$	$\frac{\Delta C_{L1}}{A_K} \frac{c}{2}$ Rad.	$\phi_{L1}$ Rad.	$\frac{\Delta C_{D1}}{A_K} \frac{c}{2}$ Rad.	$\phi_{D1}$ Rad.	$\frac{\Delta C_{M1}}{A_K} \frac{c}{2}$ Rad.	$\phi_{M1}$ Rad.
12328	8.21	.166	5	10	18.90	19.52	.380	.0327	-.0608	.0980	1.483	.00273	-1.04	-.00194	0.683
12330	8.28	.191	5	10	32.80	29.64	.413	.0304	-.0477	.0492	1.363	.00089	-2.30	-.00176	0.237
12334	7.99	.175	5	-5	23.00	23.02	.209	.0192	-.0427	.0996	1.312	.00207	-1.65	-.00442	0.736
12336	8.26	.175	5	-5	31.70	29.22	.223	.0164	-.0161	.0724	1.315	.00103	-0.525	-.00316	0.701
12338	8.13	.207	5	0	22.70	22.68	.294	.0235	-.0459	.0628	1.270	.00267	-1.74	-.00582	0.749
12340	8.22	.196	5	0	32.30	29.78	.292	.0219	-.0480	.0634	1.131	.00063	-0.99	-.00628	0.536
12342	7.95	.188	5	5	21.70	22.12	.334	.0284	-.0733	.0826	1.372	.00242	-0.84	-.00354	0.885
12344	8.17	.193	5	5	32.80	30.21	.330	.0233	-.0480	.0498	1.239	.00037	-0.30	-.00062	0.363
12318	7.47	.176	-5	10	21.50	22.28	-.173	.0343	-.0673	.0986	1.872	.01121*	-1.12	-.00872	1.337
12320	8.12	.158	-5	10	31.25	29.78	-.166	.0322	-.0770	.0904	1.965	.01045*	-1.11	-.00526	1.013
12310	7.73	.160	0	10	20.20	21.59	.117	.0155	-.0434	.1026	1.252	.00408	-1.32	-.00780	0.950
12312	8.12	.174	0	10	32.30	29.78	.117	.0148	-.0751	.0766	1.370	.00274	-1.23	-.00034	0.745
12306	8.18	.182	10	10	22.00	22.05	.598	.0611	-.0484	.1102	1.058	.00268	-1.73	-.00352	0.684
12308	8.12	.186	10	10	26.00	24.93	.593	.0603	-.0490	.0878	1.147	.00088	-0.40	-.00468	0.339

\* Wild Points.

Table 9. Flap Configuration 4;  $c_f/c = 0.2$ ,  $b_f/b = 0.8$ ; Tests in Regular Head Seas,  
Flaps Fixed, Static  $h/c = 1.0$

Run No.	$\lambda_K$ Ft.	$A_K$ Ft.	$\alpha$ Deg.	$\delta_f$ Deg.	$U$ Ft./Sec.	$\nu$ Rad./Sec.	$C_{L1}$	$C_{D1}$	$C_{M1}$	$\frac{C_{L1}}{A_K} \frac{c}{2}$ Rad.	$\frac{\phi_{L1}}{2}$ Rad.	$\frac{\Delta C_{D1}}{A_K} \frac{c}{2}$ Rad.	$\frac{\phi_{D1}}{2}$ Rad.	$\frac{\Delta C_{M1}}{A_K} \frac{c}{2}$ Rad.	$\phi_{M1}$ Rad.
12228	8.27	.186	5	10	21.10	20.94	.395	.0299	-.0742	.0802	1.236	.00410	-1.28	-.00103	0.796
12230	8.21	.189	5	10	30.30	27.92	.438	.0344	-.0644	.0414	1.117	.00140	-1.56	-.00426	0
12238	8.29	.187	5	-5	19.40	19.94	.200	.0126	-.0043	.1204	1.476	.00237	-0.59	-.00476	0.638
12240	8.07	.207	5	-5	29.40	27.56	.207	.0138	+.0082	.0696	1.185	.00137	+0.29	-.00492	0.689
12242	8.17	.210	5	0	19.90	20.27	.273	.0192	-.0326	.1014	1.480	.00155	-1.14	+.00362	0.892
12244	8.27	.193	5	0	30.80	28.82	.263	.0181	-.0296	.0614	0.980	.00073	+0.43	-.00480	0.576
12246	8.20	.203	5	5	21.30	21.30	.321	.0240	-.0486	.0890	1.448	.00123	-0.94	-.00098	1.022
12248	8.09	.177	5	5	31.30	29.22	.337	.0238	-.0398	.0658	1.227	.00082	-1.79	-.00288	0.438
12288	8.15	.187	-5	10	20.80	20.94	-.155	.0406	-.1173	.1132	1.654	.01112*	-0.77	-.00672	1.424
12290	7.88	.187	-5	10	30.30	29.36	-.135	.0317	-.0854	.0806	1.585	.00307*	-1.17	-.00478	0.998
12294	8.09	.201	0	10	20.80	21.16	.136	.0206	-.0799	.1156	1.142	.00388	-0.73	-.00338	0.825
12296	8.32	.200	0	10	30.30	28.31	.149	.0168	-.0784	.0760	0.991	.00253	-1.06	-.00311	0.396
12298	8.02	.177	10	10	20.60	21.23	.621	.0684	-.1011	.1060	1.061	.00343	-2.04	-.00380	0.531
12300	8.12	.162	10	10	26.70	25.96	.621	.0677	-.0800	.1122	0.831	.00278	+0.13	-.00880	0.363

\* Wild points.

Table 10. Flap Configuration 1;  $c_f/c = 0.3$ ,  $b_f/b = 0.6$ ; Tests in Following Seas, Flaps Fixed

Run No.	$\lambda_K$ Ft.	$A_K$ Ft.	$H_O$ In.	$\alpha$ Deg.	$\delta_f$ Deg.	$U_\infty$ Ft./Sec.	$\nu$ Rad./Sec.	$C_{L1}$	$CD_1$	$C_{M1}$	$\frac{\Delta C_{L1}}{A_K}$	$\phi_{L1}$ Rad.	$\frac{\Delta CD_1}{A_K}$	$\phi_{D1}$ Rad.	$\frac{\Delta C_{M1}}{A_K}$	$\phi_{M1}$ Rad.
12186	3.58	.079	4	5	10	21.2	29.90	.451	.0442	-.0894	.1098	-2.080	.00570	+0.150	.0045	-3.498
12188	3.53	.058	4			30.3	46.50	.427	.0411	-.0690	.1218	-2.230	.00490	-1.628	.0098	-3.162
12182	5.10	.098	4			21.3	19.92	.427	.0431	-.0868	.0818	-1.733	.00582	-0.040	.0044	-2.092
12184	4.94	.131	4			30.3	32.20	.435	.0424	-.0738	.0750	-1.739	.00262	-0.644	.0012	-3.091
12204	8.40	.198	3			21.7	11.30	.452	.0429	-.0432	.0702	-1.650	.00458	+0.339	.0023	-1.831
12206	8.21	.168	3			30.8	18.63	.435	.0399	-.0461	.0616	-1.435	.00163	+0.317	.0073	-1.900
12200	8.35	.186	5			21.7	11.47	.459	.0405	-.0377	.0642	-1.812	.00384	+0.574	.0049	-1.893
12202	8.31	.188	5			30.8	18.30	.450	.0417	-.0551	.0434	-1.867	.00124	-0.988	.0069	-2.086
12194	8.40	.179	4			21.7	11.37	.424	.0400	-.0720	.0778	-1.819	.00428	+0.728	.0067	-1.944
12196	8.26	.195	4	5	10	30.8	18.45	.429	.0392	-.0555	.0506	-1.476	.00260	+0.793	.0037	-1.919

Table 11. Flap Configuration 2;  $c_f/c = 0.3$ ,  $b_f/b = 0.8$ ; Tests in Following Seas, Flaps Fixed

Run No.	$\lambda_K$ Ft.	$A_K$ Ft.	$H_O$ In.	$\alpha$ Deg.	$\delta_f$ Deg.	$U_\infty$ Ft./Sec.	$\nu$ Rad./Sec.	$C_{L1}$	$C_{D1}$	$C_{M1}$	$\frac{\Delta C_{L1}}{A_K}$	$\phi_{L1}$ Rad.	$\frac{\Delta C_{D1}}{A_K}$	$\phi_{D1}$ Rad.	$\frac{\Delta C_{M1}}{A_K}$	$\phi_{M1}$ Rad.
12086	3.63	.058	4	5	10	22.5	31.42	.507	.0481	-.0533	.1078	-2.199	.00446	-0.566	.0078	-3.236
12088	3.76	.065	4			28.6	40.53	.490	.0482	-.0587	.1126	-1.945	.00426	-1.783	.0107	-2.553
12090	5.45	.124	4			21.4	18.47	.473	.0512	-.0767	.0860	-1.718	.00494	+0.277	.0090	-2.013
12092	5.04	.091	4			30.2	31.42	.514	.0482	-.0455	.0876	-1.917	.00540	+0.314	.0086	-2.514
12080	8.07	.190	3			20.4	10.81	.474	.0482	-.0599	.0652	-1.924	.00592	+0.627	.0090	-2.011
12082	8.27	.175	3			27.9	16.53	.491	.0436	-.0473	.0430	-1.537	.00472	+0.661	.0079	-1.769
12076	8.17	.223	5			18.4	8.99	.505	.0523	-.0602	.0776	-2.104	.00478	+1.025	.0039	-2.122
12078	7.84	.203	5			29.5	18.47	.522	.0473	-.0481	.0436	-2.143	.00284	+1.108	.0043	-2.327
12072	8.27	.180	4			19.6	9.99	.462	.0473	-.0647	.0950	-1.858	.00522	+0.999	.0080	-1.998
12074	8.04	.193	4	5	10	27.1	16.09	.497	.0481	-.0551	.0614	-1.979	.00372	+1.078	.0051	-2.156

Table 12. Flap Configuration 3;  $c_f/c = 0.2$ ,  $b_f/b = 0.6$ ;  
Tests in Following Seas, Flaps Fixed

Run No.	$\lambda_K$ Ft.	$A_K$ Ft.	$H_o$ In.	$\alpha$ Deg.	$\delta_f$ Deg.	$U_\infty$ Ft./Sec.	$\nu$ Rad./Sec.	$C_{L1}$	$C_{D1}$	$C_{M1}$	$\frac{\Delta C_{L1}}{A_K} \frac{c}{2}$ Rad.	$\phi_{L1}$ Rad.	$\frac{\Delta C_{D1}}{A_K} \frac{c}{2}$ Rad.	$\phi_{D1}$ Rad.	$\frac{\Delta C_{M1}}{A_K} \frac{c}{2}$ Rad.	$\phi_{M1}$ Rad.
12356	3.53	.149	4	5	10	21.0	29.78	.399	.0373	-.0711	.0534	-2.025	.00280	-0.893	.0031	-2.114
12358	3.55	.054	4			30.4	46.20	.387	.0321	-.0624	.1124	-1.848	.00956	-0.924	.0078	-3.142
12360	5.00	.133	4			21.4	20.60	.380	.0321	-.0793	.0850	-1.813	.00352	+1.030	.0022	-2.802
12364	5.05	.106	4			30.7	31.89	.376	.0298	-.0545	.0662	-1.818	.00524	-0.797	.0073	-2.041
12352	8.53	.158	4			21.3	10.83	.387	.0345	-.0799	.0684	-1.516	.00468	+0.237	.0026	-1.949
12354	8.45	.159	4			30.4	17.70	.357	.0308	-.0612	.0608	-1.947	.00298	+0.531	.0038	-2.425
12370	8.11	.187	3			21.25	11.44	.368	.0324	-.0761	.0782	-1.659	.00426	+0.641	.0038	-2.002
12372	8.17	.167	3			30.5	18.48	.349	.0311	-.0524	.0688	-1.552	.00336	+0.869	.0106	-1.903
12376	8.25	.183	5			21.4	11.36	.397	.0400	-.1163	.0838	-2.124	.00276	+1.216	.0059	-2.272
12378	7.85	.158	5	5	10	30.5	19.33	.419	.0365	-.0780	.0622	-1.991	.00194	+0.251	.0048	-2.204

Table 13. Flap Configuration 4;  $c_f/c = 0.2$ ,  $b_f/b = 0.8$ ;  
Tests in Following Seas, Flaps Fixed

Run No.	$\lambda_K$ Ft.	$A_K$ Ft.	$H_K^0$ In.	$\alpha$ Deg.	$\delta_c$ Deg.	$U_\infty$ Ft./Sec.	$\nu$ Rad./Sec.	$CL_1$	$CD_1$	$CM_1$	$\frac{\Delta CL_1}{A_K} \frac{c}{2}$ Rad.	$\frac{\Delta CD_1}{A_K} \frac{c}{2}$ Rad.	$\phi_{D_1}$ Rad.	$\frac{\Delta CM_1}{A_K} \frac{c}{2}$ Rad.	$\phi_{M_1}$ Rad.
12274	3.75	.104	4	5	10	21.1	27.92	.369	.0388	-.0828	.0658	.00364	-0.670	.0063	-3.239
12278	3.53	.101	4			30.4	46.54	.399	.0344	-.0657	.0850	.00264	-1.629	.0070	-2.327
12280	5.62	.122	4			21.0	17.46	.395	.0355	-.0688	.0784	.00146	+0.890	.0060	-1.658
12282	5.51	.132	4			30.2	28.43	.405	.0354	-.0626	.0640	.00452	+0.284	.0053	-1.535
12252	8.20	.173	4			21.4	11.55	.384	.0383	-.0919	.0856	.00344	+1.016	.0049	-1.986
12254	8.03	.158	4			30.4	18.76	.400	.0347	-.0703	.0636	.00294	0	.0031	-1.932
12264	8.37	.167	3			21.3	11.14	.392	.0395	-.0869	.0774	.00294	+0.334	.0005	-1.827
12266	8.25	.170	3			30.6	18.37	.383	.0340	-.0627	.0572	.00412	+0.184	.0041	-2.094
12256	8.40	.175	5			21.4	11.22	.420	.0400	-.0832	.0678	.00328	+0.449	.0049	-2.435
12258	8.12	.199	5	5	10	30.8	18.81	.413	.0368	+.0733	.0568	.00210	+0.564	.0076	-2.389

# 1

Table 14. Flap Configuration 1;  $c_f/c = 0.3$ ,  $b$  and Following Seas, Flaps Oscillati

Run No.	Head Following Sea	$\phi_f$ Rads.	$C_{L_{Max.}}$	$C_{L_{Min.}}$	$\Delta C_{L_3}$	$C_{L_3}$	$\phi_{L_3}$ Rads.	$C_{D_{Max.}}$	$C_{D_{Min.}}$	$\Delta C_{D_3}$	$C_{D_3}$	$\phi_{D_3}$ Rads.	$C_M$
13154	Head	$-\pi/2$	.52	.20	.16	.36	-2.36	.0400	.0131	.0134	.0266	-2.78	-.
		$-\pi$	.58	.15	.22	.36	+2.24	.0386	.0156	.0115	.0271	+1.96	-.
		$+\pi/2$	.60	.10	.25	.35	+ .883	.0371	.0177	.0097	.0274	+ .748	-.
13157	Head	$+\pi$	.49	.18	.16	.33	+2.375	.0366	.0134	.0116	.0250	-2.085	-.
		$+\pi/2$	.57	.06	.26	.31	+1.41	.0350	.0155	.0098	.0232	+1.09	-.
13160	Head	$-\pi$	.44	.19	.13	.32	+2.50	.0410	.0109	.0150	.0260	+3.06	-.
		$-\pi/2$	.43	.27	.08	.35	-1.06	.0433	.0146	.0144	.0289	-1.90	-.
13167	Following	$+\pi/2$	.35	.27	.04	.31	-2.52	.0412	.0197	.0107	.0305	+2.68	-.
		$+\pi$	.51	.09	.21	.30	-1.94	.0437	.0215	.0111	.0326	-2.90	-.
13182	Following	$-\pi$	.48	.07	.21	.28	-2.07	.0410	.0216	.0097	.0313	-2.79	-.
		$-\pi/2$	.55	.10	.23	.32	-1.89	.0417	.0216	.0101	.0316	+1.32	-.
13191	Following	$-\pi$	.50	.16	.17	.33	+1.23	.0418	.0207	.0105	.0313	+1.04	-.
		$+\pi/2$	.53	.20	.16	.36	+1.23	.0428	.0204	.0112	.0316	+2.11	-.
		$-\pi/2$	.60	.17	.21	.38	-1.70	.0435	.0200	.0117	.0318	-1.88	-.



$\alpha = 0.3$ ,  $b_f/b = 0.6$ ; Tests in Regular Head  
Oscillating; Static  $h/c = 1.0$ ,  $\alpha = 5^\circ$

$D_3$ ads.	$C_{M_{Max.}}$	$C_{M_{Min.}}$	$\Delta C_{M_3}$	$C_{M_3}$	$\phi M_3$ Rads.	$U_\infty$ Ft./Sec.	$\nu$ Rads./Sec.	$\omega_f$ Rads./Sec.	$\lambda_K$ Ft.	$A_K$ Ft.	$\Delta \delta_f$ Rads.
2.78	-.061	-.005	-.028	-.033	-3.14	23.80	49.4	46.1	3.65	.0628	.148
1.96	-.063	-.003	-.030	-.033	+1.354	23.90					
.748	-.069	-.005	-.032	-.037	0	24.40					
2.085	-.083	-.028	-.027	-.056	+2.375	22.10	21.5	20.2	8.32	.157	.149
1.09	-.101	-.007	-.047	-.054	+1.15	21.70					
1.06	-.097	-.026	-.035	-.062	+2.68	23.30	22.1	23.2	8.53	.163	.149
1.90	-.114	-.021	-.046	-.068	-1.193	23.31					
2.68	-.104	-.009	-.047	-.057	-2.57	20.83	10.45	12.17	8.58	.157	.149
2.90	-.080	-.021	-.029	-.051	-1.965						
2.79	-.090	-.019	-.035	-.055	+2.78	20.80	10.57	11.57	8.46	.154	.148
.32	-.081	-.016	-.032	-.049	-2.06						
1.04	-.114	-.012	-.051	-.063	+0.44	21.57	29.6	39.5	3.66	.072	.145
2.11	-.116	-.005	-.055	-.061	+0.44						
.88	-.100	-.006	-.047	-.053	-2.38						

# 1

Table 15. Flap Configuration 2;  $c_f/c = 0.3$ ,  $b_f/b =$   
and Following Seas, Flaps Oscillating;  $\delta$

Run No.	Head or Following Sea	$\phi_f$ Rads.	$C_{L_{Max.}}$	$C_{L_{Min.}}$	$\Delta C_{L_3}$	$C_{L_3}$	$\phi_{L_3}$ Rads.	$C_{D_{Max.}}$	$C_{D_{Min.}}$	$\Delta C_{D_3}$	$C_{D_3}$	$\phi_{D_3}$ Rads.	$C_{M_{M_2}}$
13240	Head	$-\pi/2$	.55	.04	.25	.30	-1.98	.0372	.0131	.0120	.0252	-2.125	-.105
13248	Head	$+\pi$	.59	0	.29	.30	+2.36	.0385	.0136	.0125	.0260	+2.325	-.106
		$+\pi/2$	.63	-.05	.34	.29	+ .83	.0400	.0142	.0129	.0271	+ .472	-.117
13256	Head	$-\pi/2$	.39	.17	.11	.28	-1.13	.0376	.0136	.0120	.0256	-1.775	-.124
13260	Head	$+\pi$	.48	.02	.23	.25	+2.74	.0340	.0147	.0096	.0244	+2.54	-.126
		$+\pi/2$	.58	-.05	.32	.26	+1.33	.0365	.0131	.0117	.0248	+ .942	-.136
13284	Following	$-\pi/2$	.51	.01	.25	.26	-1.79	.0357	.0194	.0082	.0275	-1.211	-.093
		$-\pi$	.49	.02	.24	.25	-2.07	.0401	.0204	.0098	.0303	+2.46	-.091
13302	Following	$+\pi/2$	.39	.18	.10	.29	+1.63	.0441	.0178	.0132	.0309	+1.315	-.119
13308	Following	$-\pi/2$	.58	-.01	.29	.29	-1.79	.0311	.0131	.0090	.0221	-1.10	-.137
13310	Following	$-\pi$	.57	.04	.27	.30	+1.87	.0375	.0136	.0119	.0256	+2.80	-.138
		$+\pi/2$	.52	.07	.22	.30	+1.23	.0396	.0143	.0126	.0270	+ .868	-.143



= 0.3,  $b_f/b = 0.8$ ; Tests in Regular Head  
Oscillating; Static  $h/c = 1.0$ ,  $\alpha = 5^\circ$

$\phi_{D_3}$ Rads.	$C_{M_{Max.}}$	$C_{M_{Min.}}$	$\Delta C_{M_3}$	$C_{M_3}$	$\phi_{M_3}$ Rads.	$U_\infty$ Ft. /Sec.	$\nu$ Rads. /Sec.	$\omega_f$ Rads. /Sec.	$\lambda_K$ Ft.	$A_K$ Ft.	$\Delta \delta_f$ Rads.
-2.125	-.105	-.001	-.052	-.053	-3.18	23.12	46.9	45.2	3.67	.066	.160
+2.325	-.106	-.011	-.047	-.059	+1.56	22.73	46.5	44.8	3.66	.063	.159
+ .472	-.117	-.003	-.057	-.060	-.28						
-1.775	-.124	+.012	-.068	-.056	-1.80	22.64	22.4	27.2	8.16	.165	.160
+2.54	-.126	-.081	-.023	-.103	+2.85	22.02	22.1	23.5	8.11	.167	.160
+ .942	-.136	-.010	-.063	-.073	+1.16						
-1.214	-.093	-.006	-.043	-.050	-1.74	21.38	11.31	10.46	8.27	.166	.162
+2.46	-.091	-.002	-.045	-.046	-2.67						
+1.315	-.119	-.009	-.055	-.064	+1.47	21.74	11.73	12.55	8.15	.140	.163
-1.10	-.137	+.012	-.075	-.062	-2.44	21.83	30.0	35.8	3.67	.075	.158
+2.80	-.138	+.025	-.082	-.056	+1.24	21.33	30.3	34.9	3.54	.068	.158
+ .868	-.143	+.021	-.082	-.061	+ .54						

# 1

Table 16. Flap Configuration 3;  $c_f/c = 0.2$ ;  $b_f/b =$   
and Following Seas, Flaps Oscillating; :

Run No.	Head or Following Sea	$\phi_f$ Rads.	$C_{LMax.}$	$C_{LMin.}$	$\Delta C_{L3}$	$C_{L3}$	$\phi_{L3}$ Rads.	$C_{DMax.}$	$C_{DMin.}$	$\Delta C_{D3}$	$C_{D3}$	$\phi_{D3}$ Rads.	$C_{MMax.}$
12702	Head	$-\pi$	.35	.22	.06	.29	+1.955	.0282	.0171	.0056	.0226	+2.89	-.031
12704	Head	$-\pi/2$	.39	.19	.10	.29	+ .116	.0261	.0172	.0044	.0217	-1.40	-.068
12706	Head	$+\pi/2$	.44	.17	.14	.30	+1.529	.0287	.0162	.0063	.0224	+1.39	-.044
12760	Head	$+\pi/2$	.47	.14	.17	.30	+ .911	.0267	.0181	.0043	.0224	+1.57	-.058
12762	Head	$-\pi/2$	.39	.21	.09	.30	+2.710	.0264	.0132	.0066	.0198	-2.365	-.047
		$-\pi$	.48	.16	.16	.32	+1.657	.0323	.0211	.0056	.0267	+2.02	-.040
12778	Following	$+\pi/2$	.30	.26	.02	.28	+2.074	.0301	.0167	.0067	.0234	+ .415	-.067
12784	Following	$+\pi$	.39	.17	.11	.28	-2.154	.0254	.0199	.0028	.0226	+1.632	-.065
12824	Following	$+\pi/2$	.35	.24	.05	.30	- .347	.0318	.0175	.0072	.0246	+ .316	-.073
12849	Following	$-\pi/2$	.42	.16	.13	.29	-2.079	.0276	.0156	.0060	.0216	-2.44	-.060
		$-\pi$	.41	.17	.12	.29	+3.095	.0263	.0194	.0035	.0228	+2.41	-.066
		$+\pi/2$	.37	.24	.07	.30	+1.032	.0253	.0206	.0024	.0229	- .698	-.061



$\beta = 0.2$ ;  $b_f/b = 0.6$ ; Tests in Regular Head  
 s Oscillating; Static  $h/c = 1.0$ ;  $\alpha = 5^\circ$

$D_3$ Rads.	$C_{M_{Max.}}$	$C_{M_{Min.}}$	$\Delta C_{M3}$	$C_{M3}$	$\phi_{M3}$ Rads.	$U_\infty$ Ft./Sec.	$\nu$ Rads./Sec.	$\omega_f$ Rads./Sec.	$\lambda_K$ Ft.	$A_K$ Ft.	$\Delta \delta_f$ Rads.
2.89	-.031	-.014	-.009	-.022	+2.066	30.77	28.4	29.75	8.24	.157	.169
1.40	-.068	+.013	-.040	-.028	-.781	30.46	26.7	29.9	8.74	.150	.167
1.39	-.044	+.003	-.024	-.020	+1.119	29.26	27.65	29.6	8.11	.164	.169
1.57	-.058	-.015	-.022	-.036	-.288	22.90	46.8	47.2	3.65	.065	.127
2.365	-.047	-.032	-.007	-.040	-1.892	21.71	43.3	47.5	3.79	.064	.124
2.02	-.040	-.020	-.010	-.030	+.741						
.415	-.067	-.016	-.025	-.042	+1.566	30.48	18.3	18.95	8.25	.158	.127
1.632	-.065	-.013	-.026	-.039	-2.428	30.61	18.85	19.0	8.07	.150	.128
.316	-.073	-.025	-.024	-.049	+.539	30.50	19.0	20.7	7.99	.161	.124
2.44	-.060	-.015	-.022	-.038	-2.800	30.37	43.3	42.0	3.77	.066	.126
2.41	-.066	-.019	-.024	-.042	+1.705						
.698	-.061	-.020	-.021	-.040	0						

# 1

Table 17. Flap Configuration 4;  $c_f/c = 0.2$ ,  $b_f = 0.8$   
and Following Seas, Flaps Oscillating; Sta

Run No.	Head or Following Sea	$\phi_f$ Rads.	$C_{LMax.}$	$C_{LMin.}$	$\Delta C_{L3}$	$C_{L3}$	$\phi_{L3}$ Rads.	$C_{DMax.}$	$C_{DMin.}$	$\Delta C_{D3}$	$C_{D3}$	$\phi_{D3}$ Rads.	$C_{MMax.}$
2996	Head	$+\pi/2$	.47	.13	.17	.30	+1.174	.0268	.0198	.0035	.0233	+ .328	-.088
2999	Head	$-\pi/2$	.36	.26	.05	.31	-1.011	.0277	.0189	.0044	.0233	-2.01	-.072
3002	Head	$-\pi$	.41	.17	.12	.29	+1.708	.0264	.0132	.0066	.0198	+2.28	-.069
3012	Head	$+\pi/2$	.50	.13	.18	.32	+1.024	.0269	.0157	.0056	.0213	+ .752	-.058
		$+\pi$	.47	.14	.17	.30	+1.714	.0291	.0146	.0073	.0218	+1.99	-.066
		$-\pi/2$	.42	.21	.11	.31	-2.405	.0263	.0160	.0052	.0211	-3.47	-.062
3005	Head	$-\pi/2$	.39	.24	.07	.32	-2.173	.0286	.0203	.0042	.0244	-3.46	-.065
3008		$+\pi/2$	.50	.11	.20	.30	+ .879	.0341	.0208	.0066	.0275	+ .72	-.068
2965	Following	$-\pi/2$	.45	.15	.15	.30	-1.294	.0292	.0199	.0046	.0246	-2.68	-.072
2967	Following	$-\pi$	.39	.17	.11	.28	-2.261	.0317	.0206	.0055	.0262	+1.57	-.082
2990	Following	$+\pi/2$	.41	.22	.10	.31	- .320	.0359	.0175	.0092	.0267	+ .274	-.033
2947	Following	$-\pi/2$	.45	.13	.16	.29	-2.003	.0322	.0188	.0067	.0255	-2.295	-.073
		$+\pi$	.39	.18	.10	.29	+2.493	.0292	.0196	.0048	.0244	+1.385	-.081
2952	Following	$+\pi/2$	.41	.19	.11	.30	+ .553	.0333	.0191	.0071	.0262	+ .128	-.073



$b_f = 0.2$ ,  $b_f = 0.8$ ; Tests in Regular Head  
 Oscillating; Static  $h/c = 1.0$ ,  $\alpha = 5^\circ$

$\phi_{D_3}$ Rads.	$C_{M_{Max.}}$	$C_{M_{Min.}}$	$\Delta C_{M_3}$	$C_{M_3}$	$\phi_{M_3}$ Rads.	$U_\infty$ Ft./Sec.	$\nu$ Rads./Sec.	$\omega_f$ Rads./Sec.	$\lambda_K$ Ft.	$A_K$ Ft.	$\Delta \delta_f$ Rads.
+ .328	-.088	0	-.044	-.044	+ .411	34.20	31.4	32.2	8.41	.173	.124
-2.01	-.072	-.017	-.027	-.045	-2.173	34.50	30.2	33.4	8.55	.173	.120
+2.28	-.069	-.010	-.029	-.040	+1.130	32.60	28.9	34.1	8.53	.176	.119
+ .752	-.058	-.038	-.010	-.048	+ .578	20.93	43.3	49.0	3.66	.068	.120
+1.99	-.066	-.048	-.009	-.057	+1.218						
-3.47	-.062	-.054	-.004	-.058	+2.229						
-3.46	-.065	-.040	-.012	-.053	-3.303	21.90	45.2	46.9	3.64	.064	.120
- .72	-.068	-.032	-.018	-.050	+ .259	22.70	48.0	46.2	3.53	.073	.119
-2.68	-.072	-.012	-.030	-.042	-1.595	30.60	17.6	17.4	8.53	.161	.127
-1.57	-.082	-.012	-.035	-.047	+2.744	31.30	18.3	20.3	8.49	.160	.124
- .274	-.033	-.005	-.014	-.019	.553	29.80	17.7	13.6	8.27	.163	.124
-2.295	-.073	-.010	-.031	-.042	-3.184	29.65	39.0	39.2	4.04	.065	.128
-1.385	-.081	+ .001	-.041	-.040	+1.532						
- .128	-.073	-.021	-.026	-.047	0	29.10	44.5	39.7	3.51	.065	.124

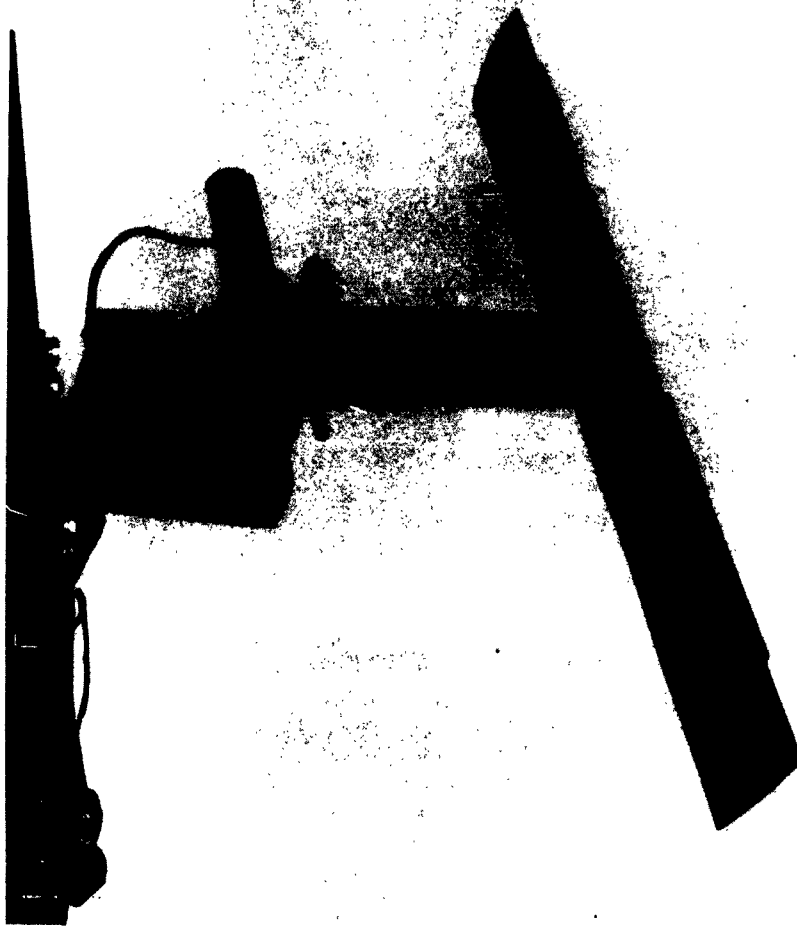


Figure 1. MODEL WITH  $c_f/c = 0.2$ ,  $b_f/b = 0.6$ , FLAPS INSTALLED

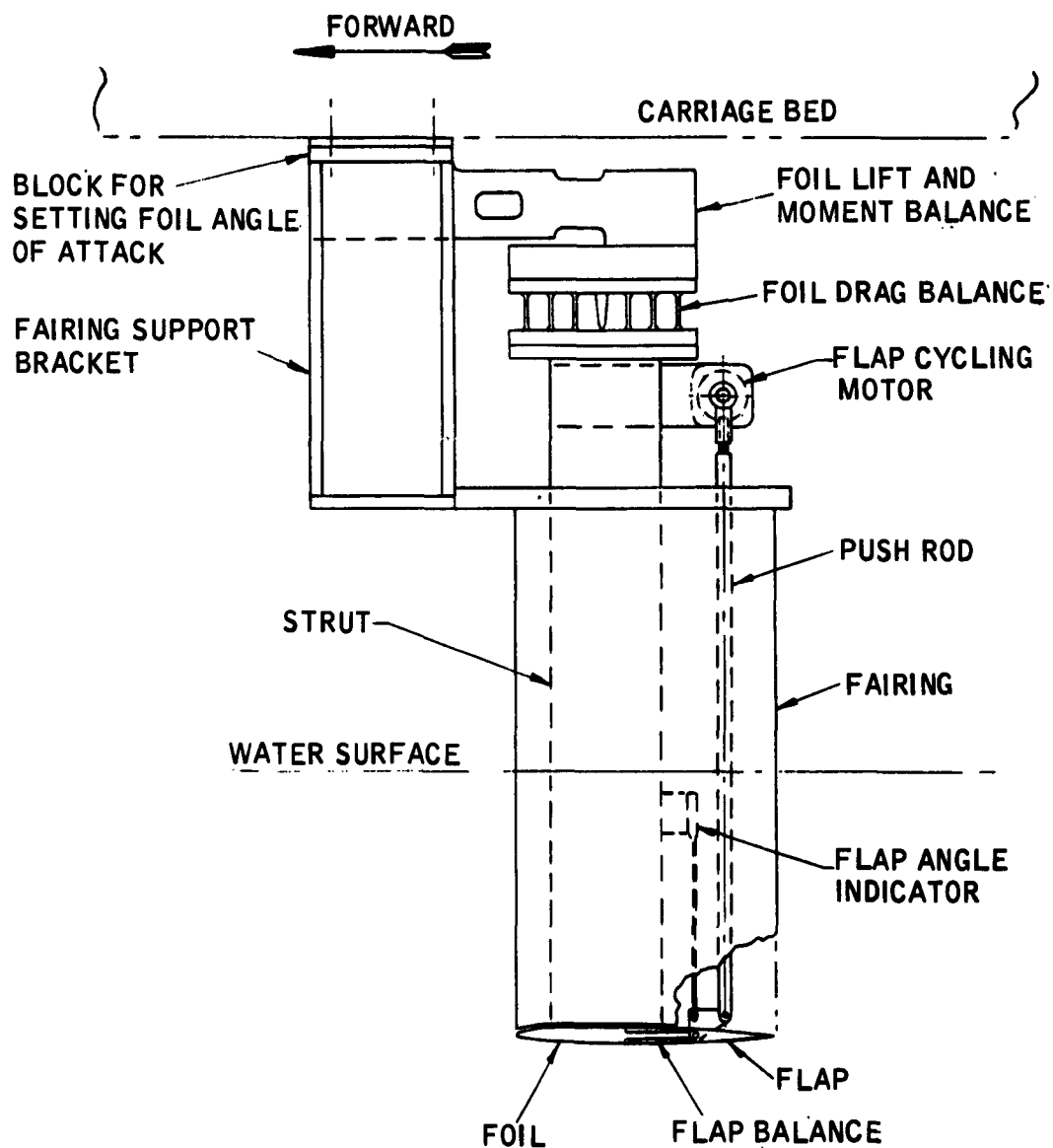


Figure 2. Model and Balances

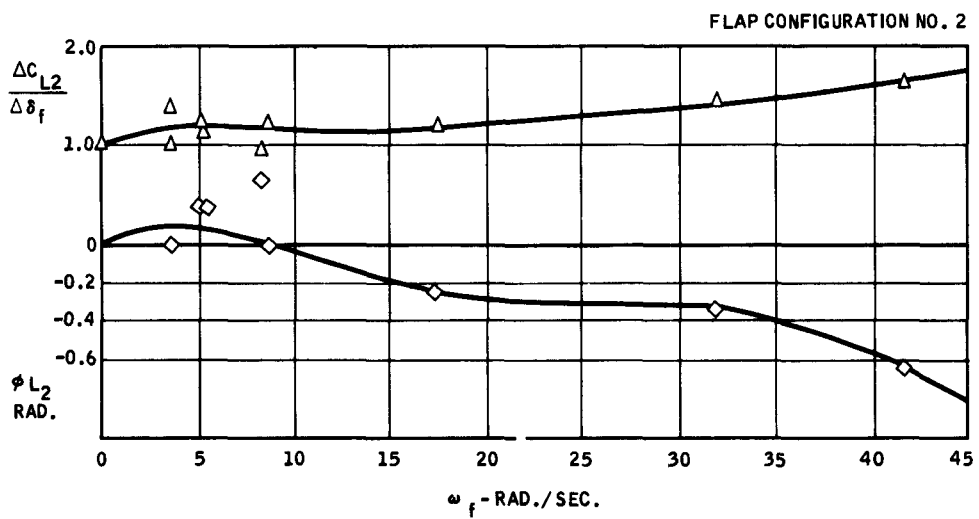
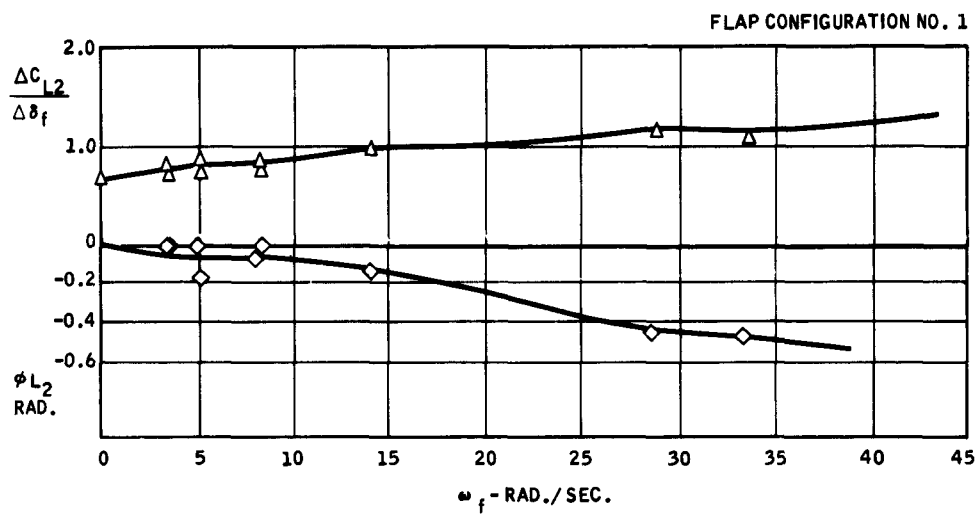
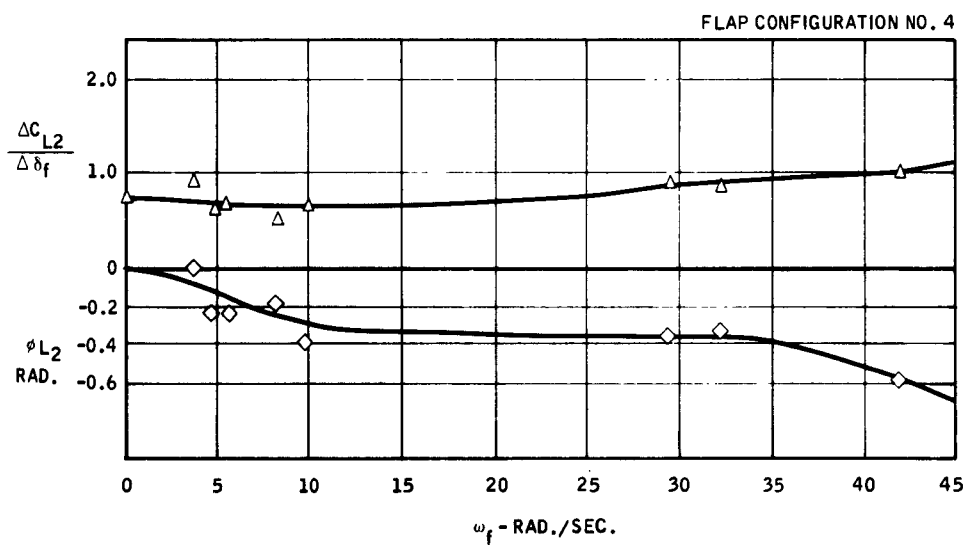
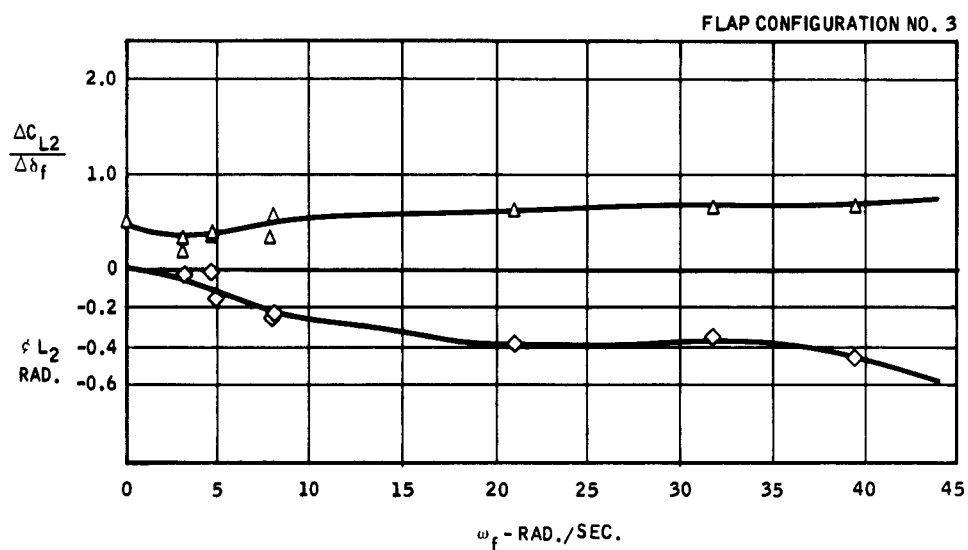


Figure 3. Lift Frequency Response,  
Flaps Oscillating, Smooth Water



**Figure 4. Lift Frequency Response,  
Flaps Oscillating, Smooth Water**

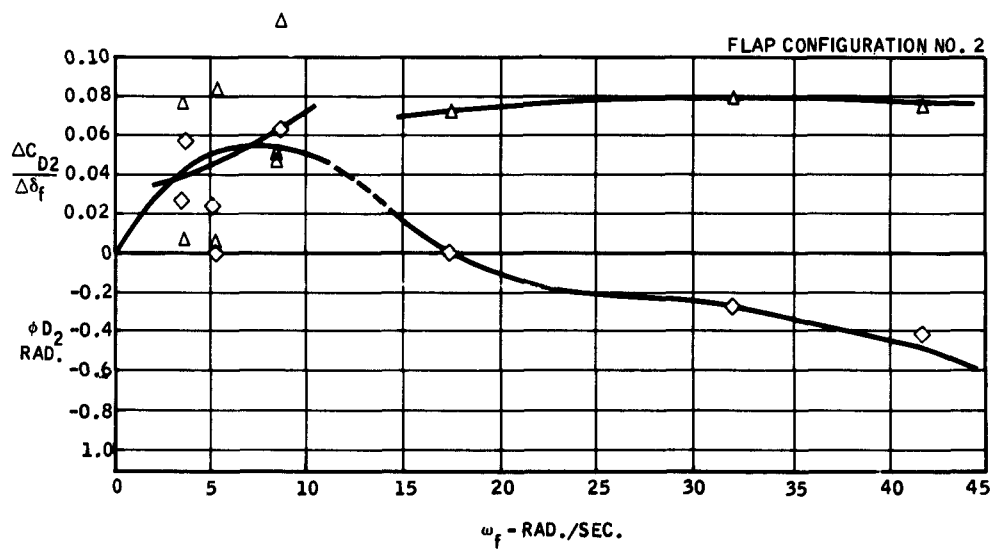
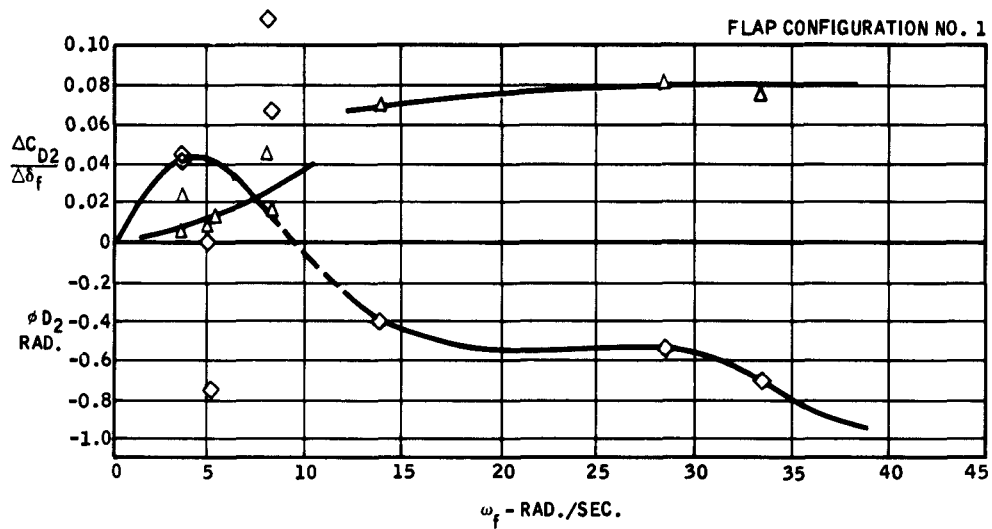


Figure 5. Drag Frequency Response,  
Flaps Oscillating, Smooth Water

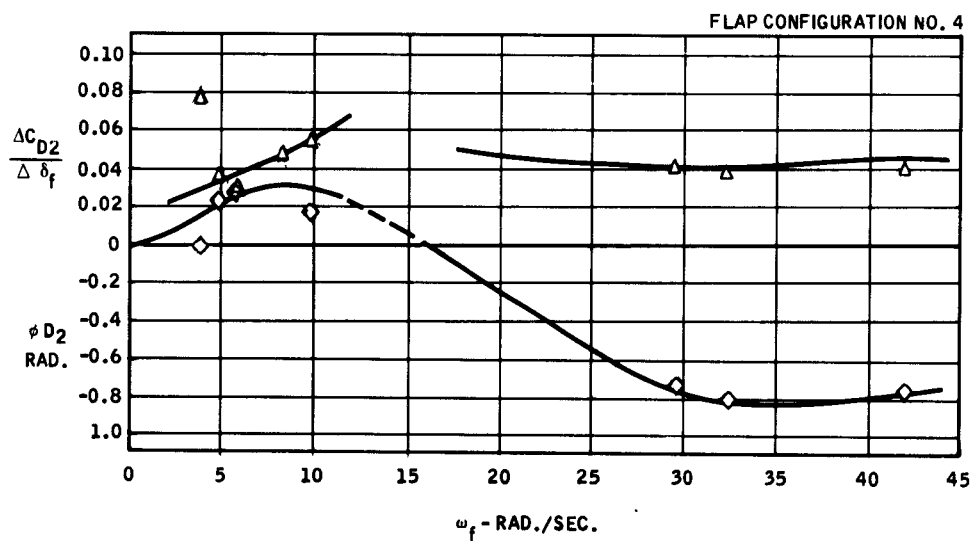
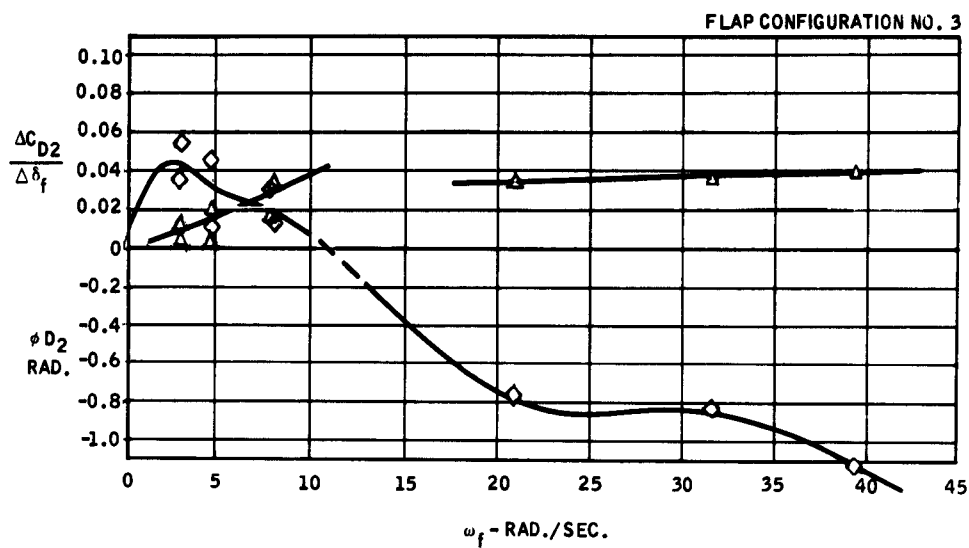


Figure 6. Drag Frequency Response,  
Flaps Oscillating, Smooth Water

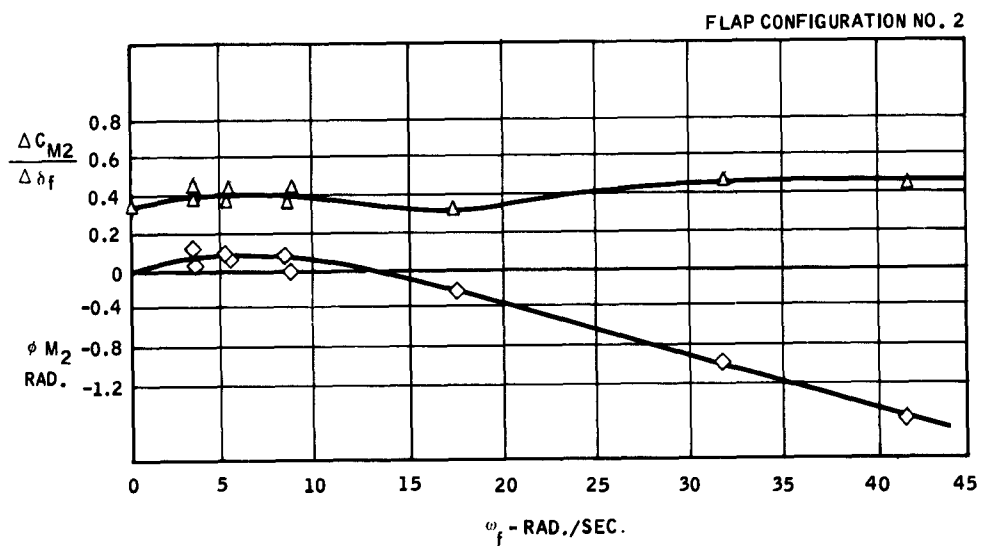
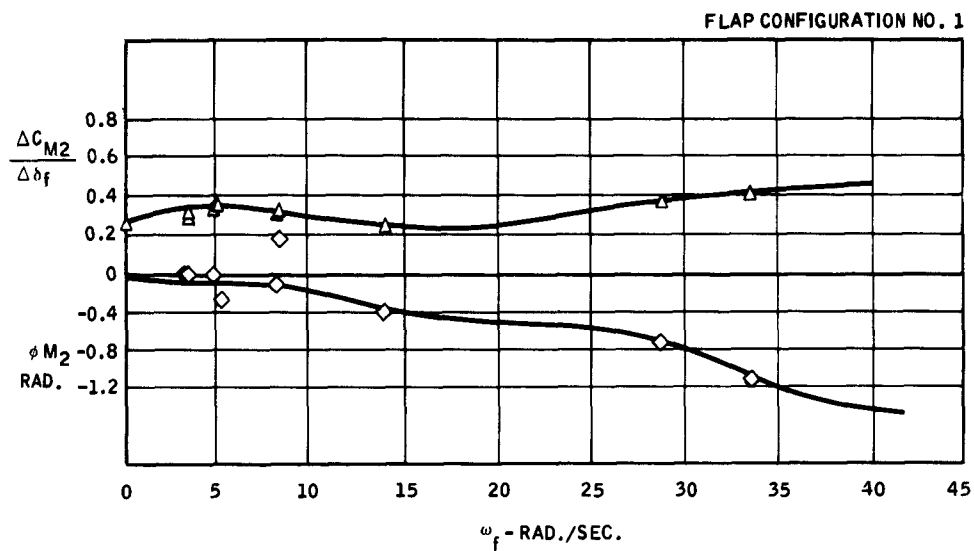


Figure 7. Pitching Moment Frequency Response,  
Flaps Oscillating, Smooth Water

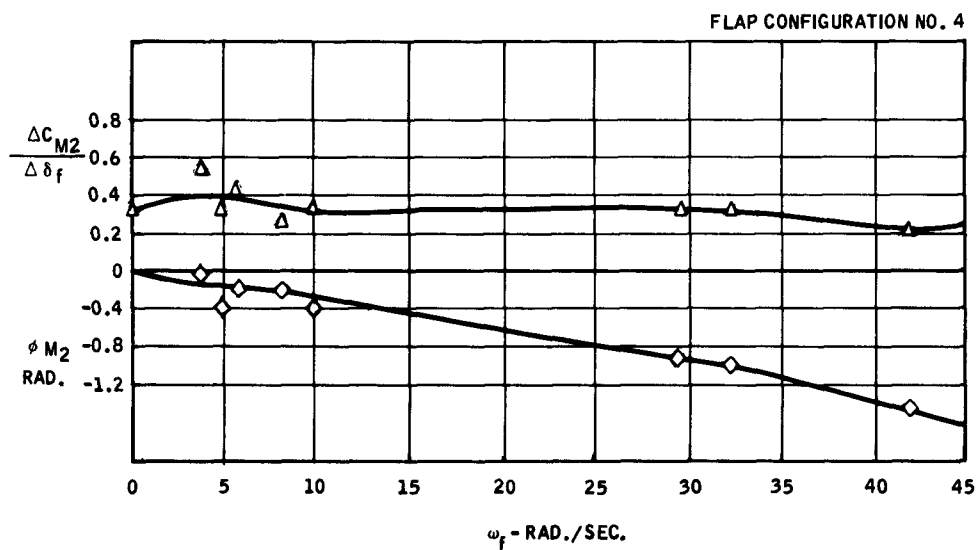
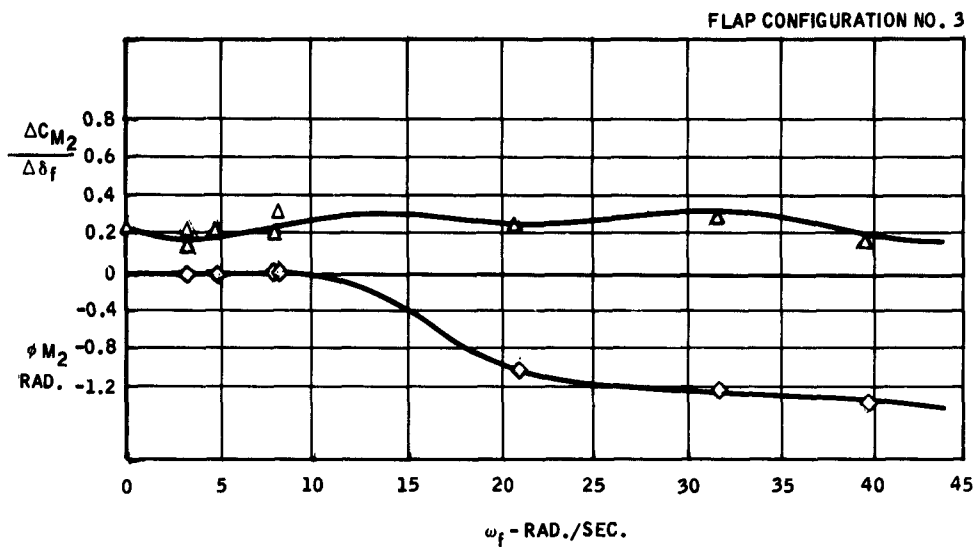


Figure 8. Pitching Moment Frequency Response,  
Flaps Oscillating, Smooth Water

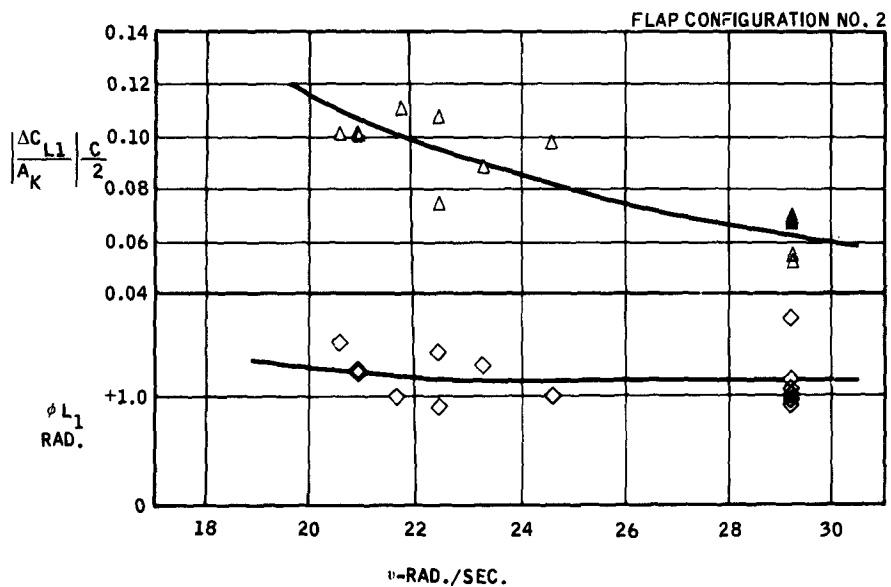
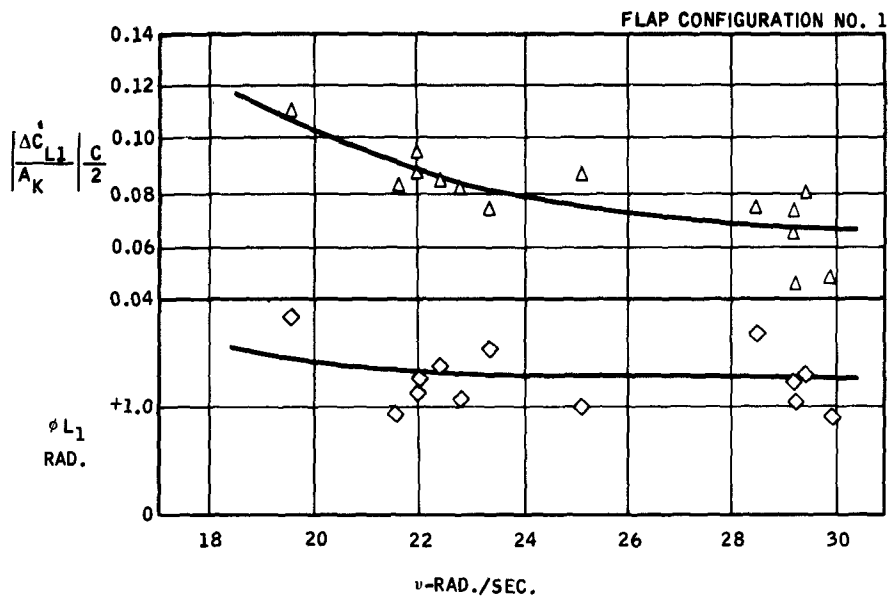
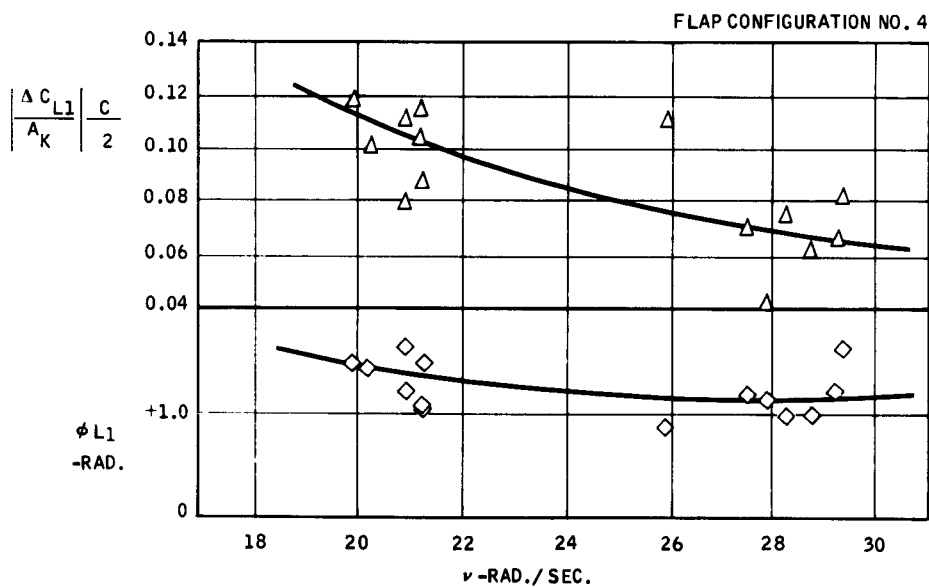
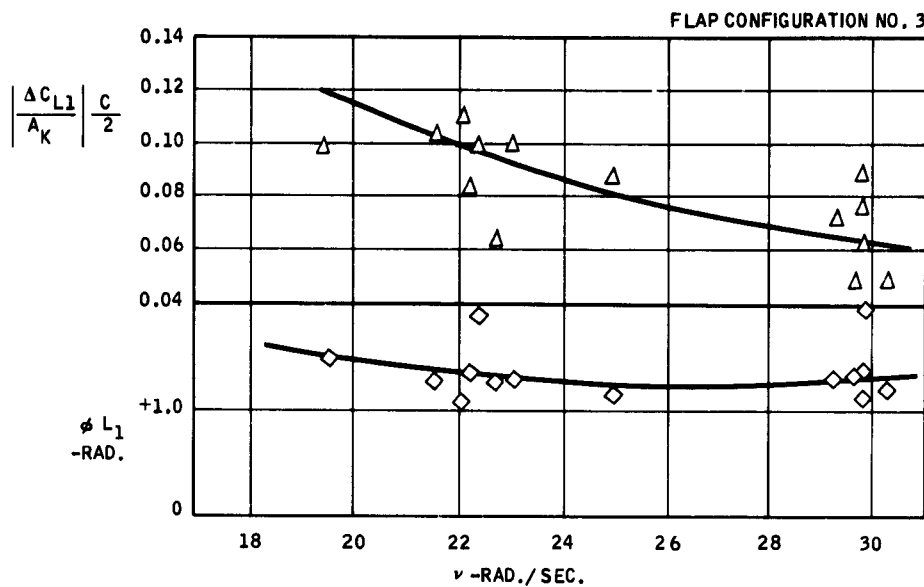


Figure 9. Lift Frequency Response, Head Seas, Flaps Fixed



**Figure 10. Lift Frequency Response, Head Seas, Flaps Fixed**

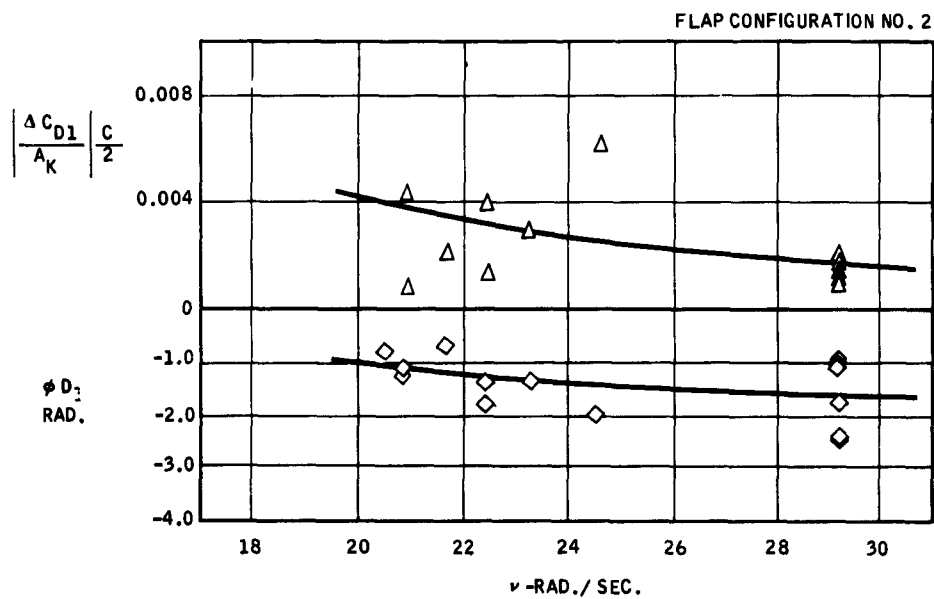
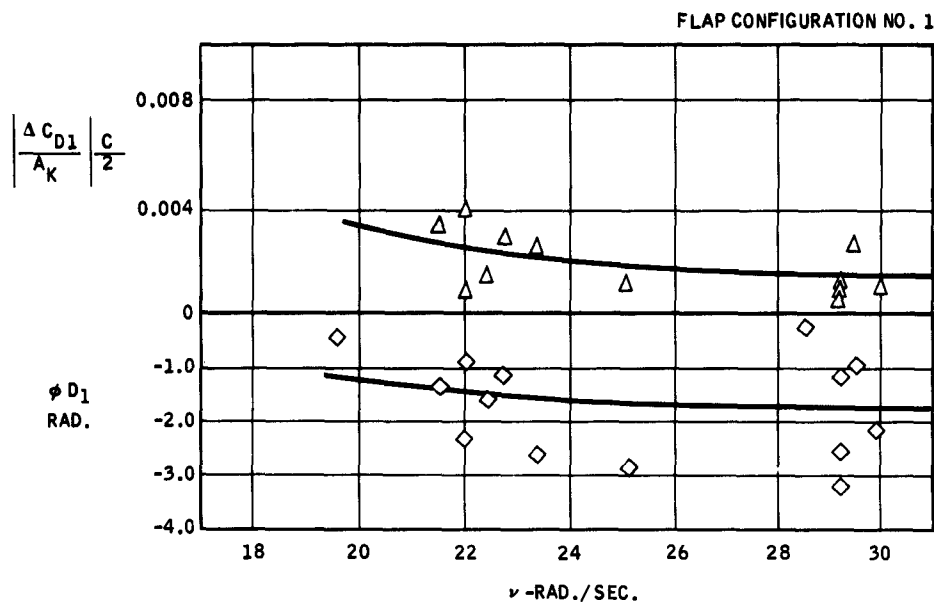


Figure 11. Drag Frequency Response, Head Seas, Flaps Fixed

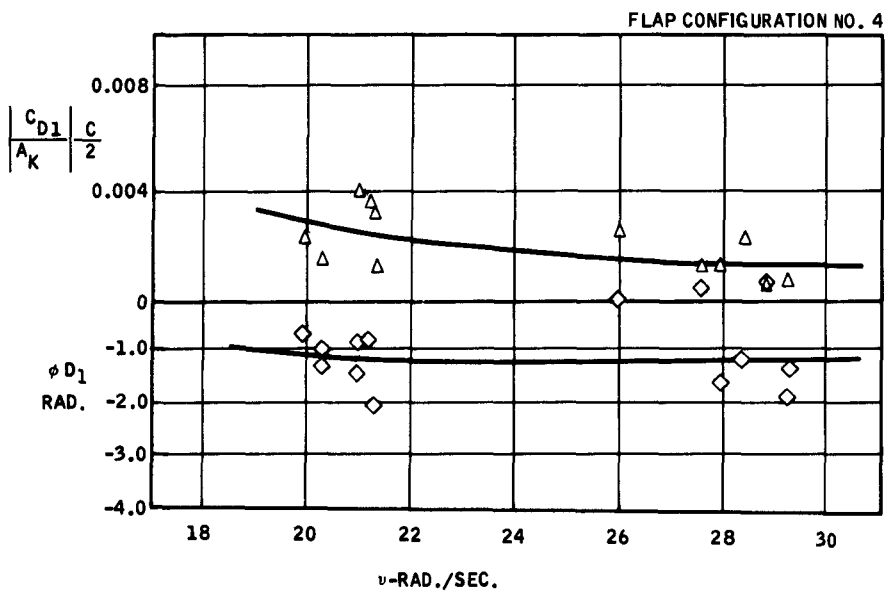
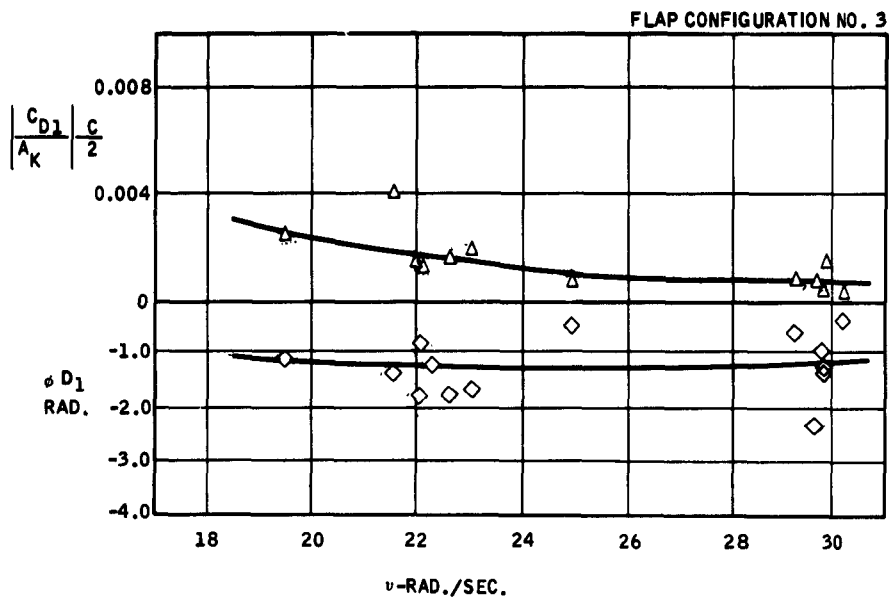


Figure 12. Drag Frequency Response, Head Seas, Flaps Fixed

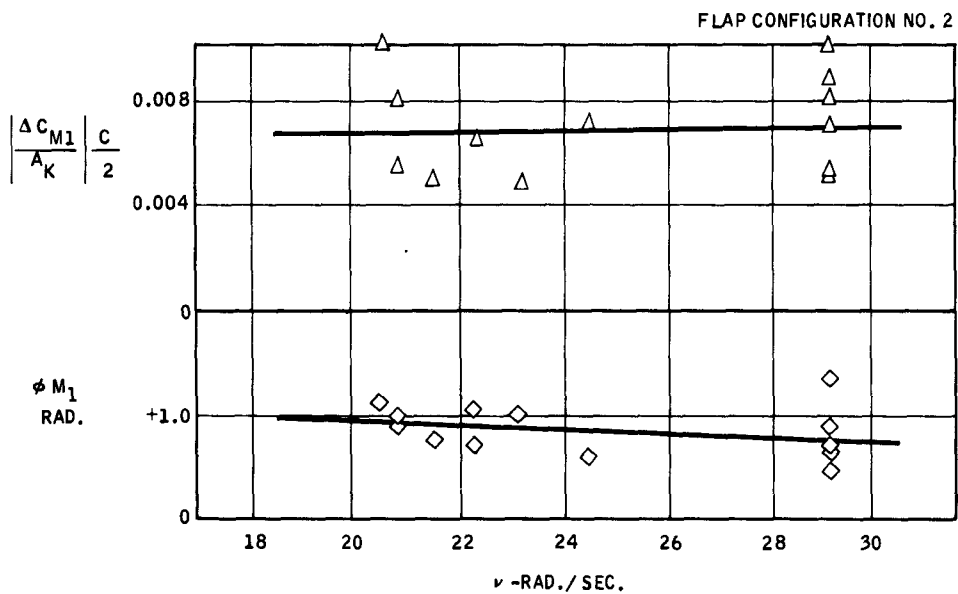
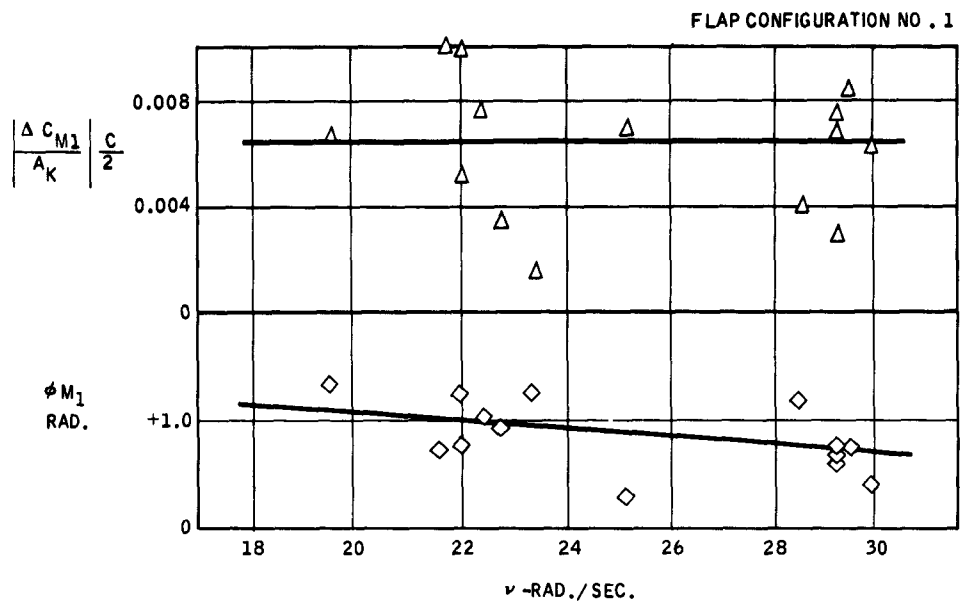
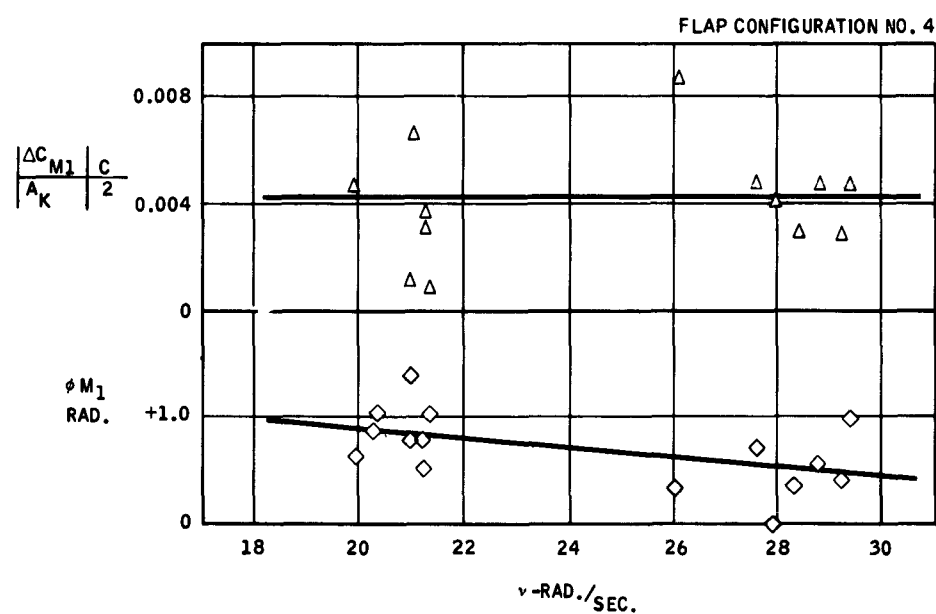
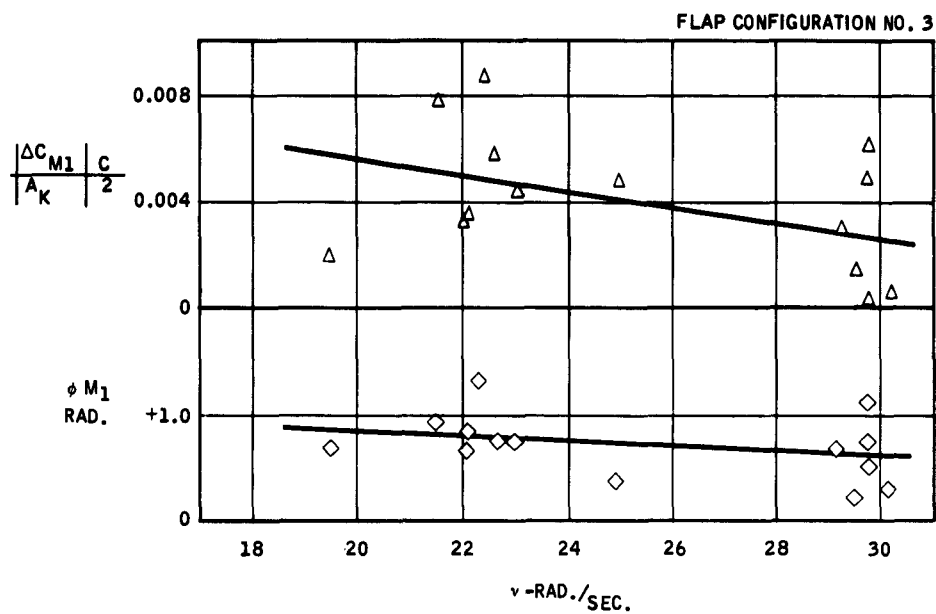


Figure 13. Pitching Moment Frequency Response, Head Seas, Flaps Fixed



**Figure 14. Pitching Moment Frequency Response, Head Seas, Flaps Fixed**

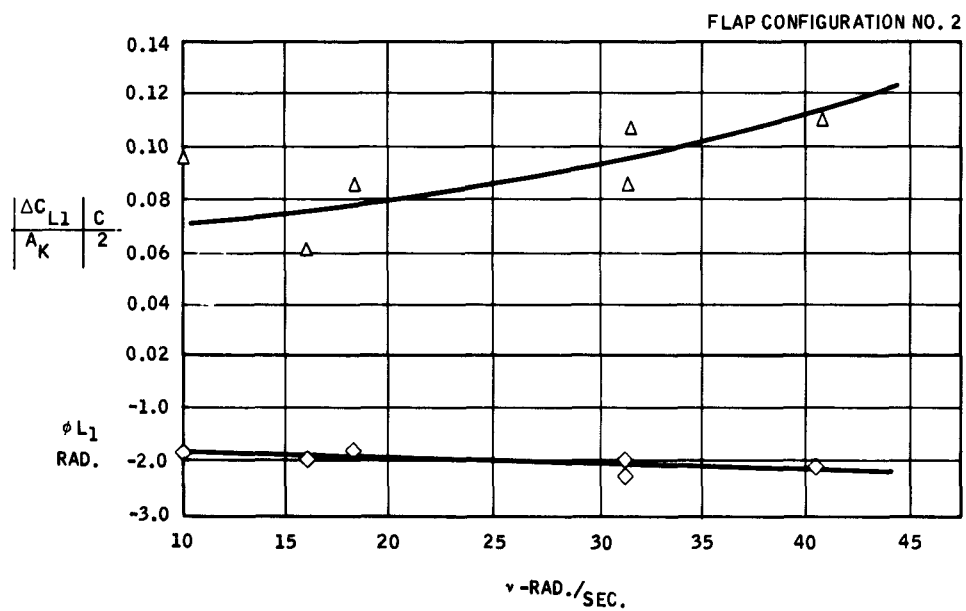
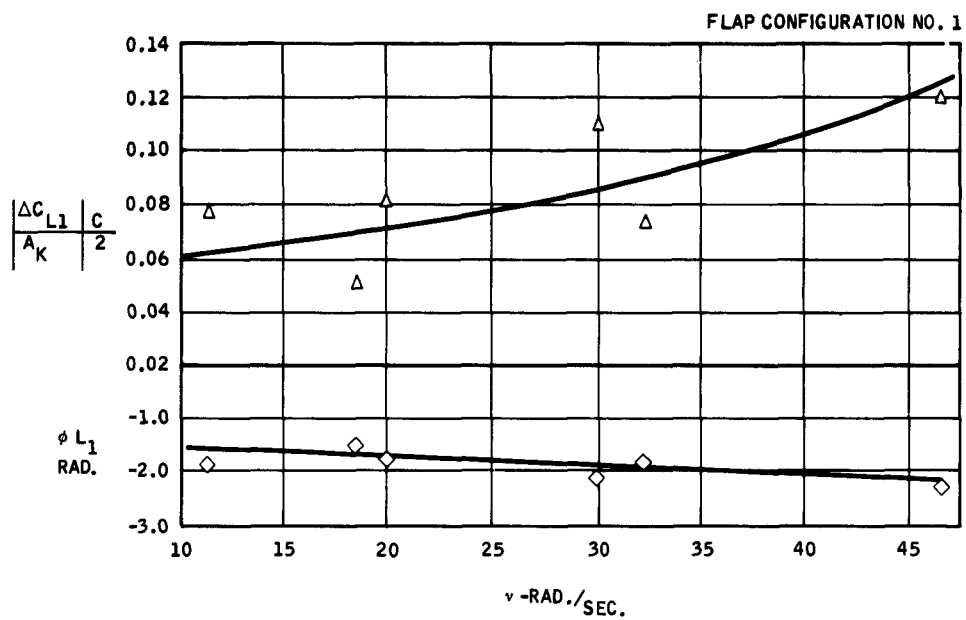


Figure 15. Lift Frequency Response, Following Seas, Flaps Fixed

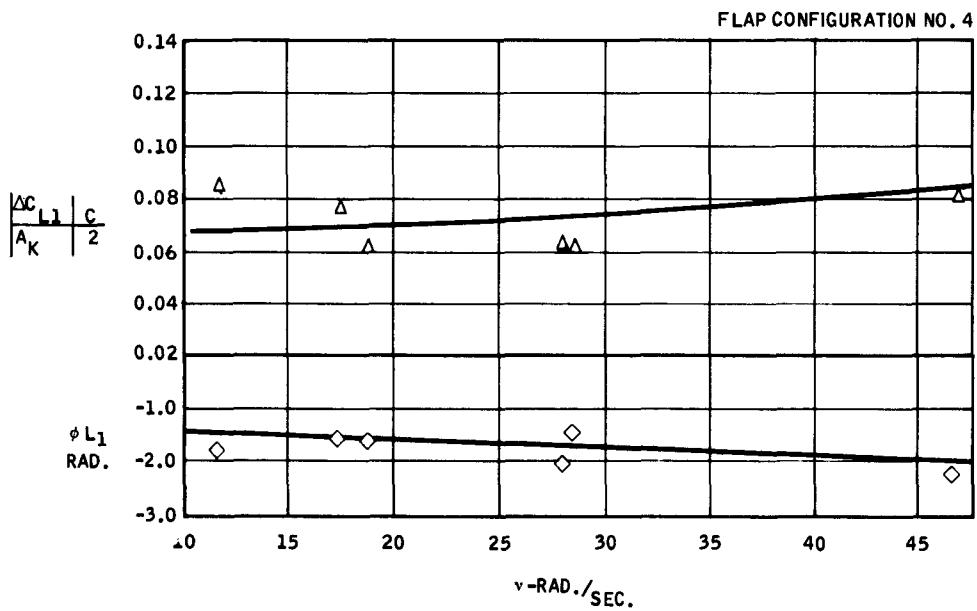
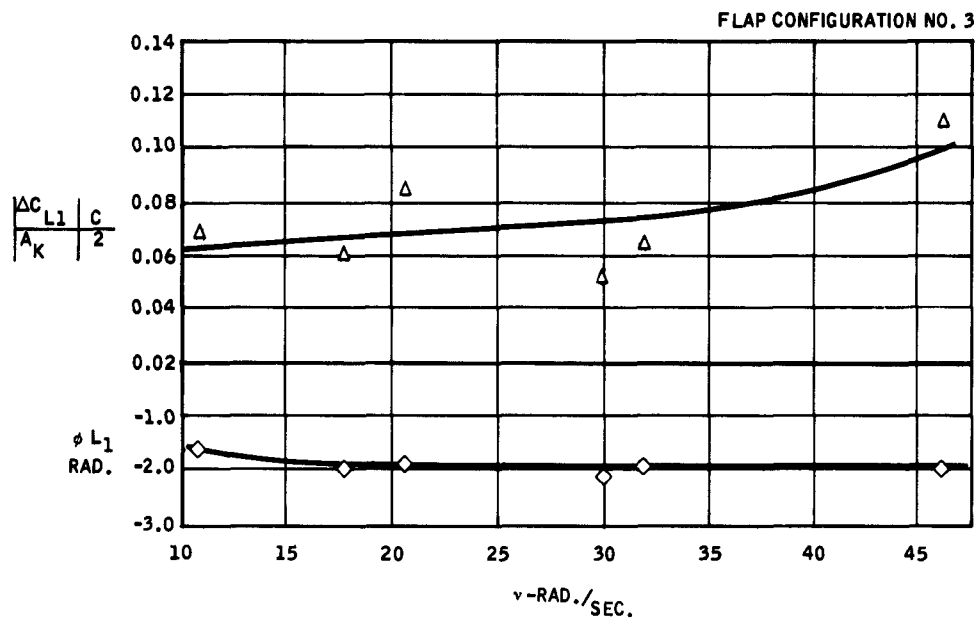


Figure 16. Lift Frequency Response, Following Seas, Flaps Fixed

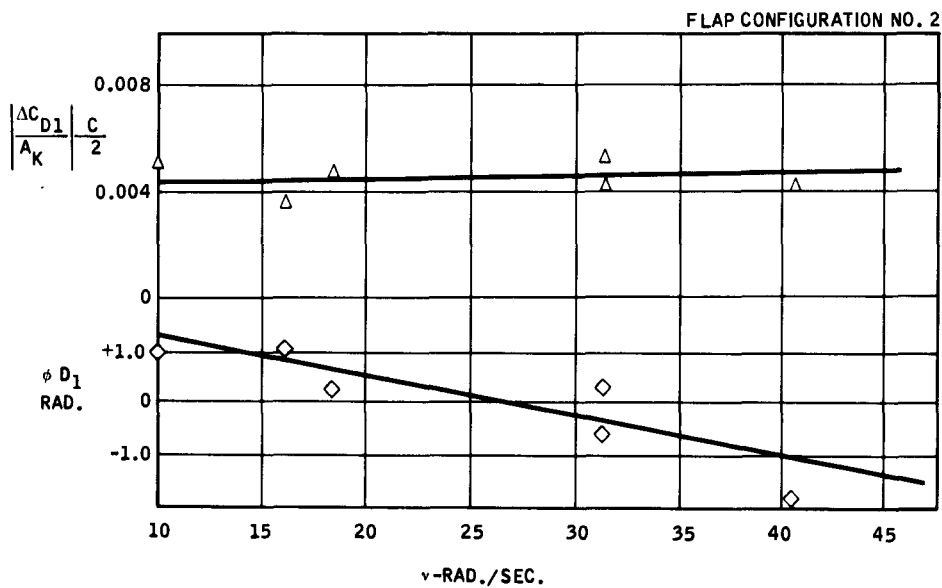
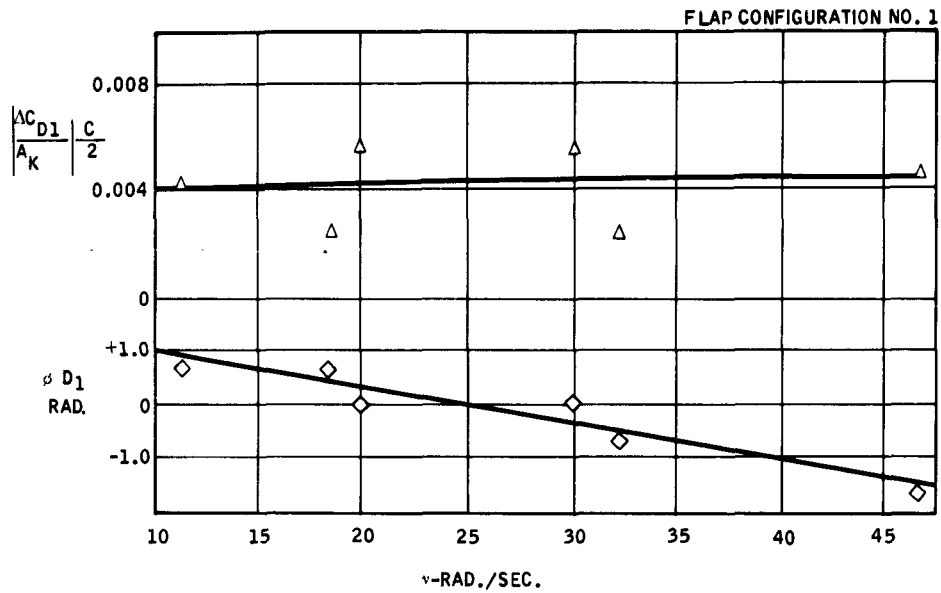


Figure 17. Drag Frequency Response, Following Seas, Flaps Fixed

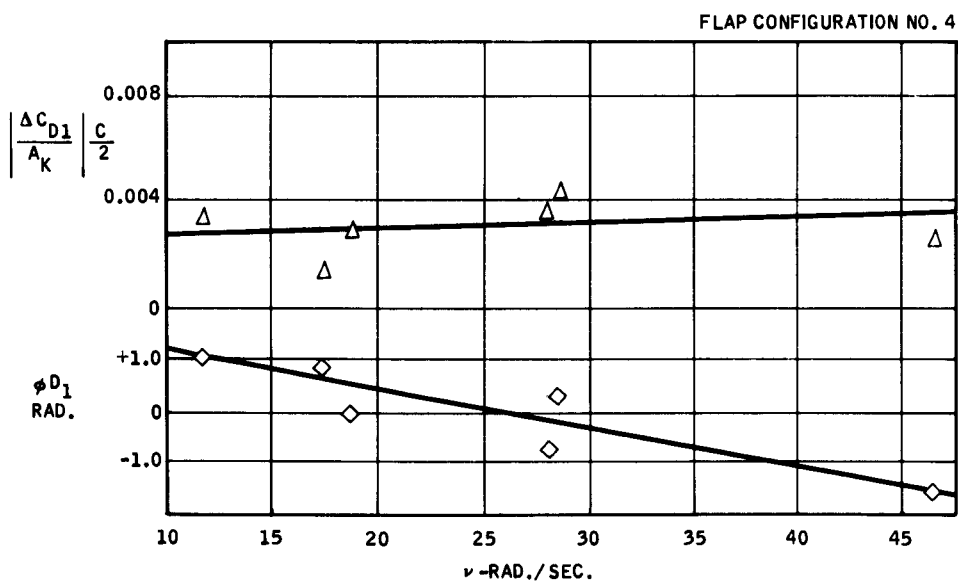
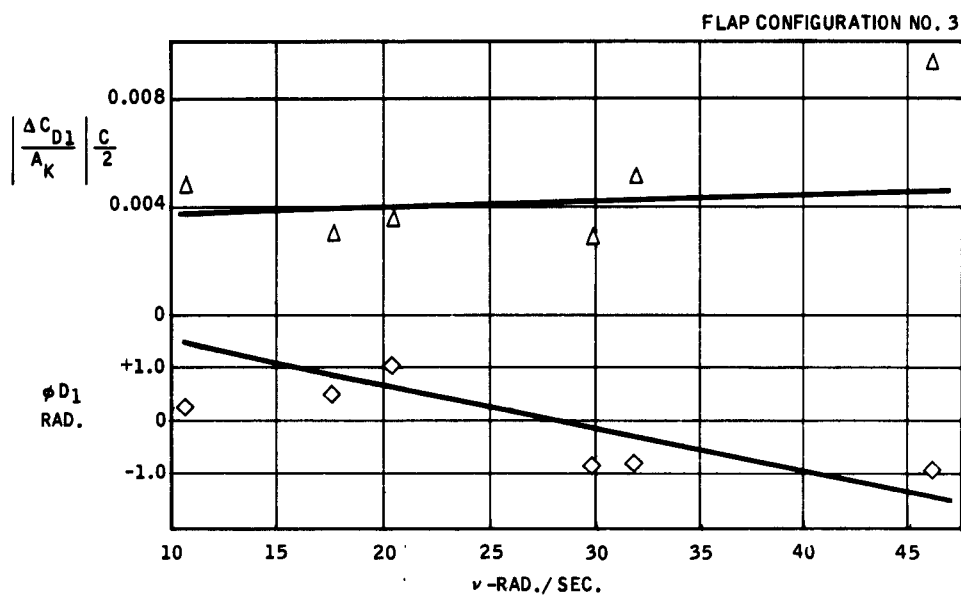
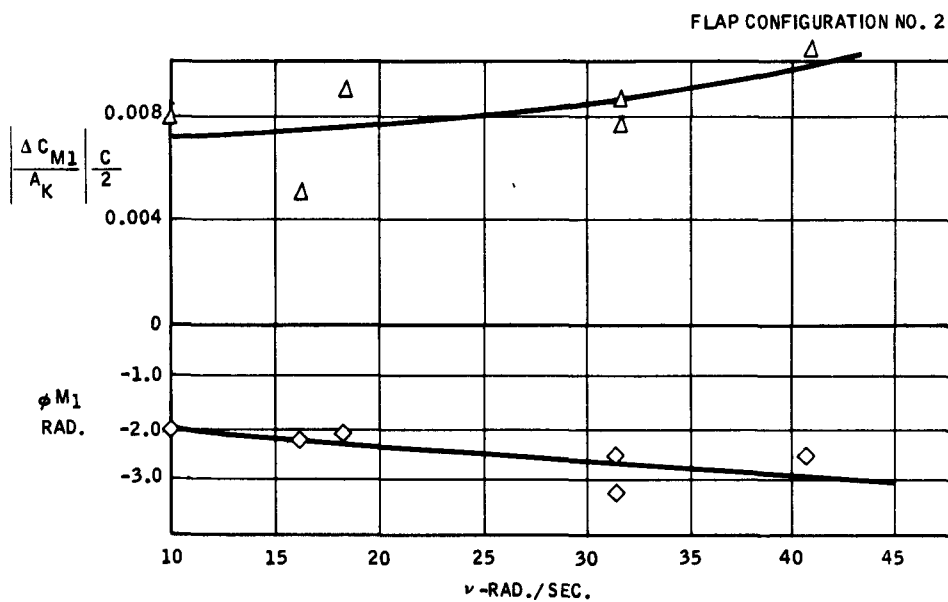
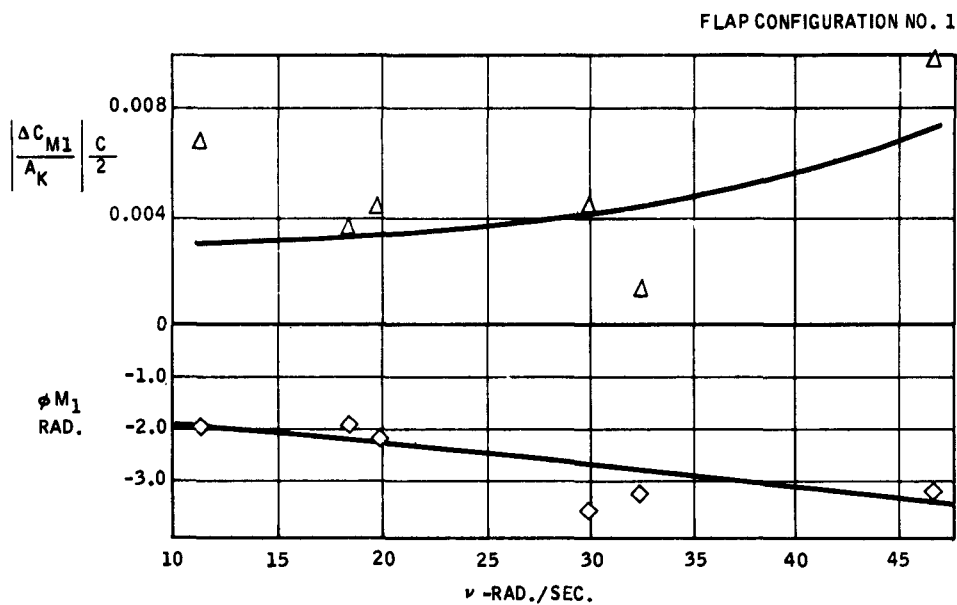
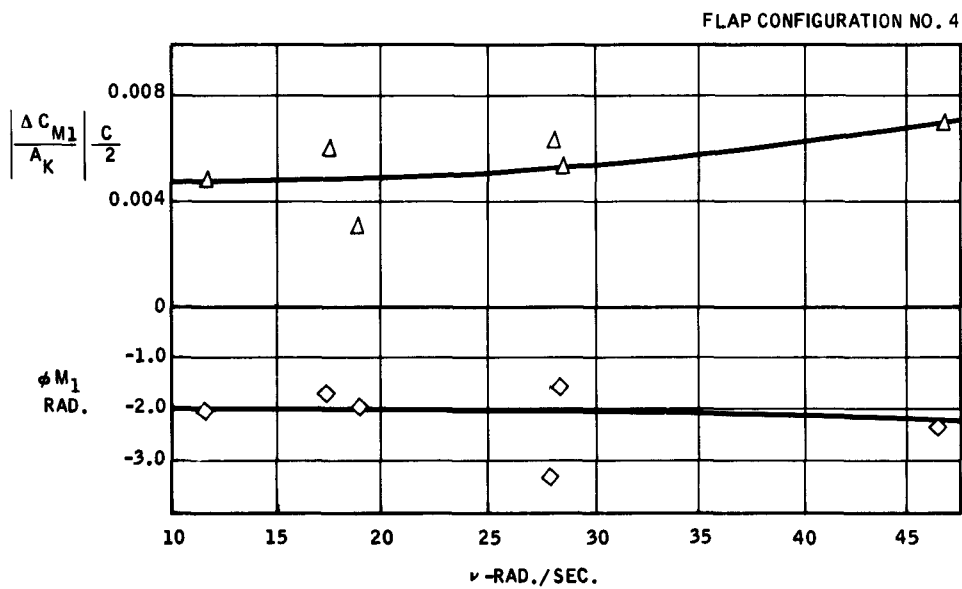
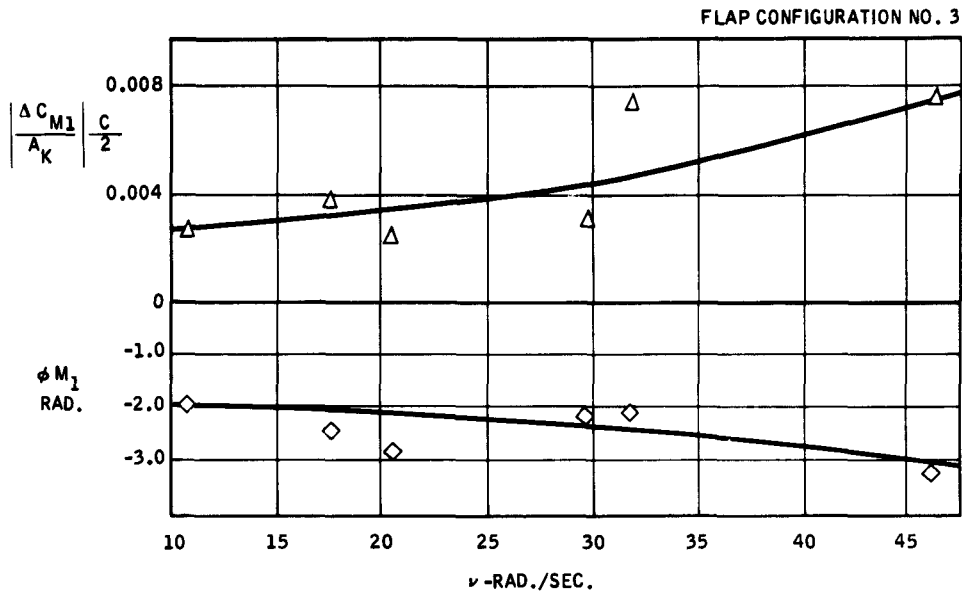


Figure 18. Drag Frequency Response, Following Seas, Flaps Fixed



**Figure 19. Pitching Moment Frequency Response,  
Following Seas, Flaps Fixed**



**Figure 20. Pitching Moment Frequency Response,  
Following Seas, Flaps Fixed**

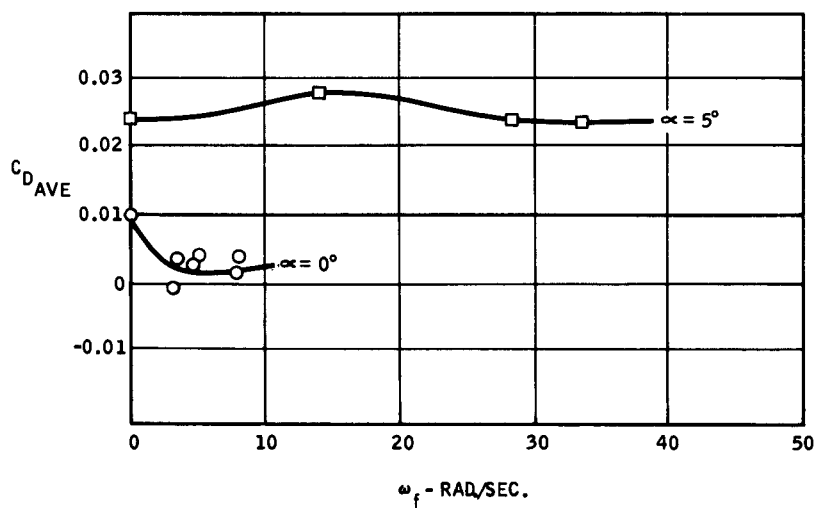
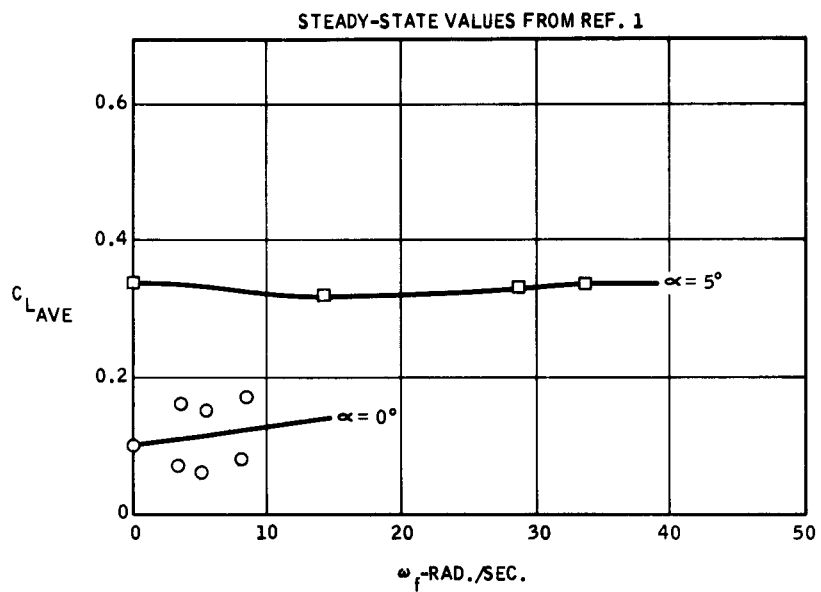


**Figure 21. Flaps Configuration 1 — Mean Values of Force Coefficients, Flaps Cycling in Smooth Water**

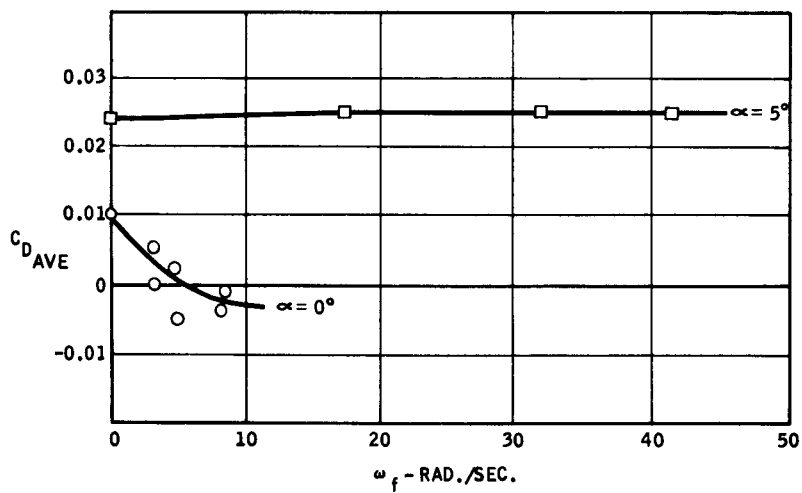
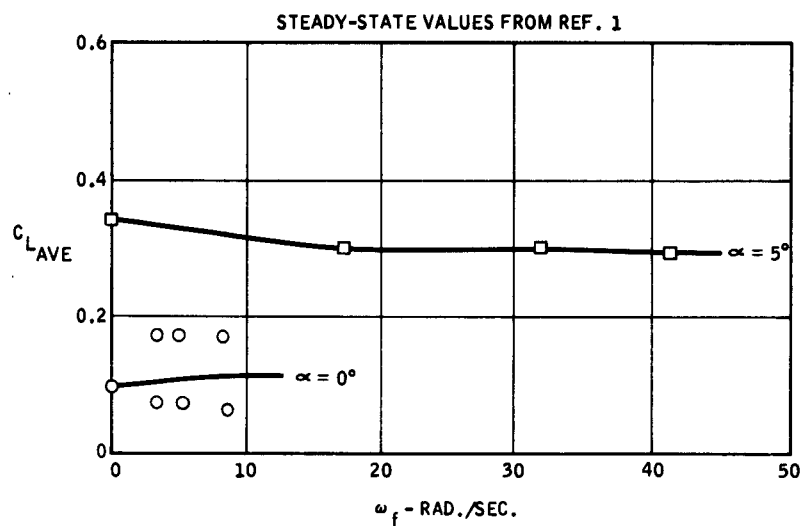


**Figure 22. Flap Configuration 2 — Mean Value of Force Coefficients, Flaps Cycling in Smooth Water**

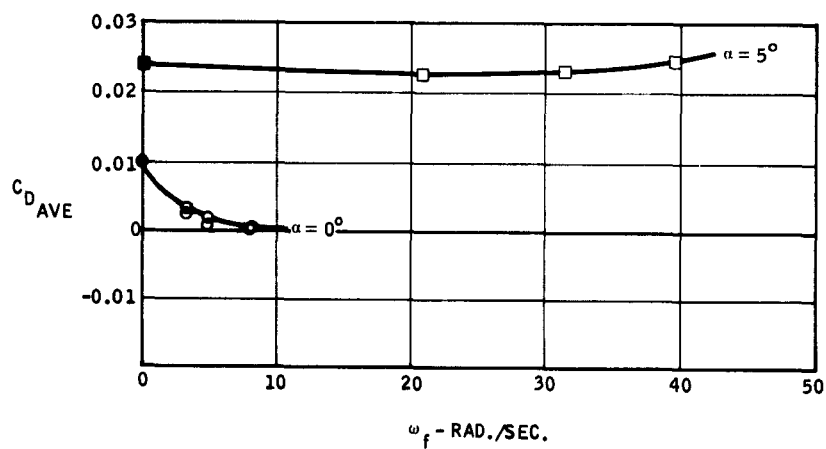
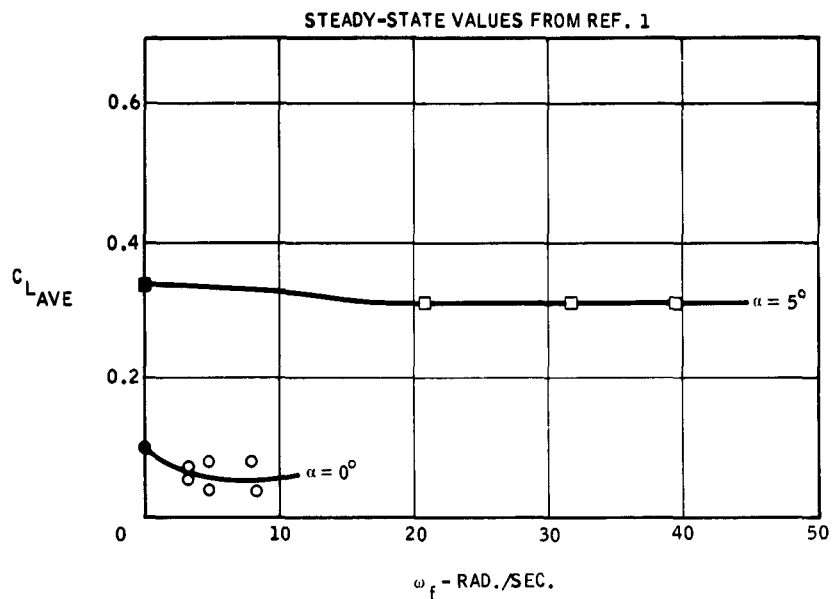


**Figure 23. Flap Configuration 3 — Mean Values of Force Coefficients, Flaps Cycling in Smooth Water**

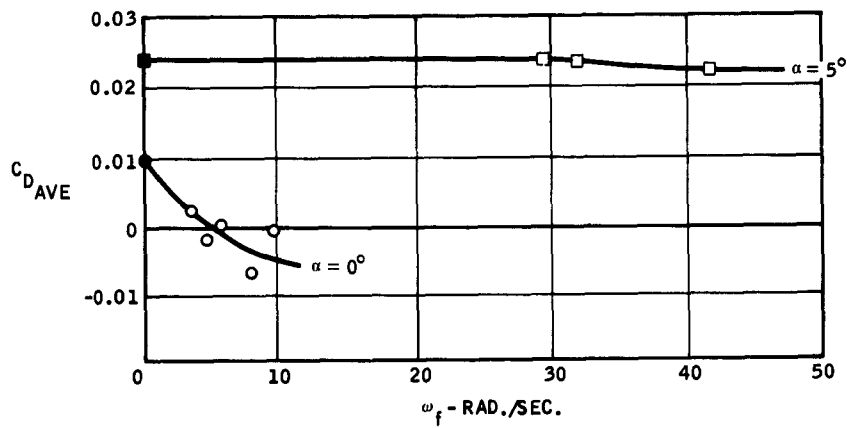
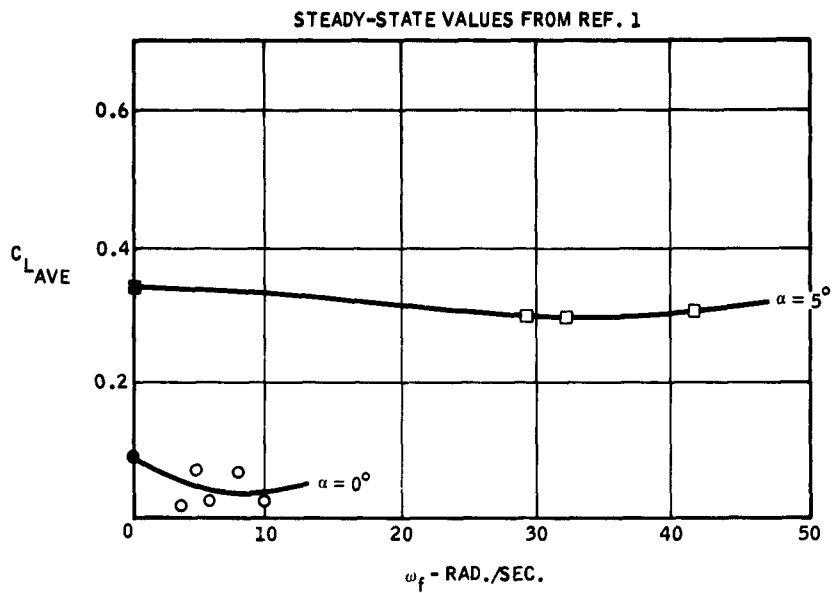


**Figure 24. Flap Configuration 4 — Mean Value of Force Coefficients, Flaps Cycling in Smooth Water**

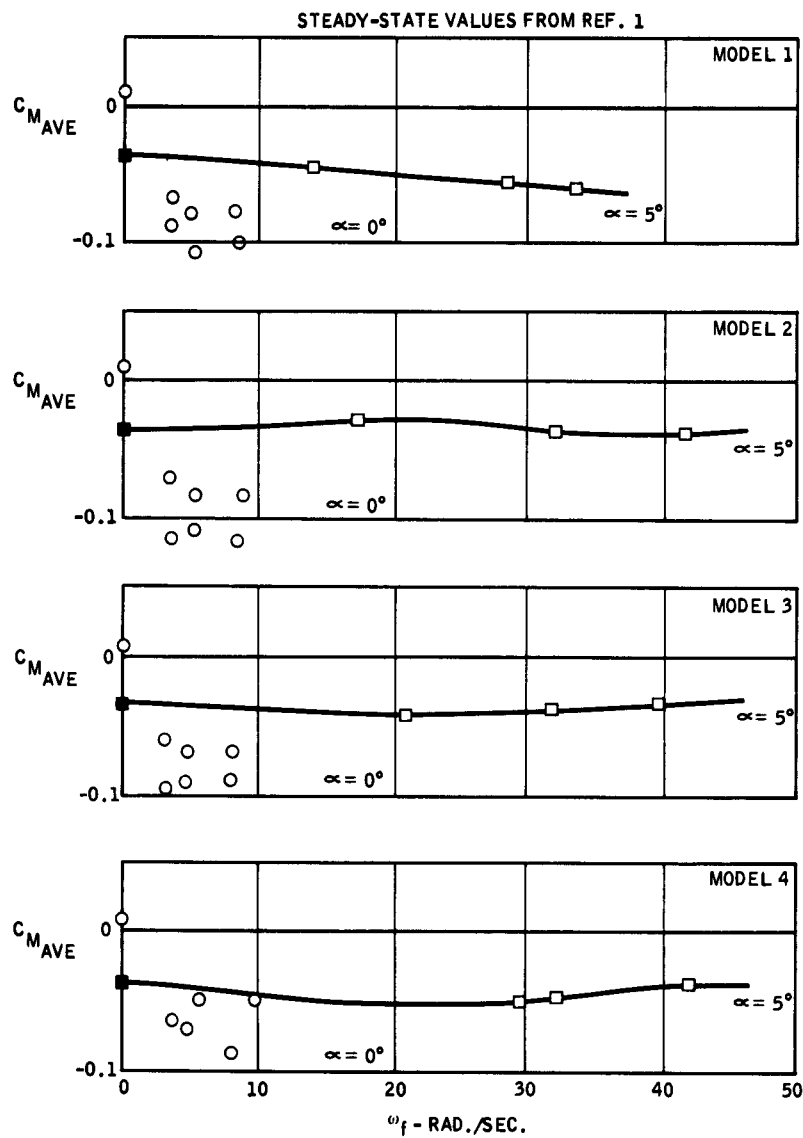


**Figure 25. Mean Pitching Moment Coefficients —  
All Models, Flaps Cycling in Smooth Water**

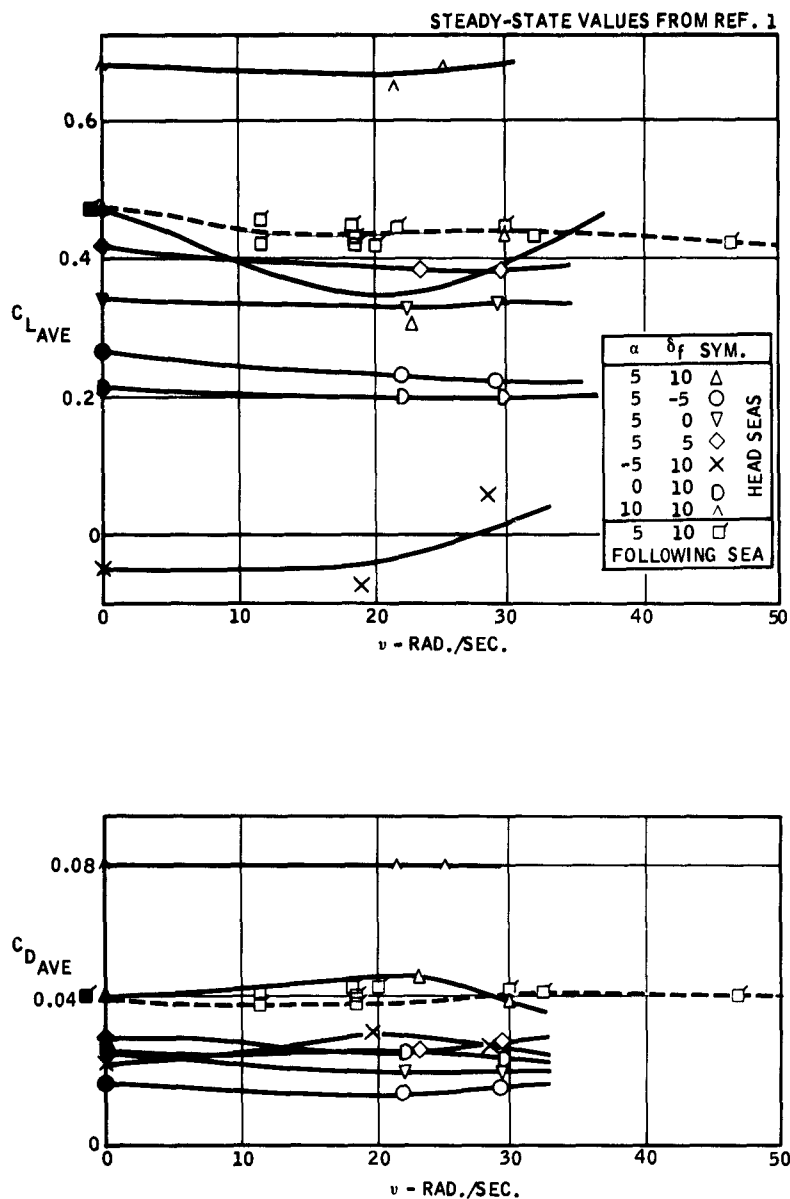


**Figure 26. Flap Configuration 1 — Mean Value of Force Coefficients, Flaps Fixed in Waves**

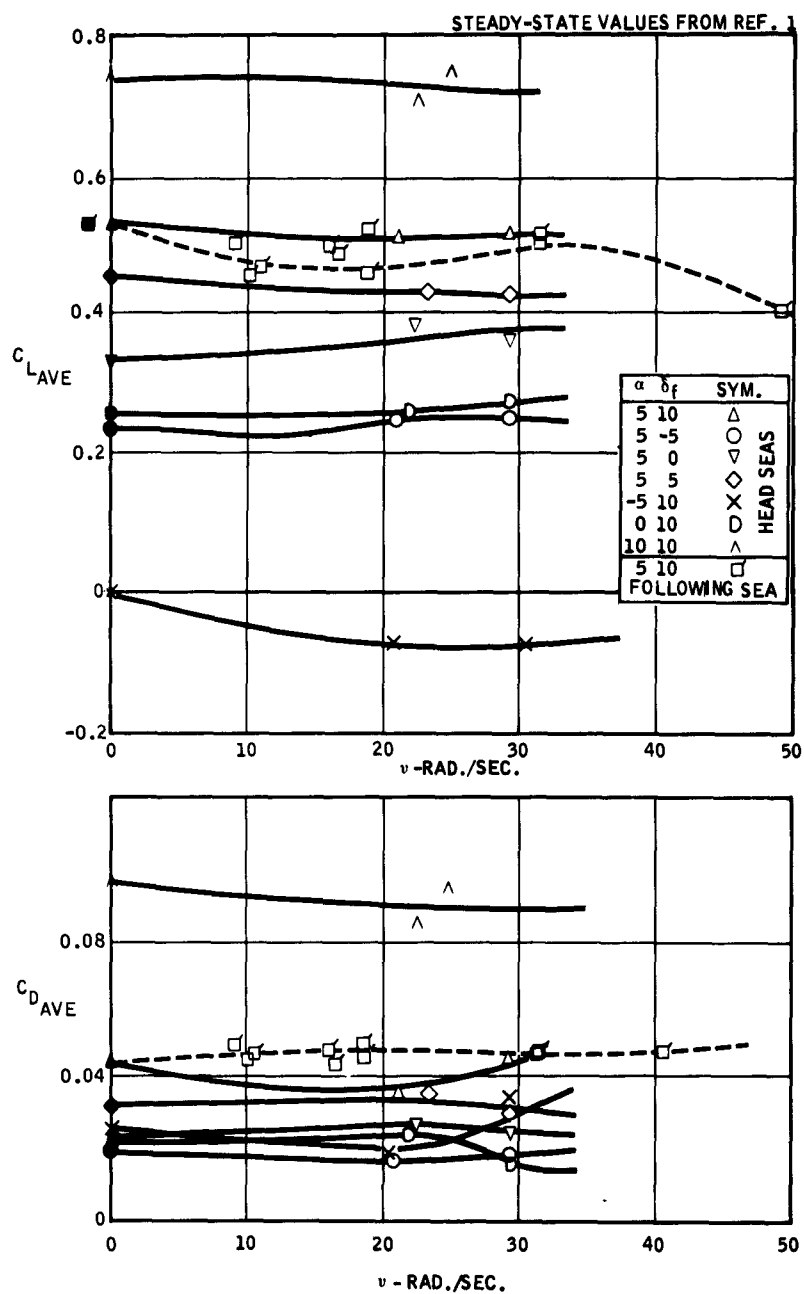


**Figure 27. Flap Configuration 2 — Mean Values of Force Coefficients, Flaps Fixed in Waves**

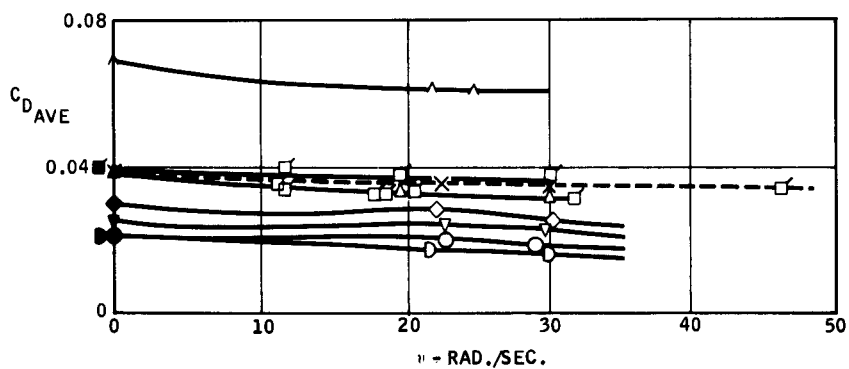
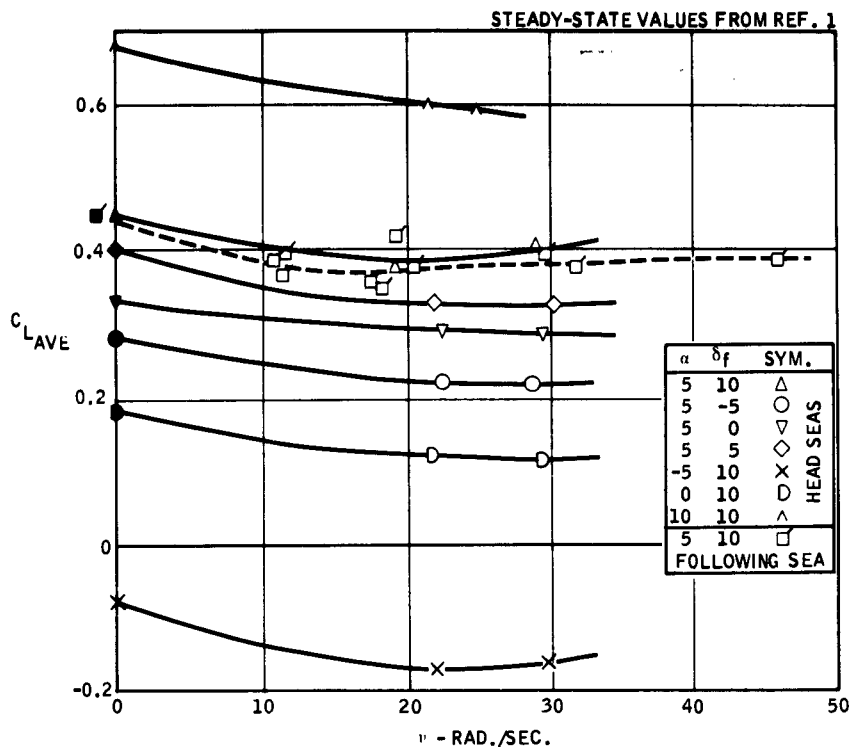


**Figure 28. Flap Configuration 3 — Mean Values of Force Coefficients, Flaps Fixed in Waves**

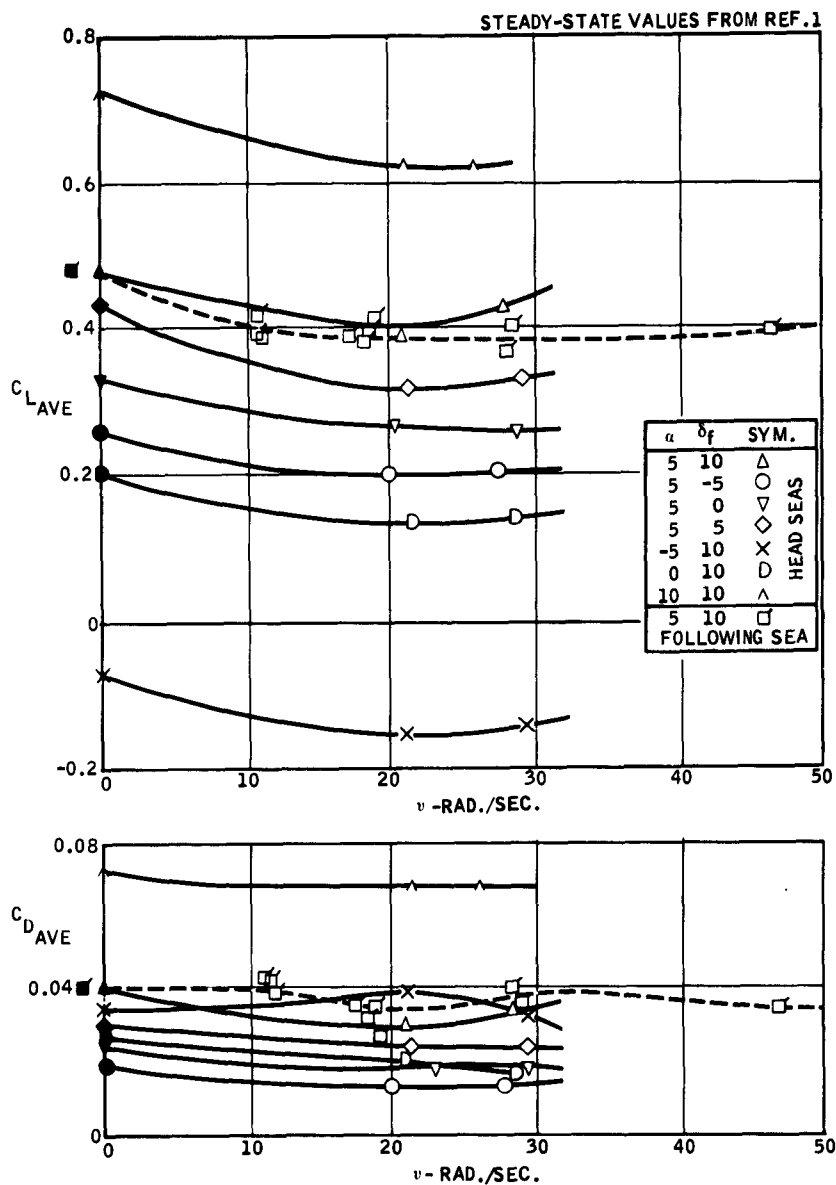


**Figure 29. Flap Configuration 4 — Mean Values of Force Coefficients, Flaps Fixed in Waves**

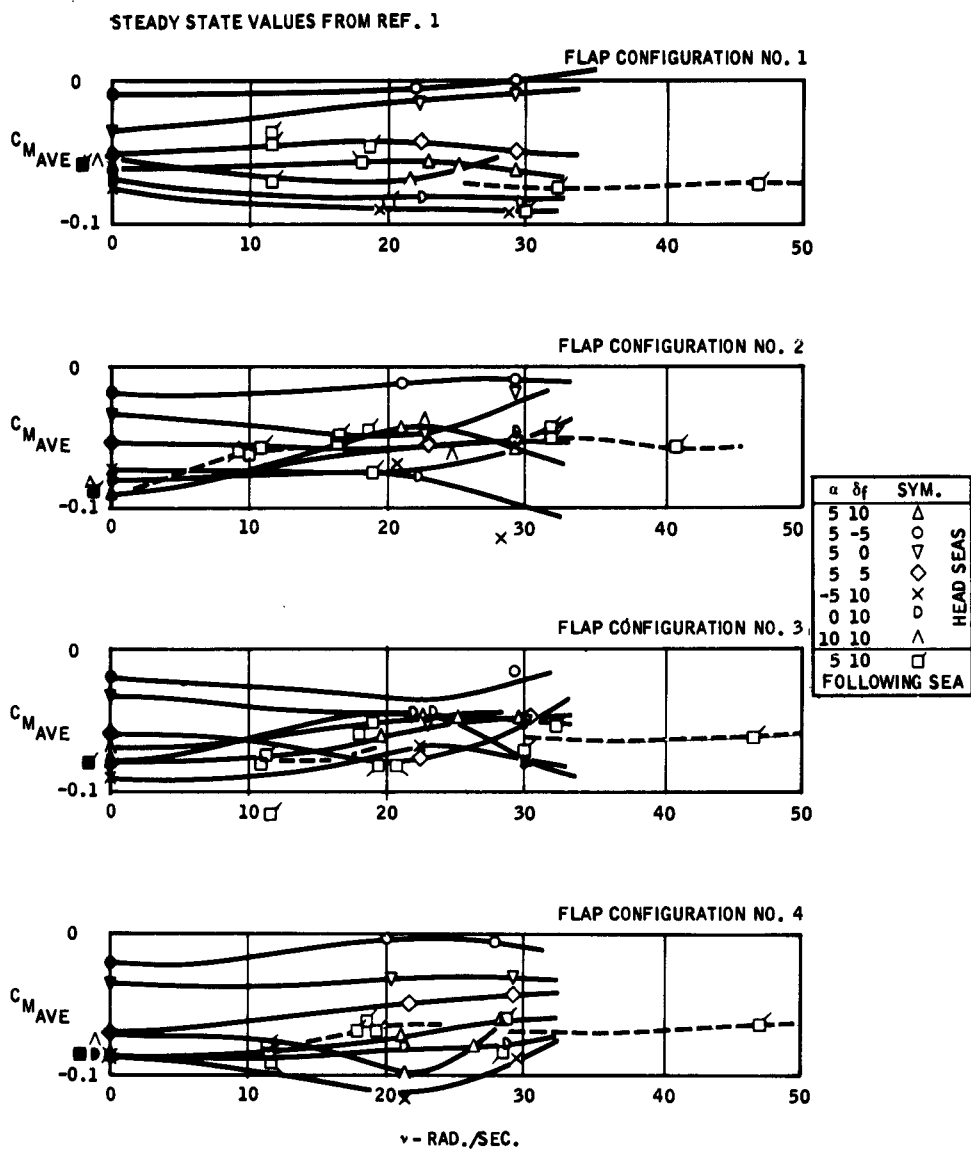


Figure 30. Mean Pitching Moment Coefficients — All Models, Flaps Fixed in Waves

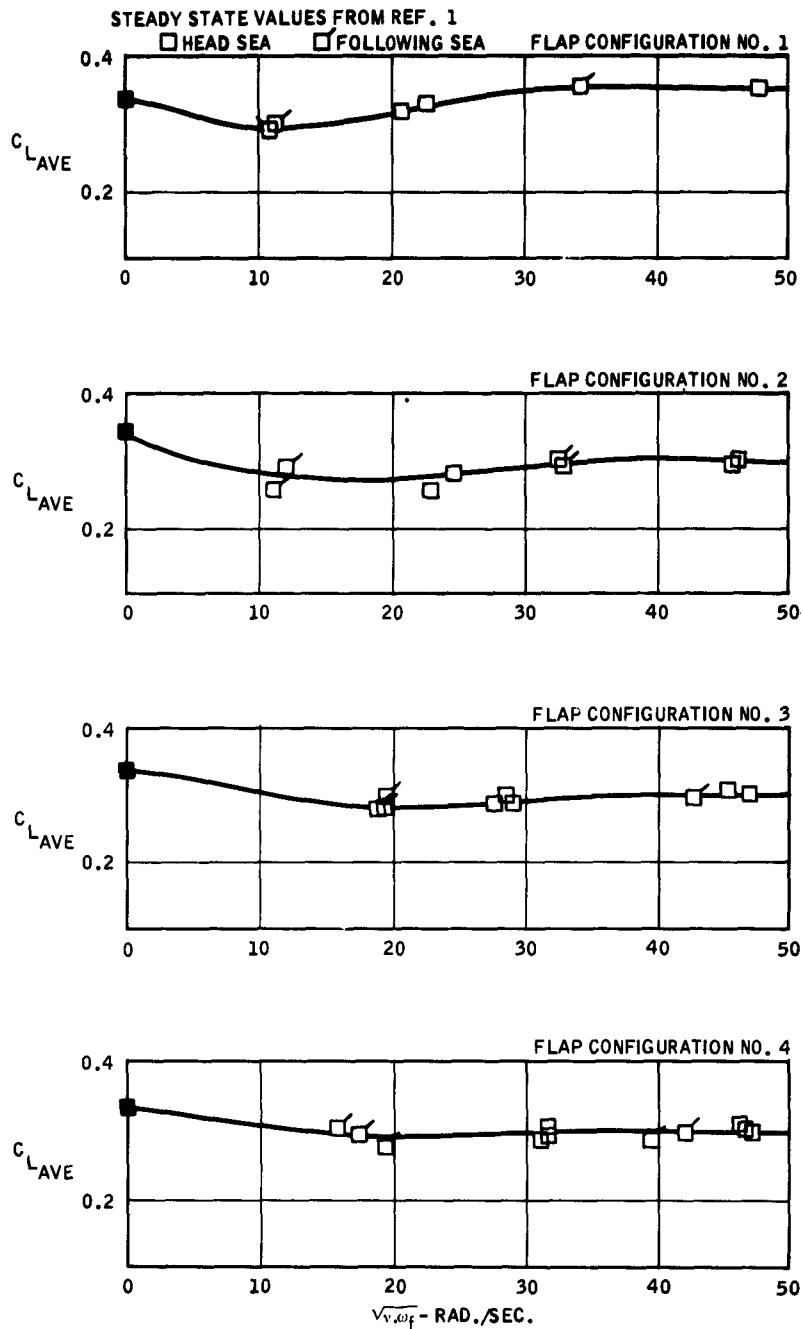


Figure 31. Mean Values of Lift Coefficients — All Models, Flaps Cycling in Waves,  $\alpha = 5^\circ$

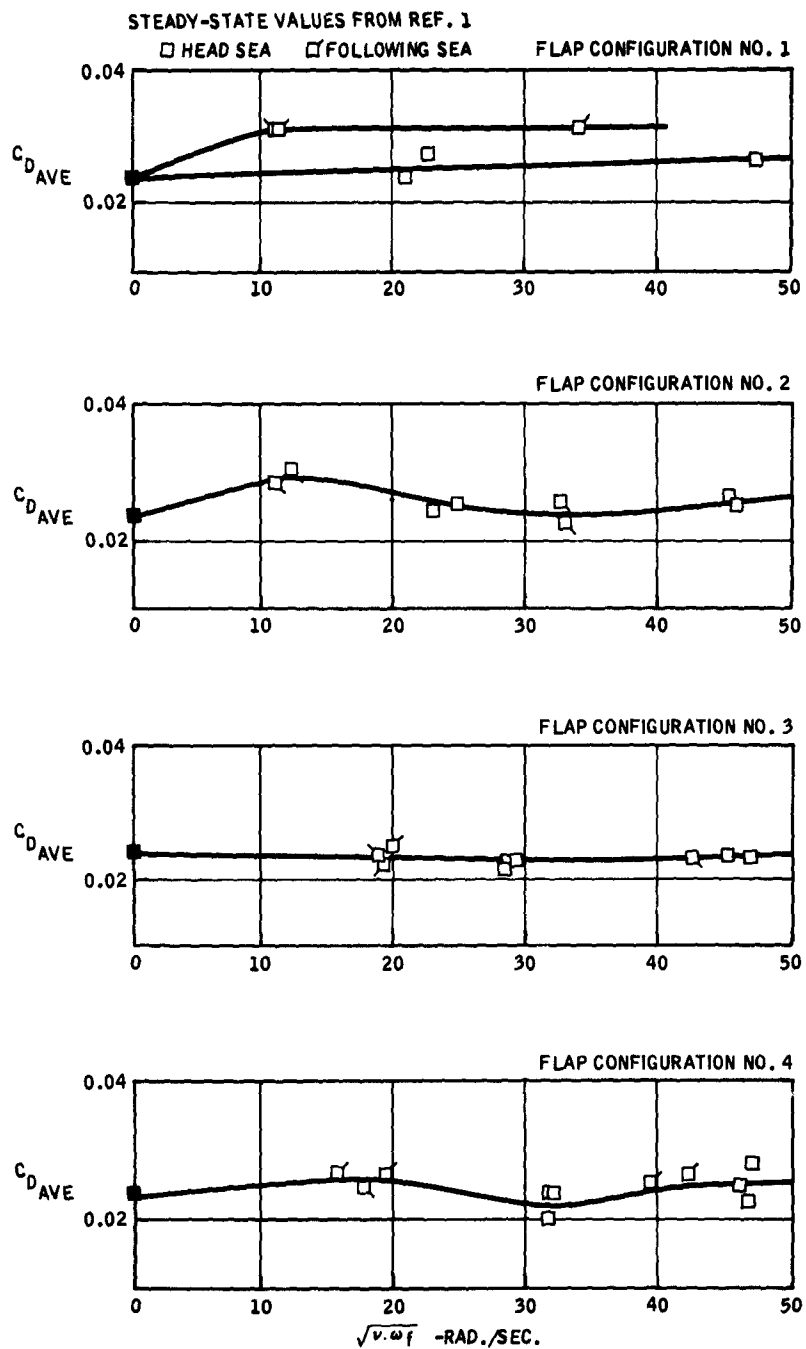


Figure 32. Mean Values of Drag Coefficients — All Models, Flaps Cycling in Waves,  $\alpha = 5^\circ$

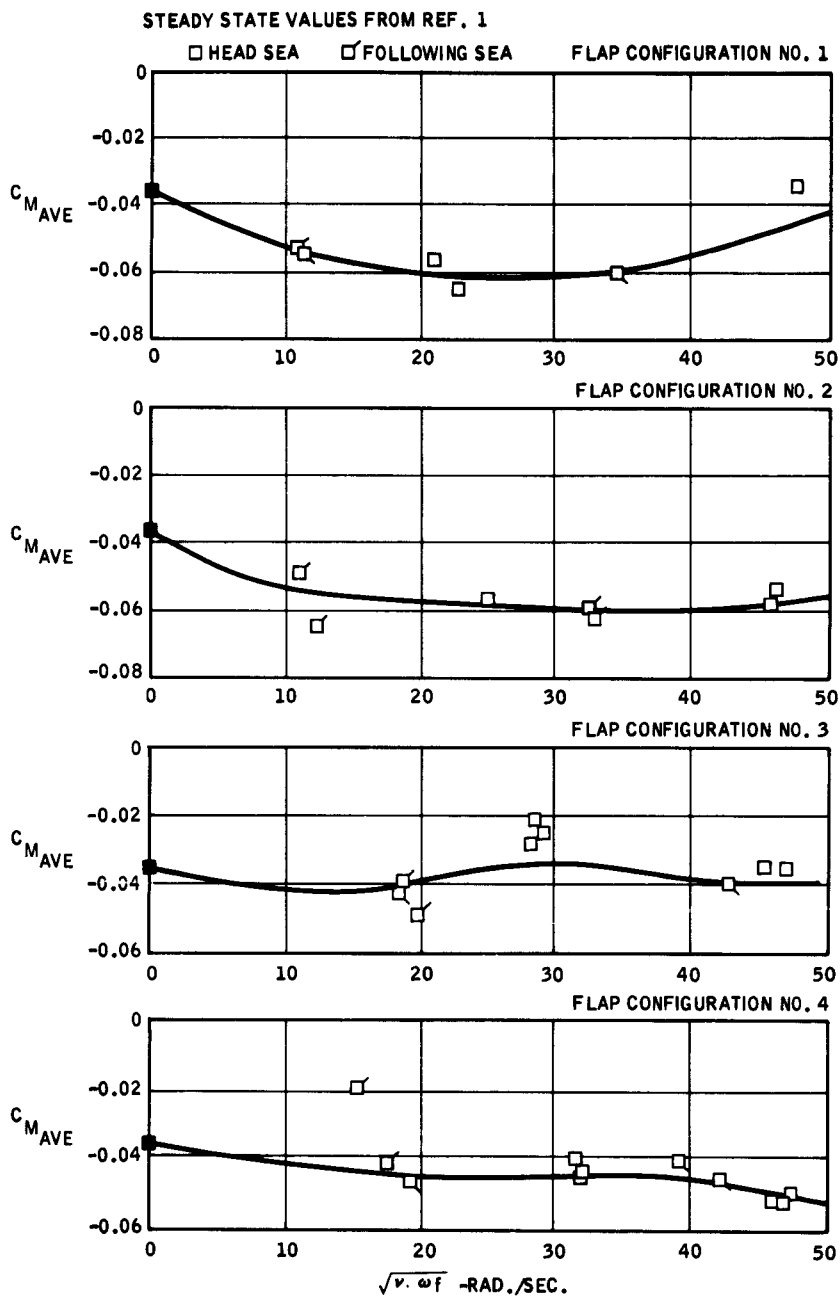


Figure 33. Mean Values of Pitching Coefficients — All Models, Flaps Cycling in Waves,  $\alpha = 5^\circ$

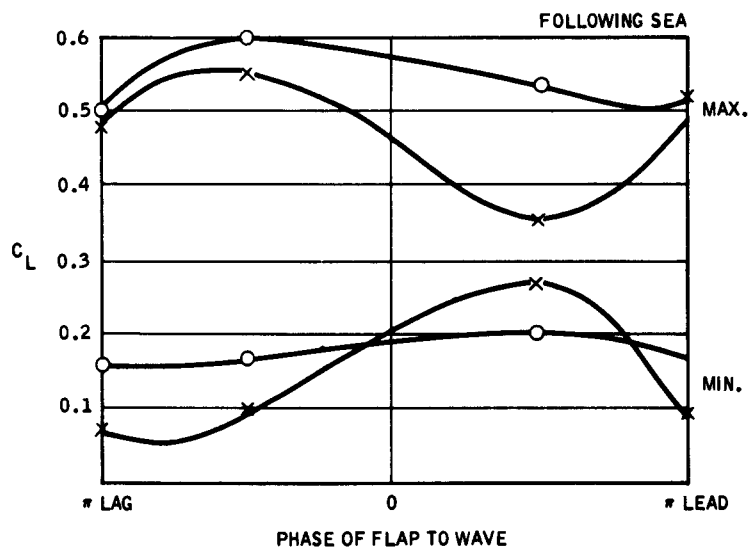
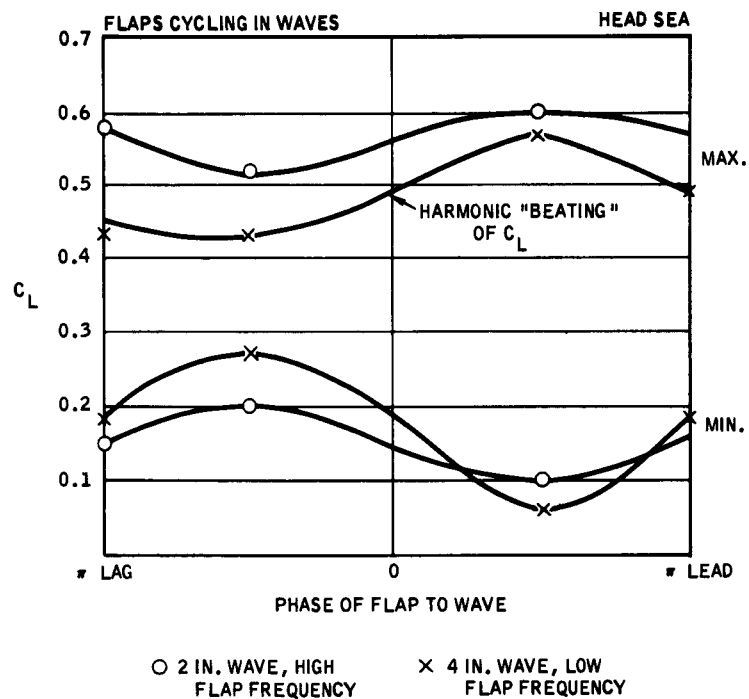


Figure 34. Flap Configuration 1 — Maximum and Minimum  $C_L$  Vs. Phase of Flap to Wave

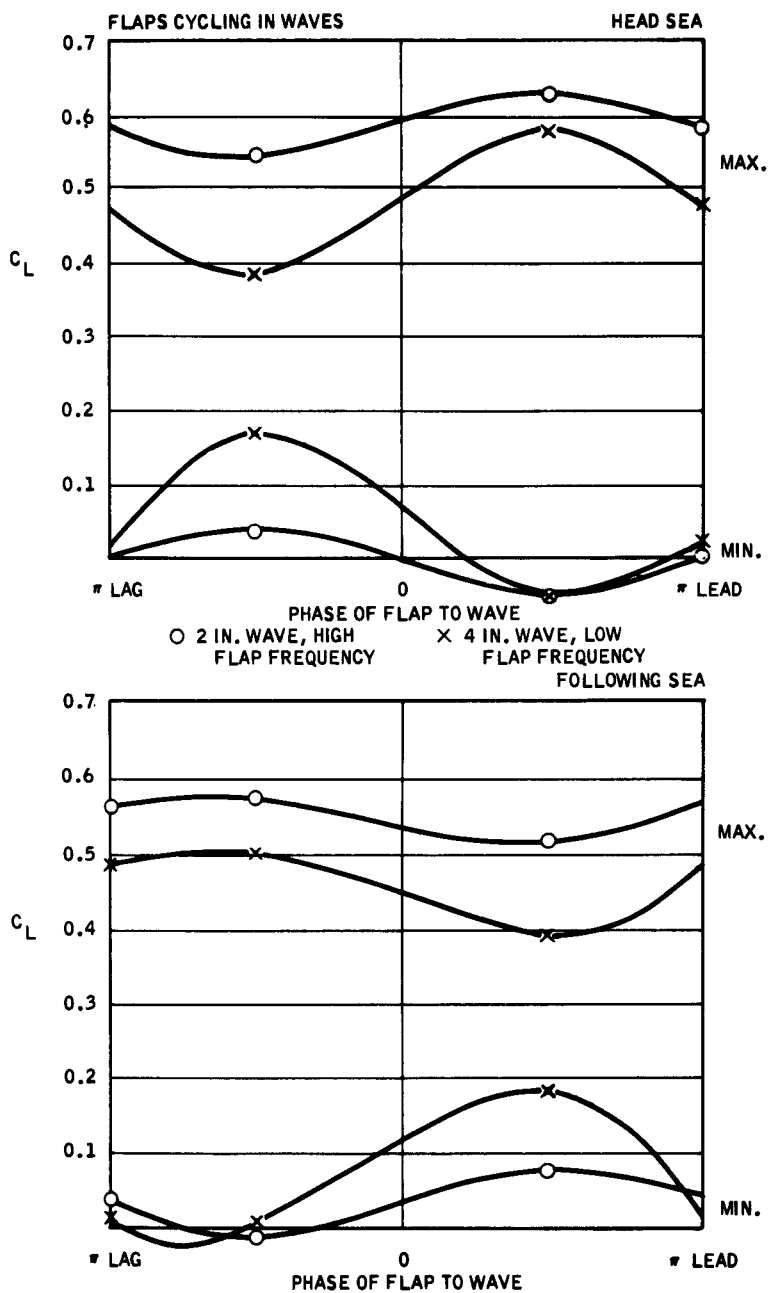


Figure 35. Flap Configuration 2 — Maximum and Minimum  $C_L$  Vs. Phase of Flap to Wave

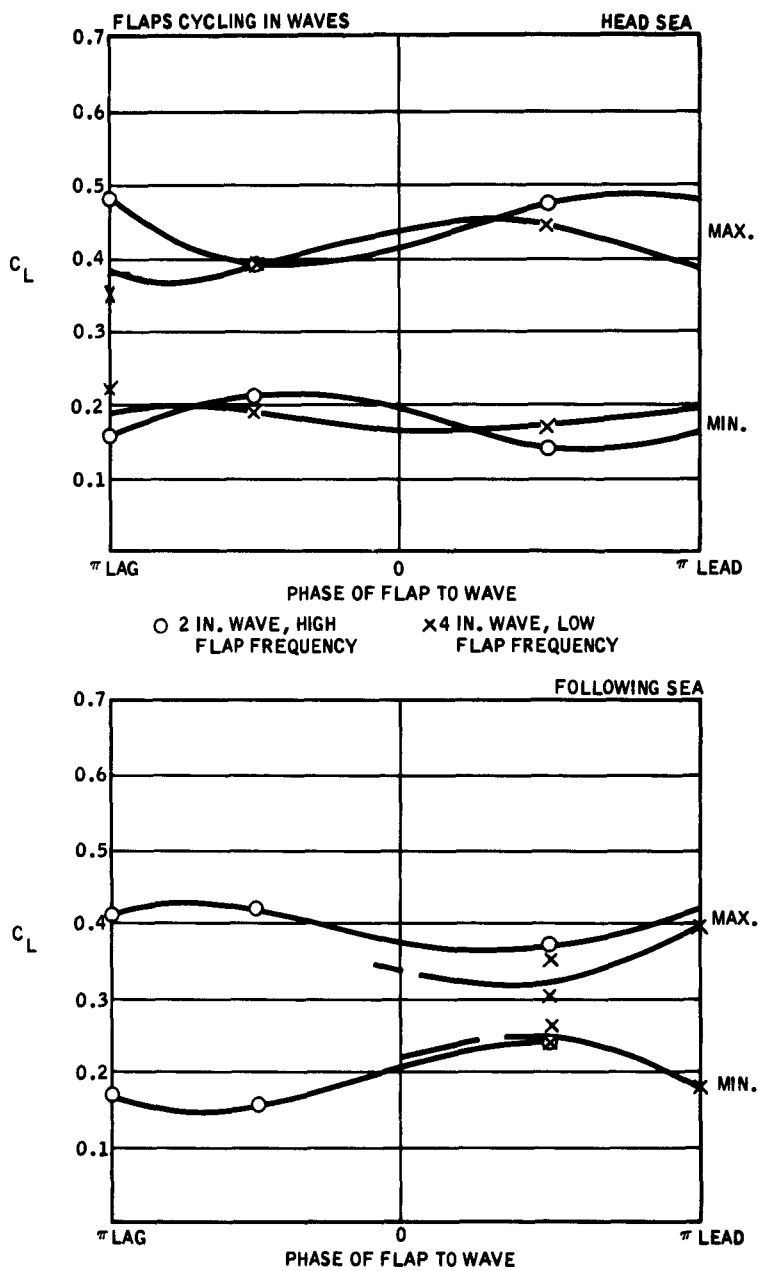


Figure 36. Flap Configuration 3 — Maximum and Minimum  $C_L$  Vs. Phase of Flap to Wave

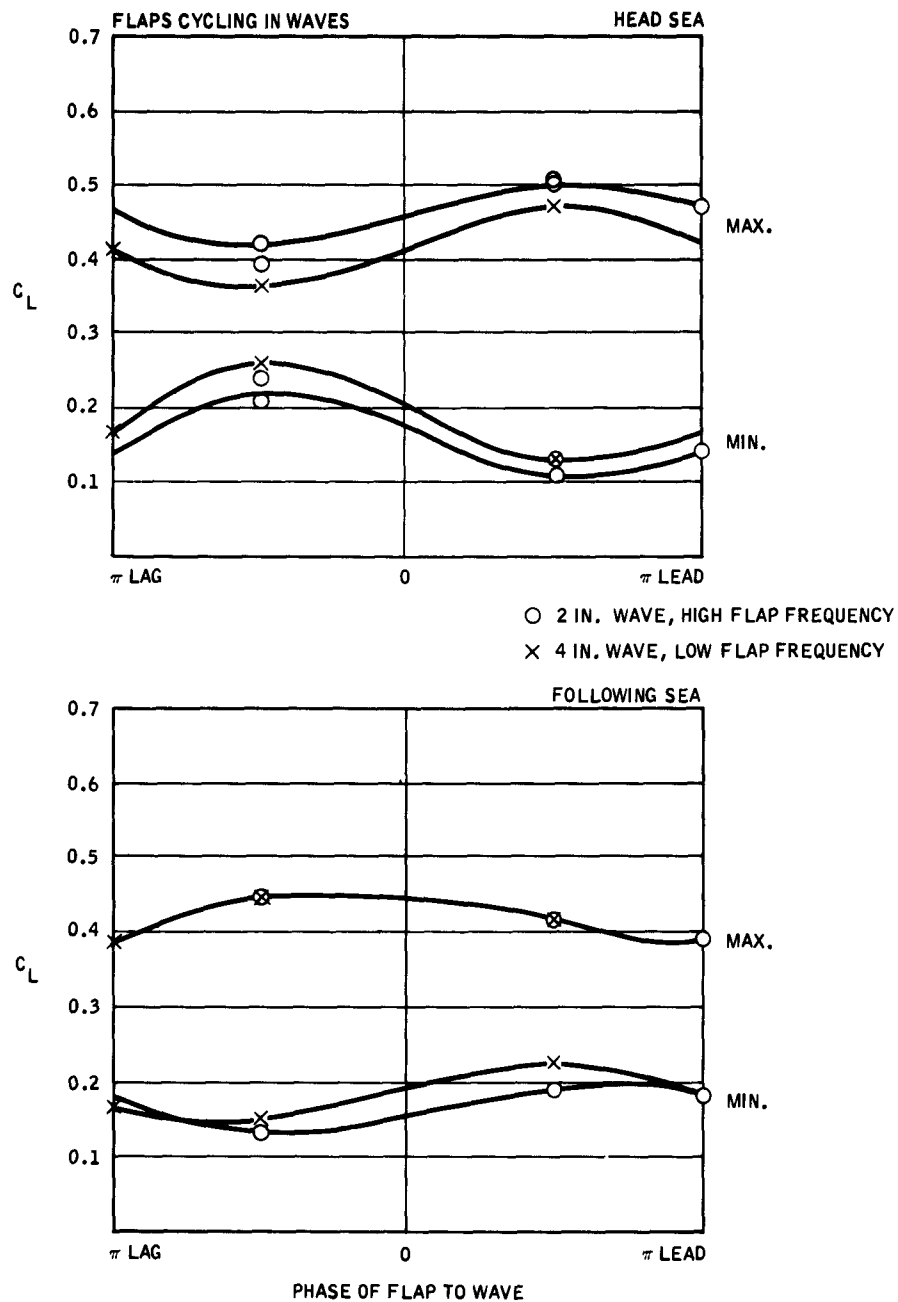
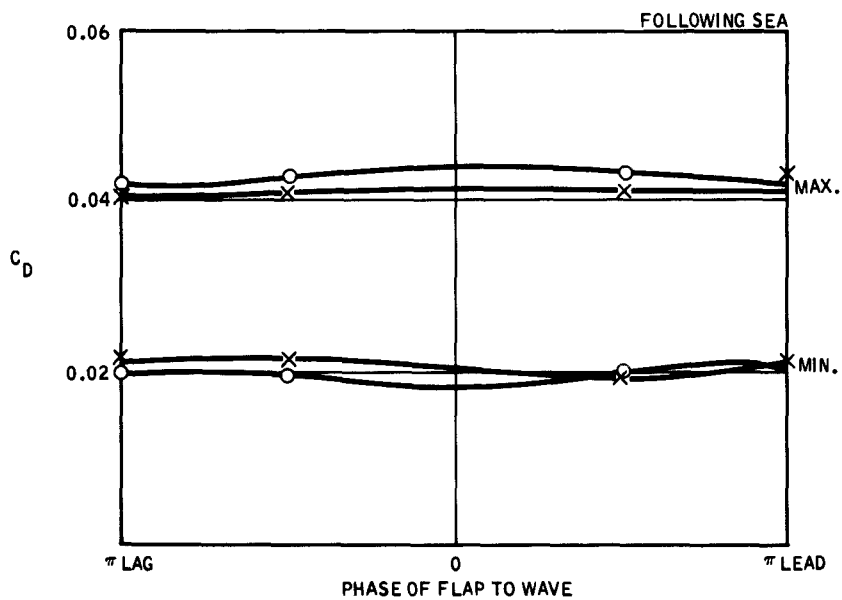
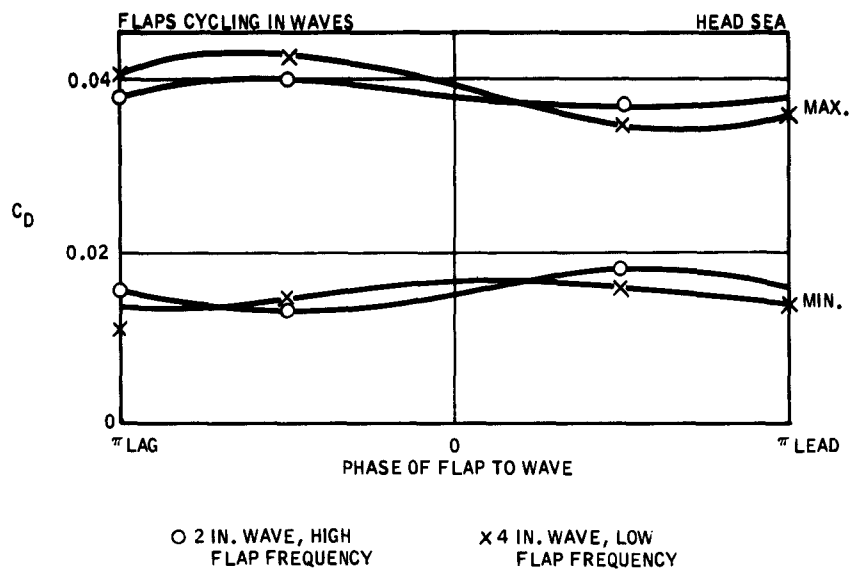


Figure 37. Flap Configuration 4 — Maximum and Minimum  $C_L$  Vs. Phase of Flap to Wave



**Figure 38. Flap Configuration 1 — Maximum and Minimum  $C_D$  Vs. Phase of Flap to Wave**

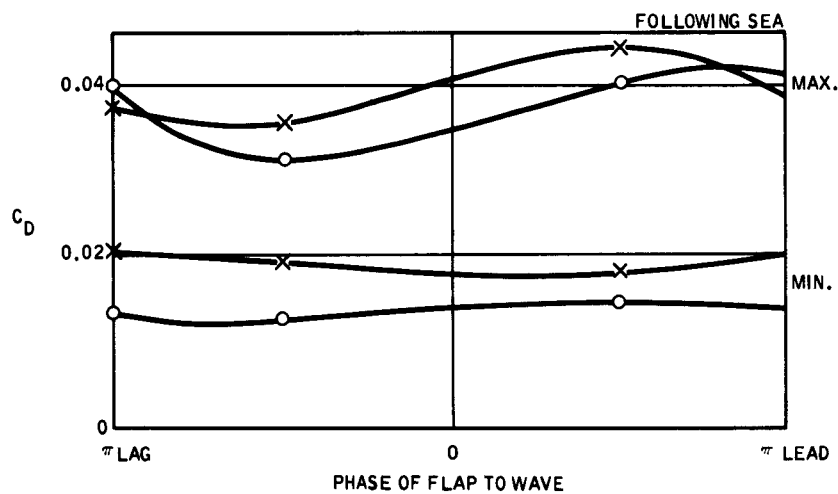
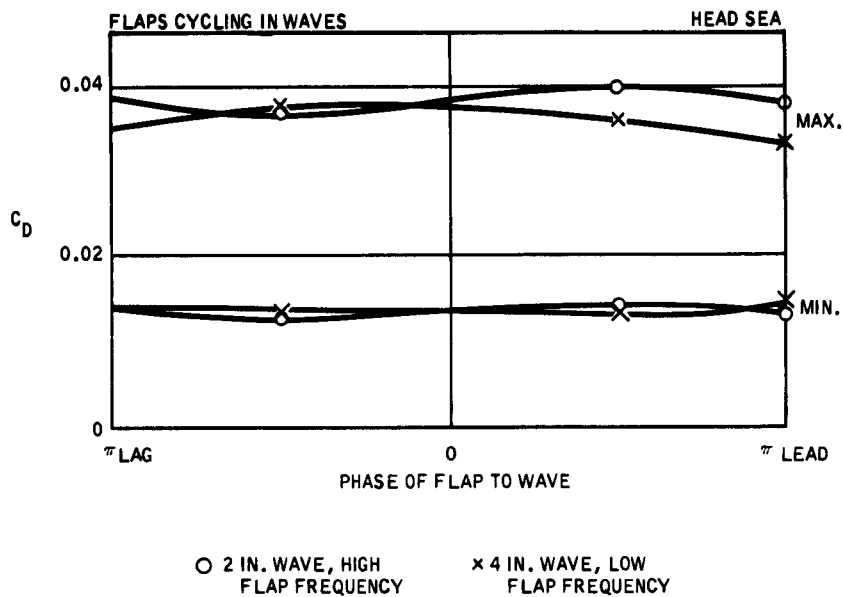
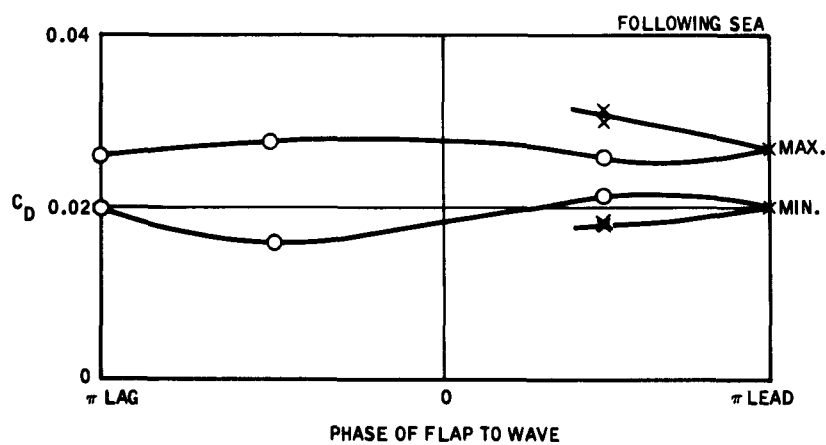
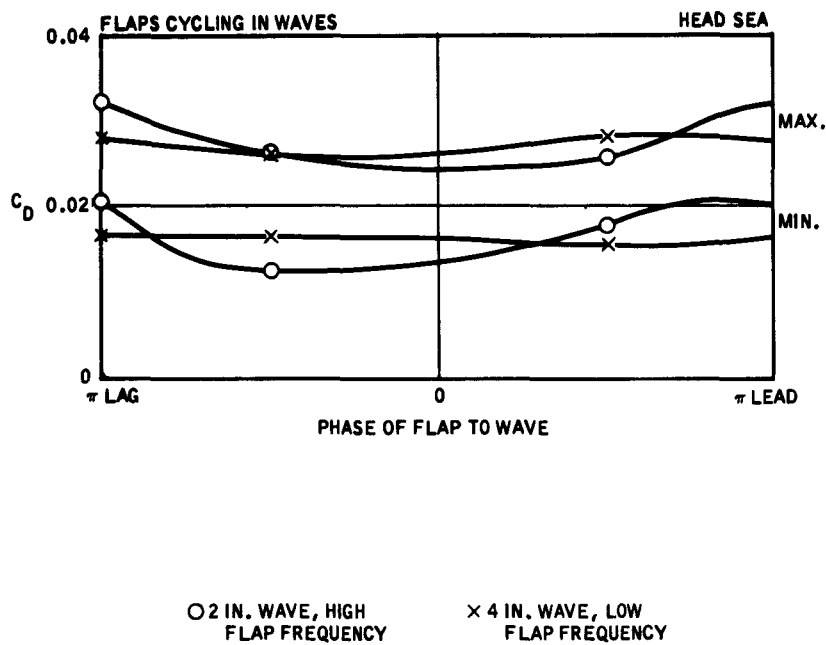
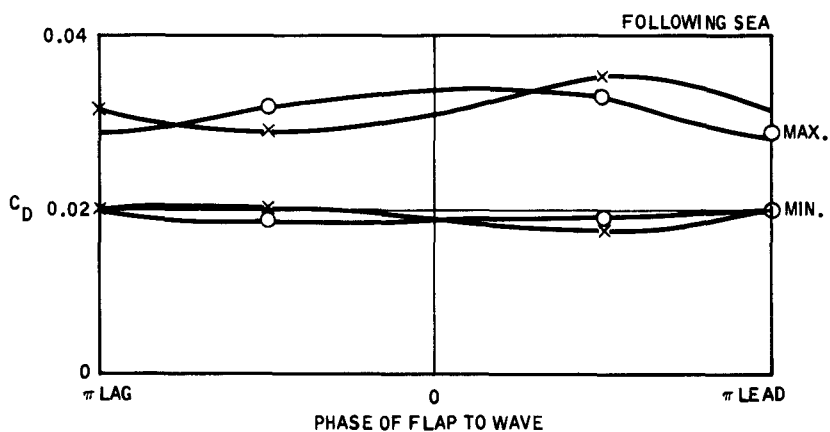
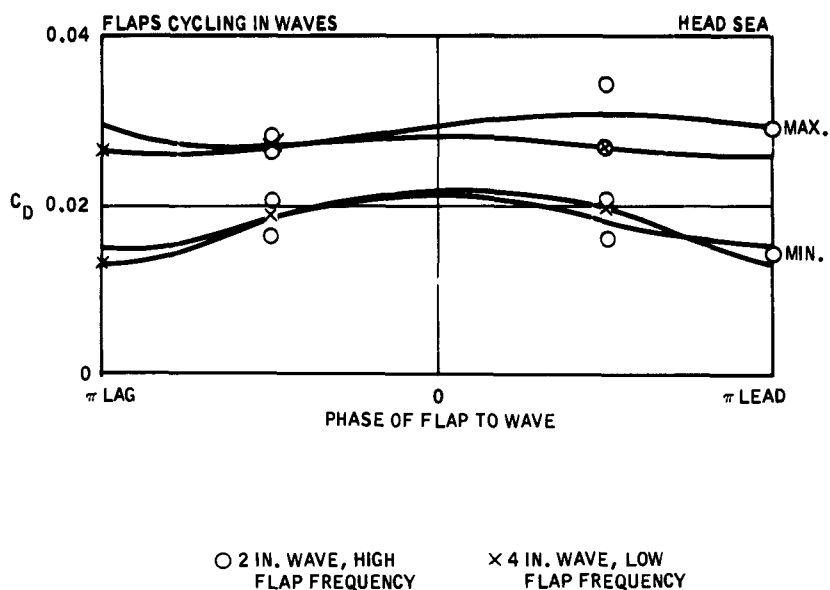


Figure 39. Flap Configuration 2 — Maximum and Minimum  $C_D$  Vs. Phase of Flap to Wave



**Figure 40. Flap Configuration 3 — Maximum and Minimum  $C_D$  Vs. Phase of Flap to Wave**



**Figure 41. Flap Configuration 4 — Maximum and Minimum  $C_D$  Vs. Phase of Flap to Wave**

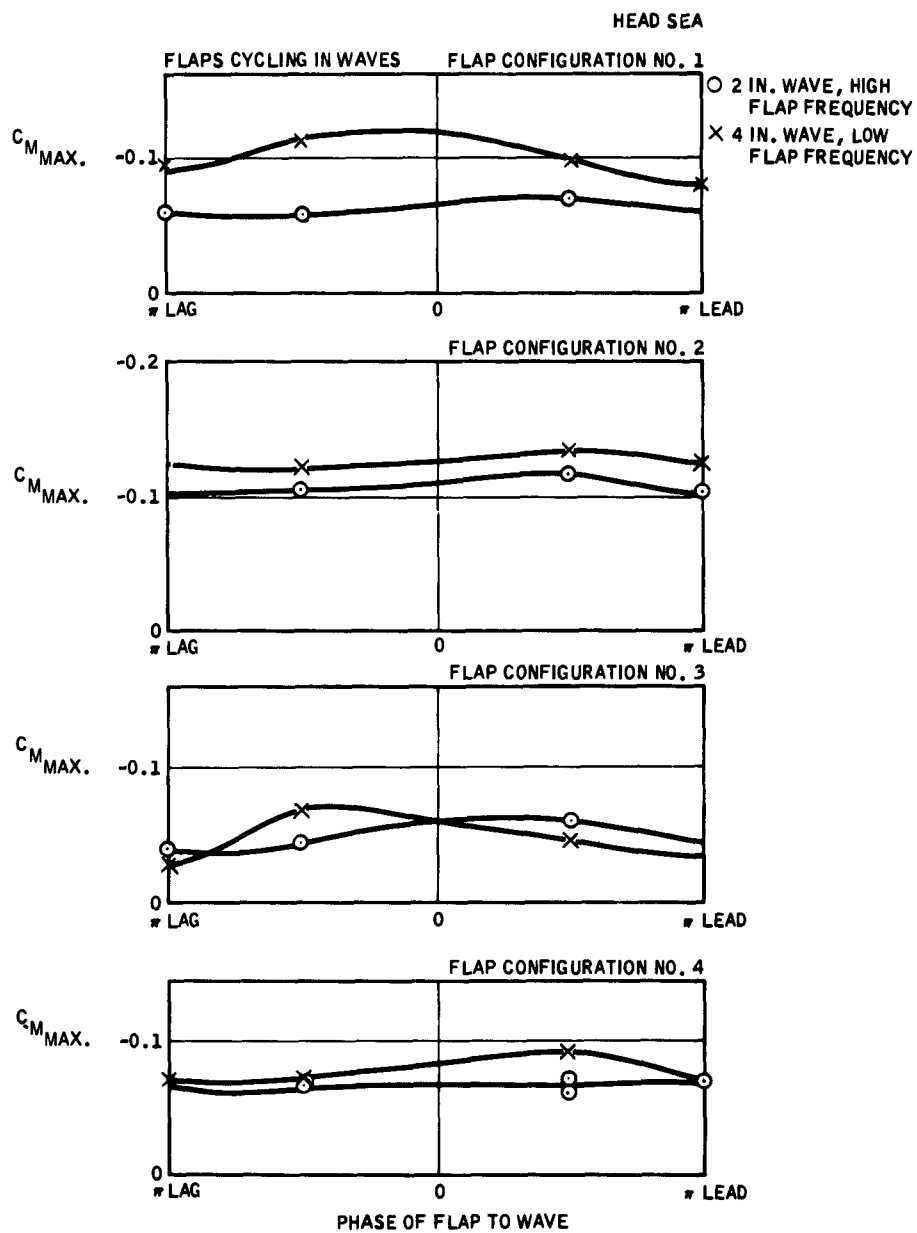


Figure 42. Maximum  $-C_M$  Vs. Phase of Flap to Wave

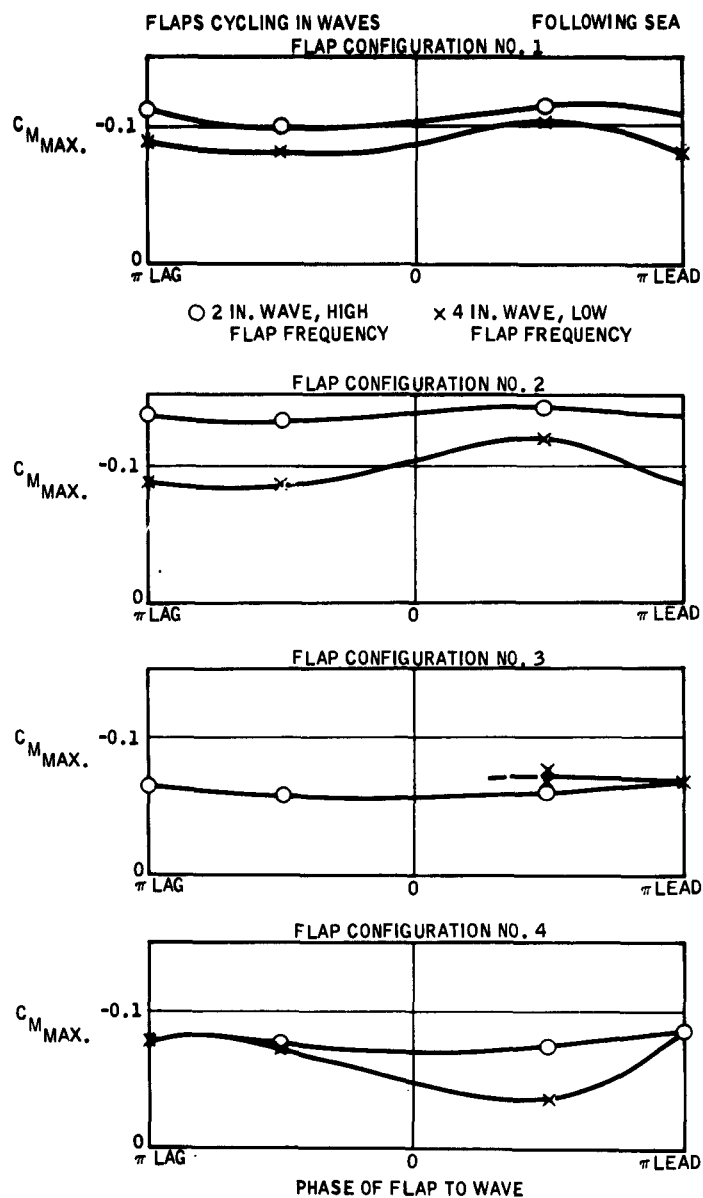


Figure 43. Maximum  $-C_M$  Vs. Phase of Flap to Wave

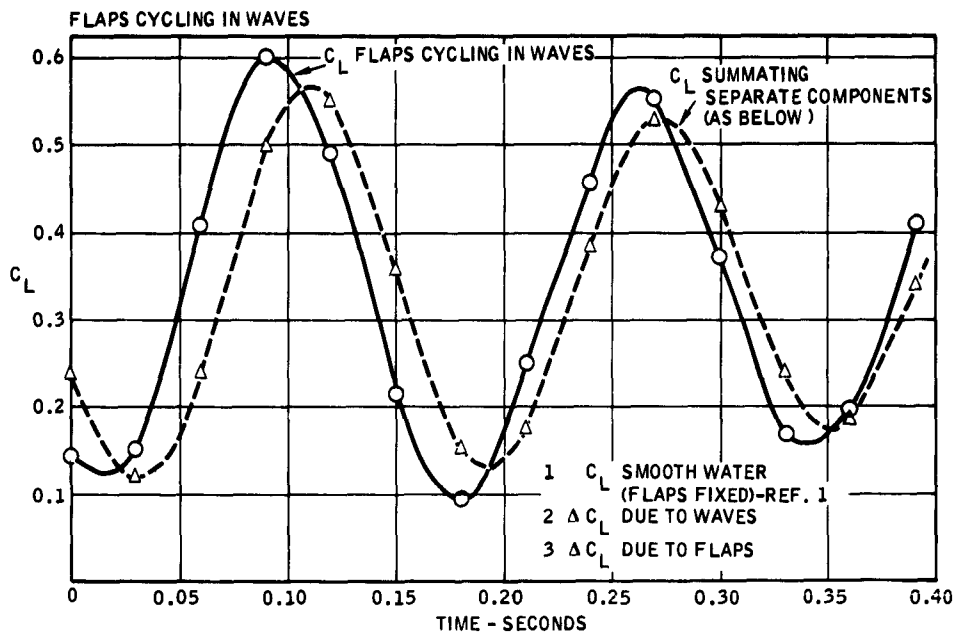


Figure 44. Run 13191, Flap Configuration 1 -  $C_L$   
Time History, Following Sea

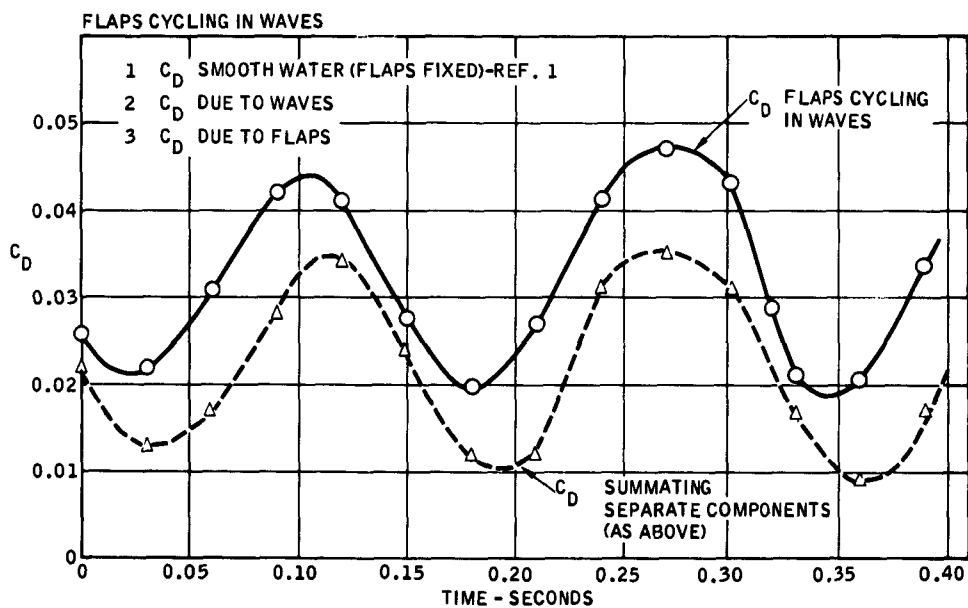


Figure 45. Run 13191, Flap Configuration 1 -  $C_D$   
Time History, Following Sea

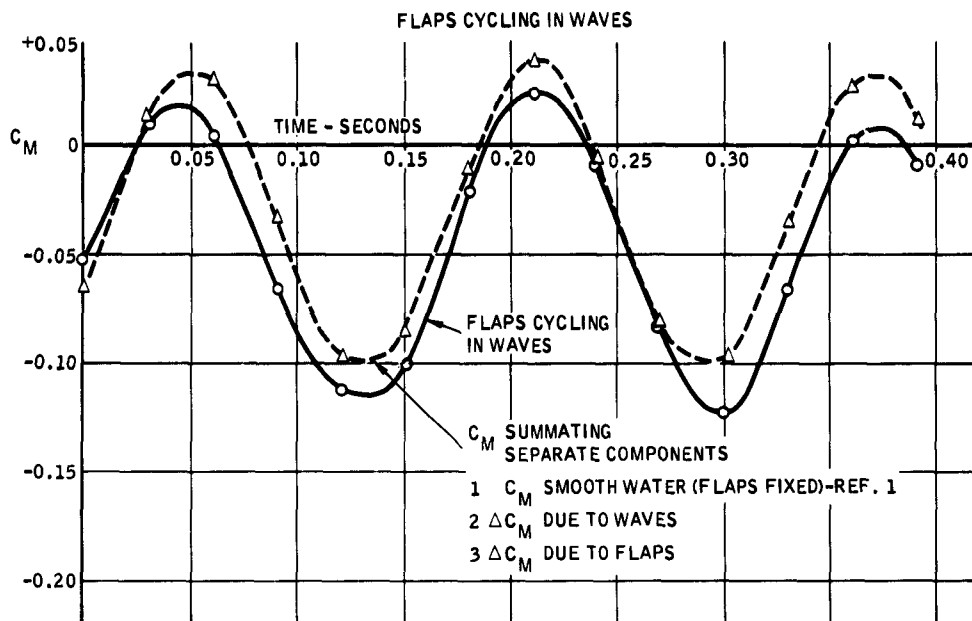


Figure 46. Run 13191, Flap Configuration 1 -  $C_M$  Time History, Following Sea

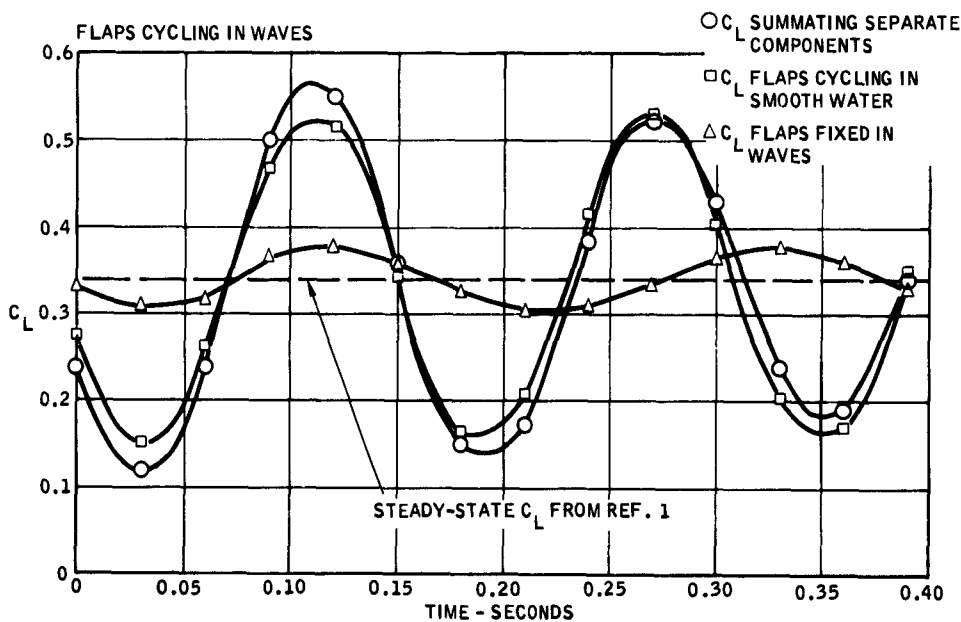


Figure 47. Run 13191, Flap Configuration 1 -  $C_L$  Time History, Comparison of Flap and Wave Effects

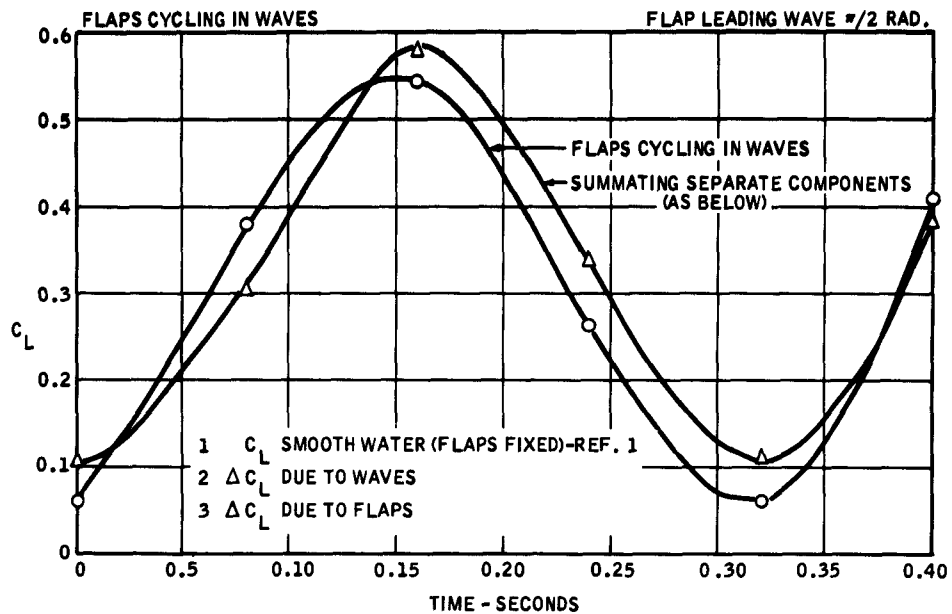


Figure 48. Run 13157, Flap Configuration 1 —  $C_L$   
Time History, Head Sea

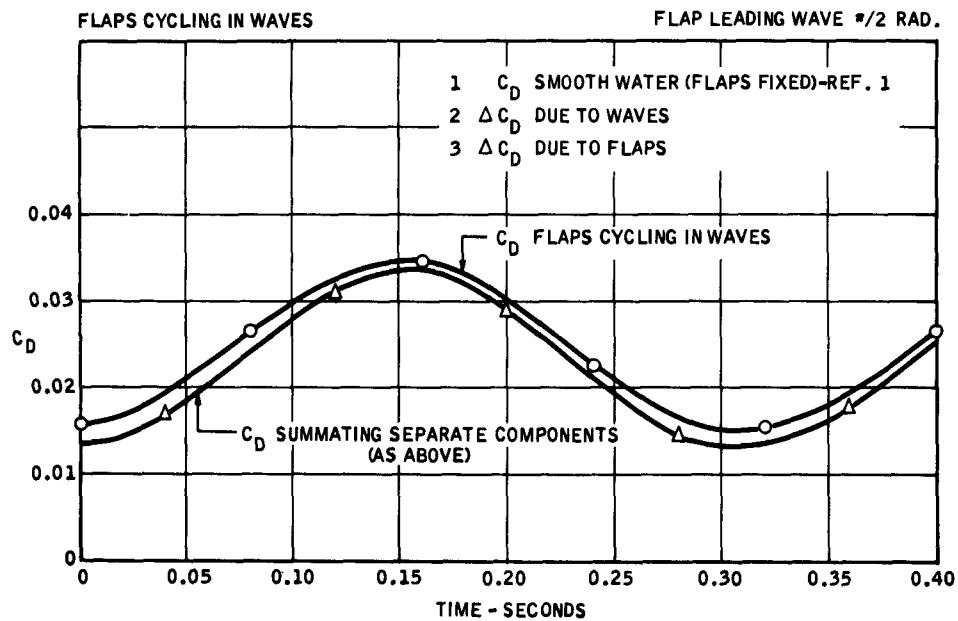


Figure 49. Run 13157, Flap Configuration 1 —  $C_D$   
Time History, Head Sea

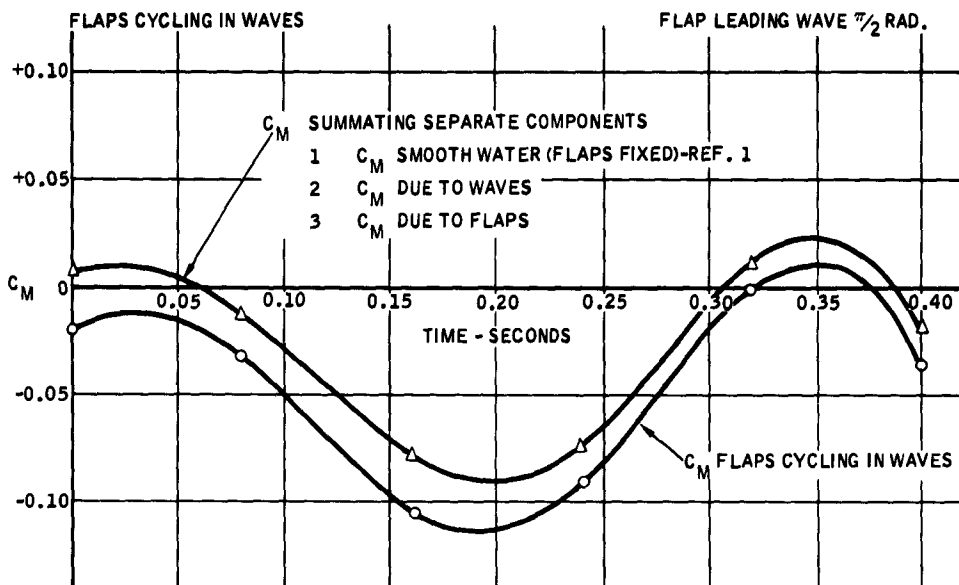


Figure 50. Run 13157, Flap Configuration 1 -  $C_M$  Time History, Head Sea

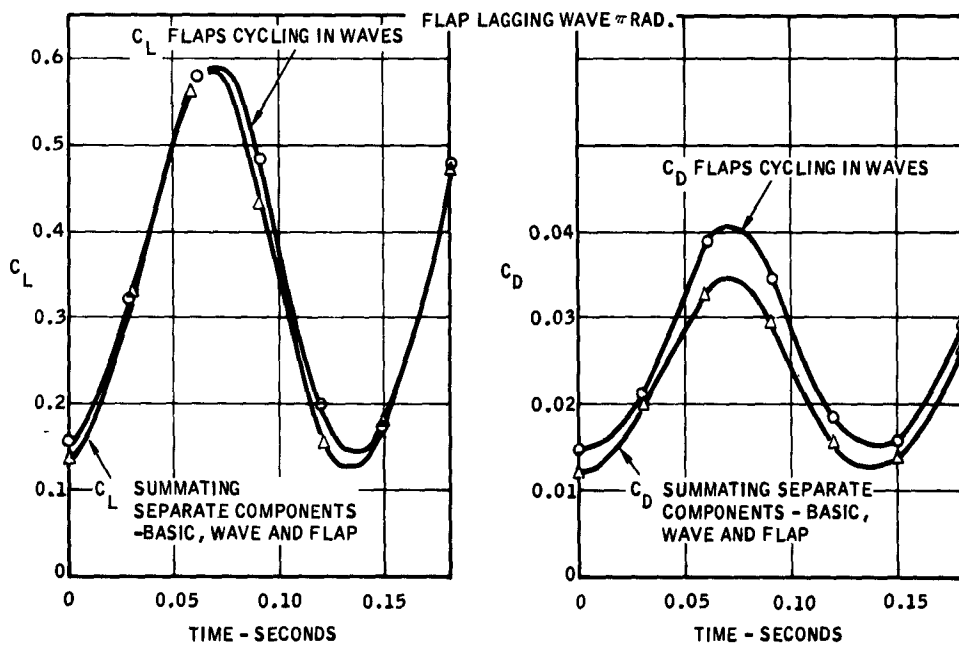


Figure 51. Run 13154, Flap Configuration 1 -  $C_L$  and  $C_D$  Time History, Head Sea

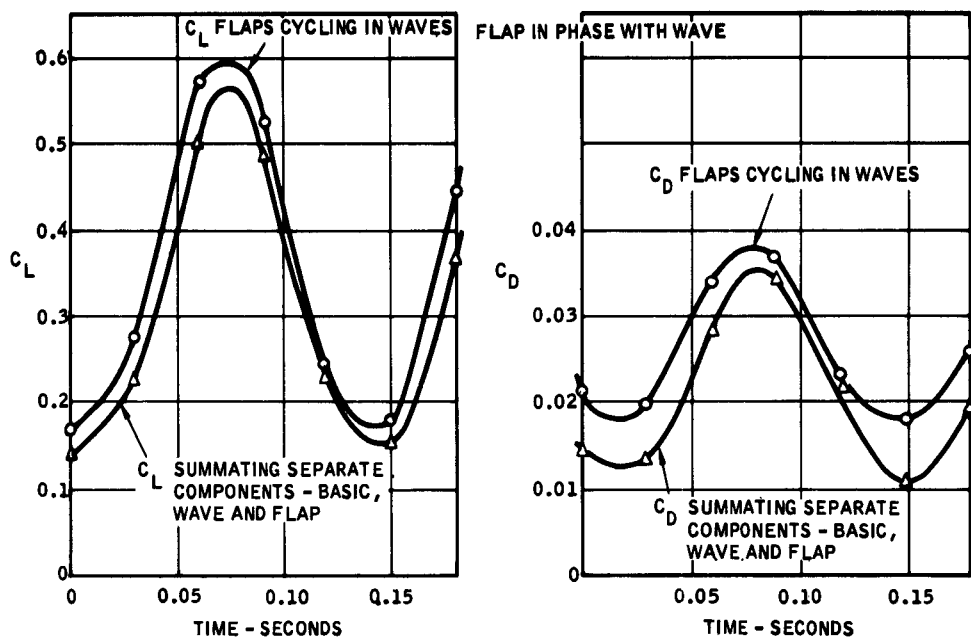


Figure 52. Run 13154, Flap Configuration 1 —  $C_L$  and  $C_D$  Time History, Head Sea

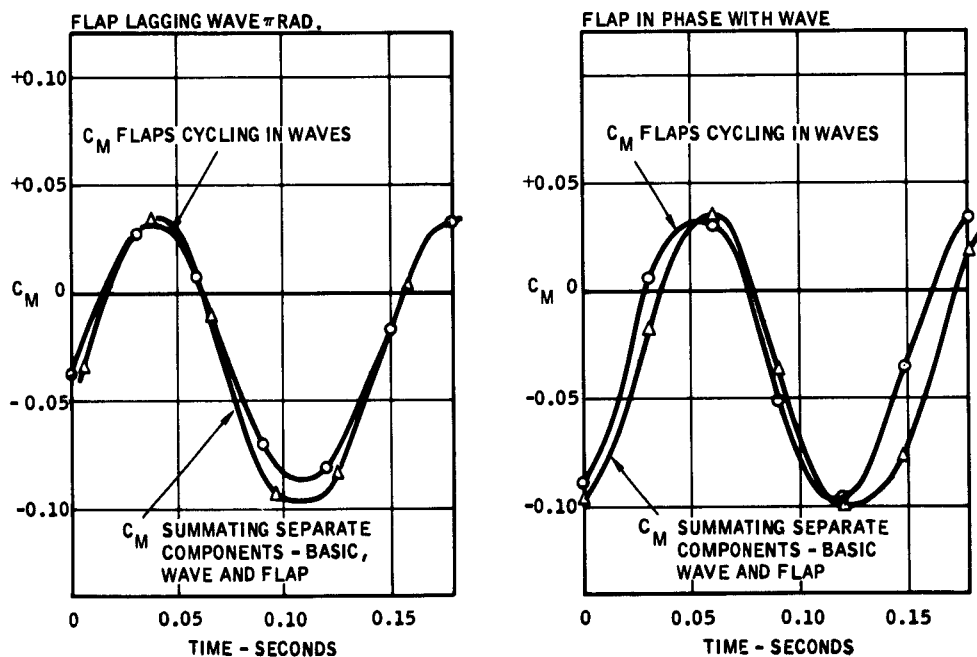
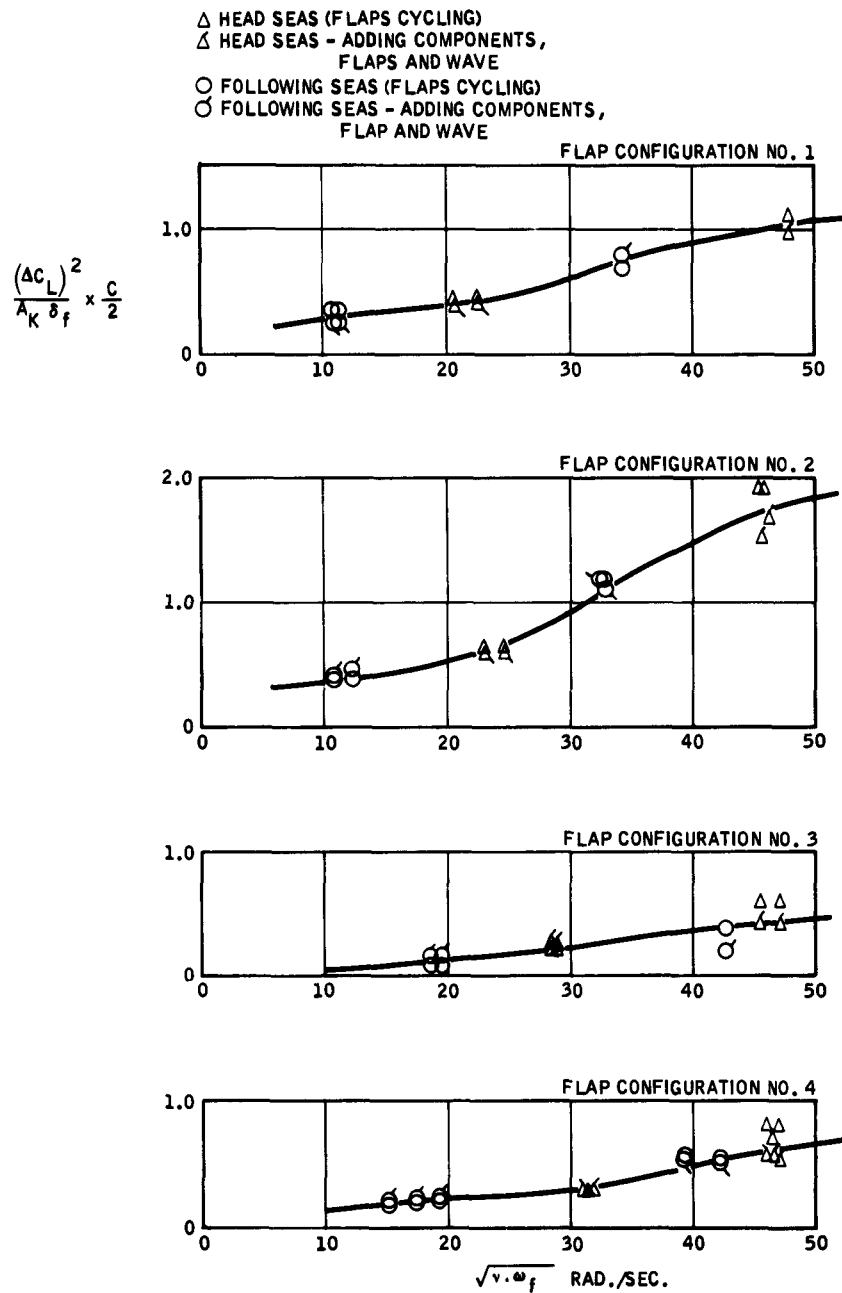
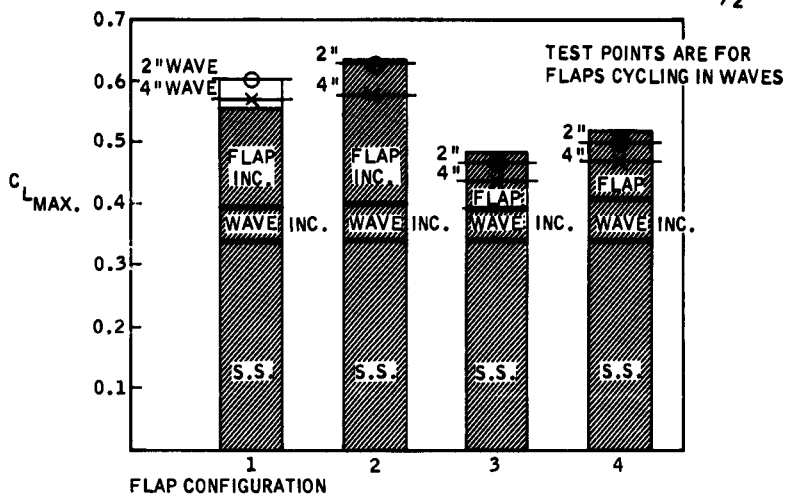


Figure 53. Run 13154, Flap Configuration 1 —  $C_M$  Time History, Head Sea



**Figure 54. Maximum Lift Frequency Response, Flaps Oscillating in Waves, All Models — Comparisons with Separate Tests**

ALL FLAP CONFIGURATIONS  $\alpha = 5^\circ$   
 HEAD SEA - MAX. FLAP DOWN LEADING WAVE BY  $\pi/2$  RAD.



FOLLOWING SEA - MAX. FLAP DOWN LAGGING WAVE BY  $\pi/2$  RAD.

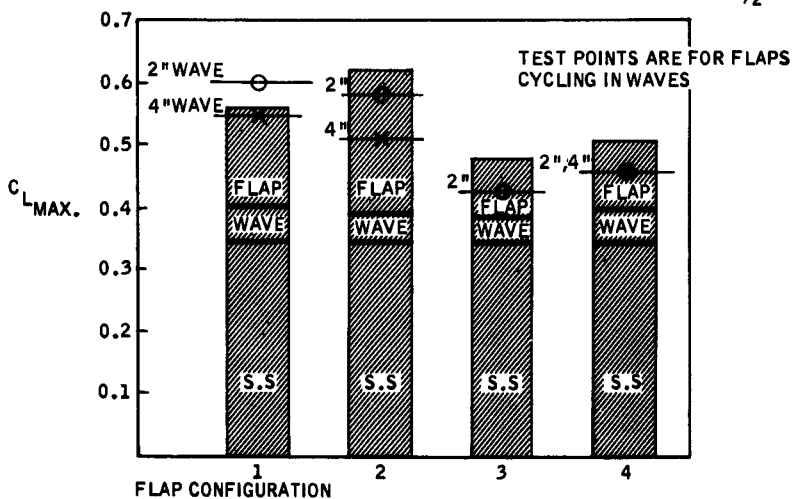


Figure 55. Summary of Flap and Wave Effectiveness

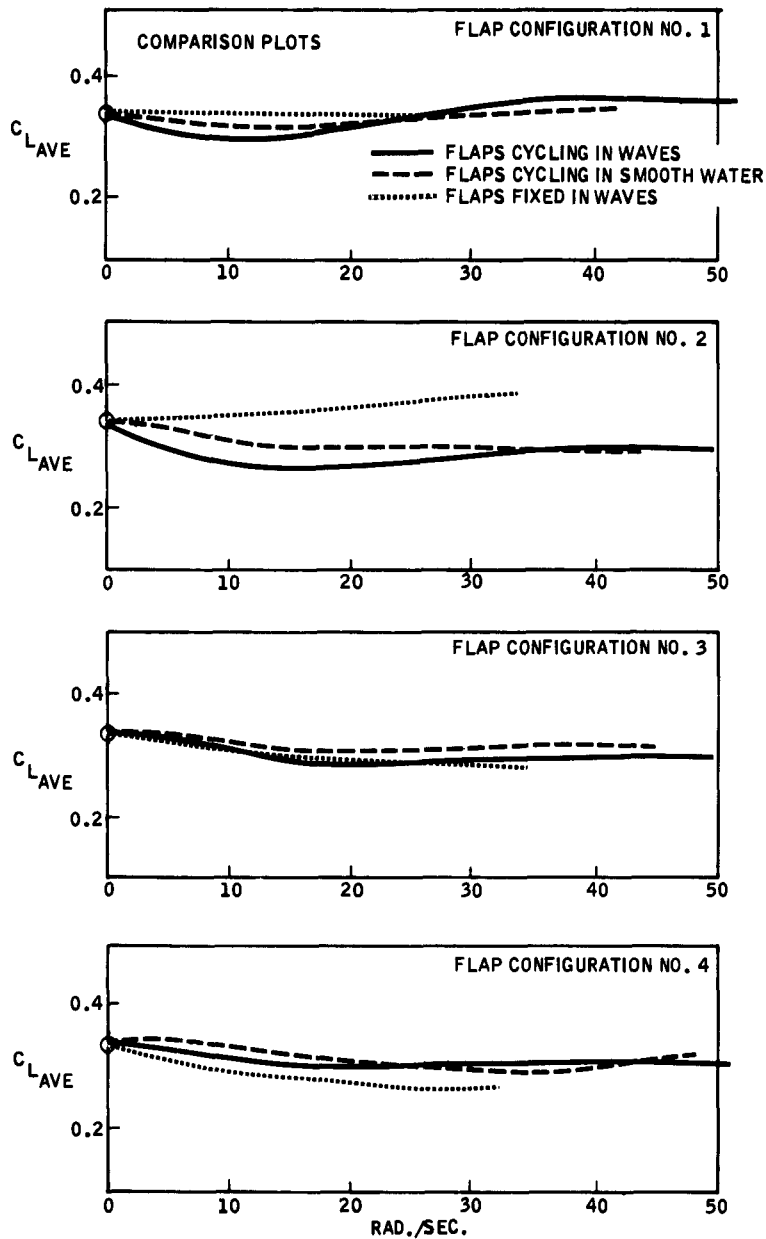
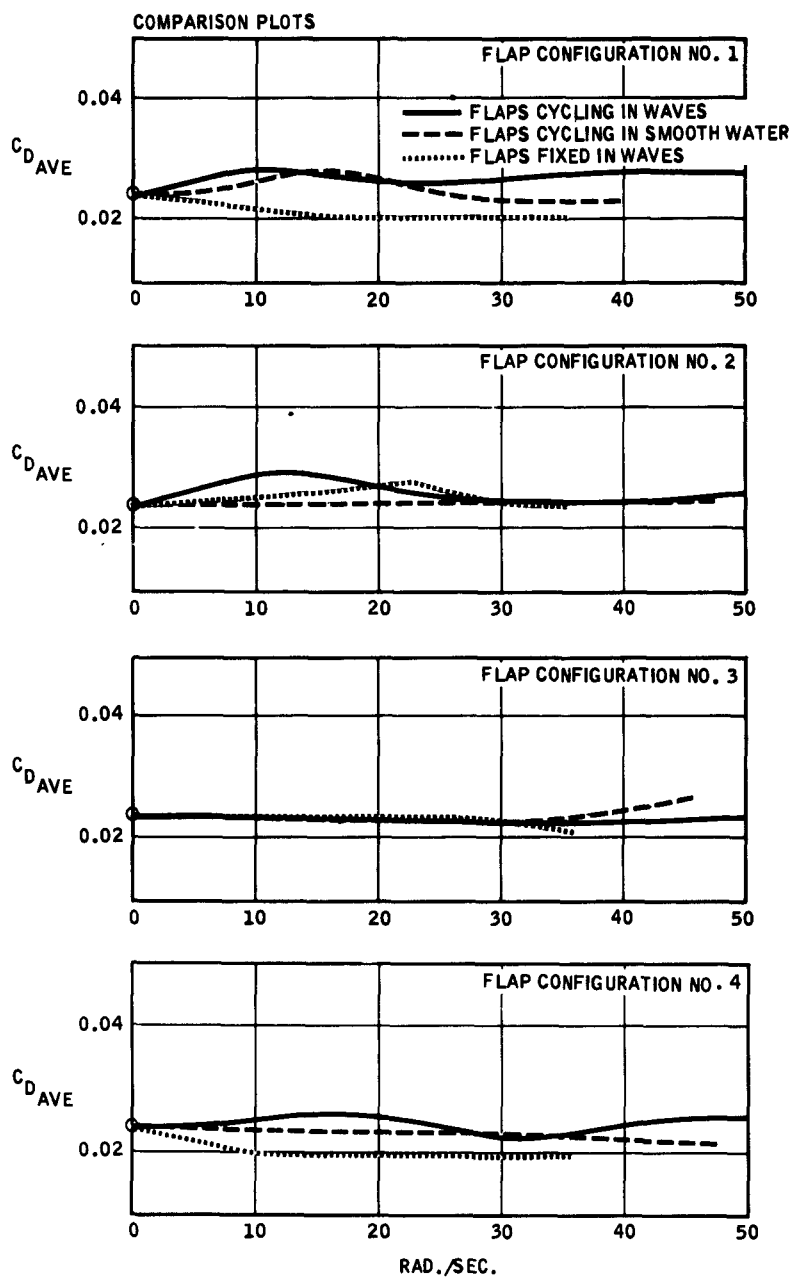


Figure 56. Mean Values of Lift Coefficients — All Models



**Figure 57. Mean Values of Drag Coefficients — All Models**

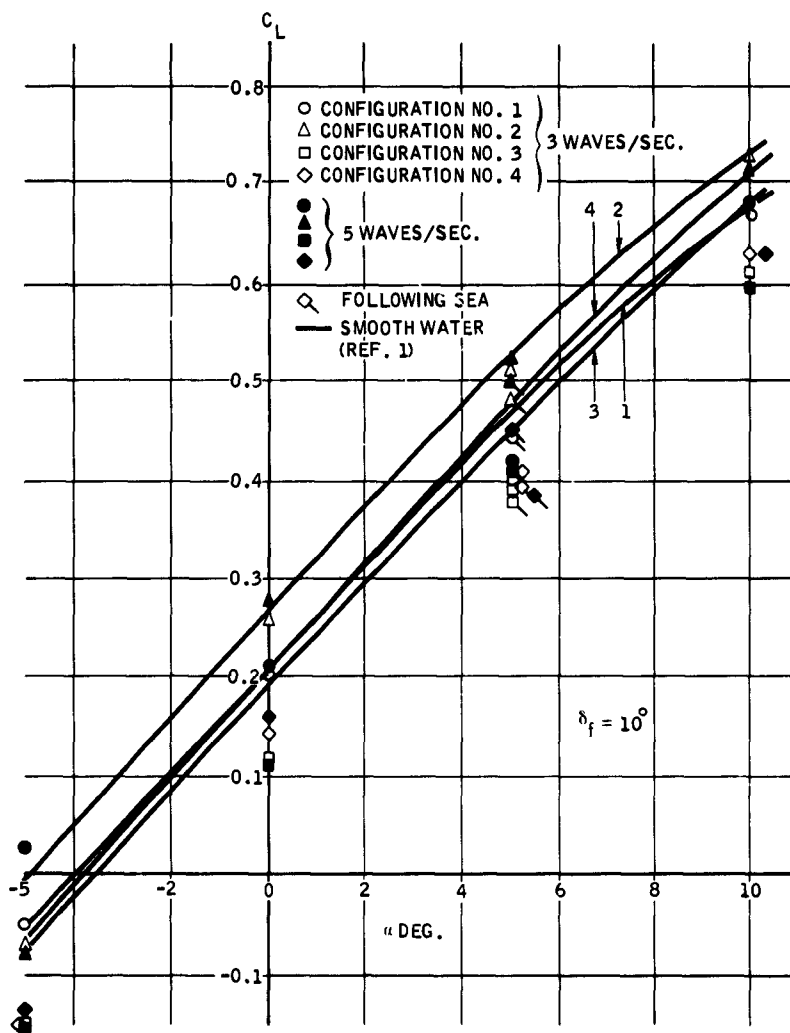


Figure 58. Average  $C_L$  Vs.  $\alpha$ , Flaps Fixed in Waves, and Smooth Water (Ref. 1)

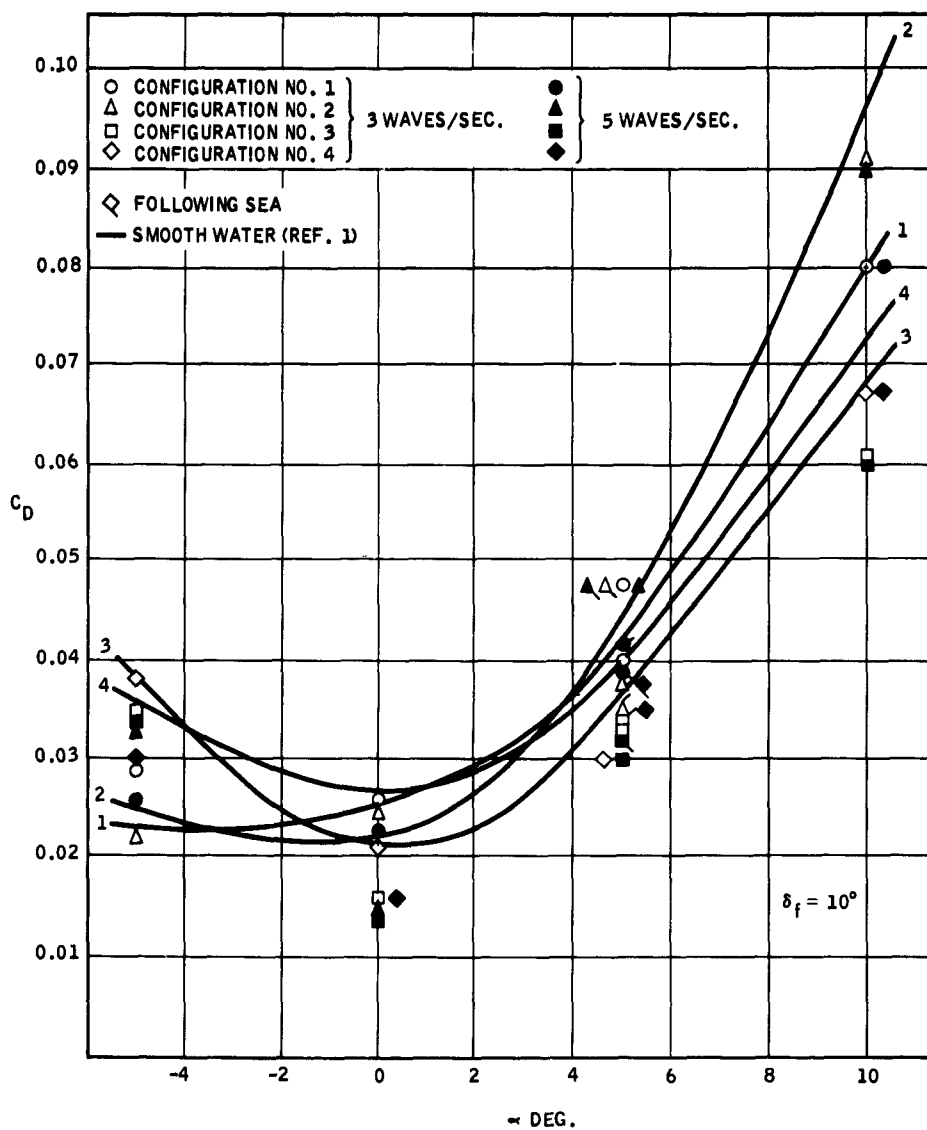


Figure 59. Average  $C_D$  Vs.  $\alpha$ , Flaps Fixed in Waves, and Smooth Water (Ref. 1)

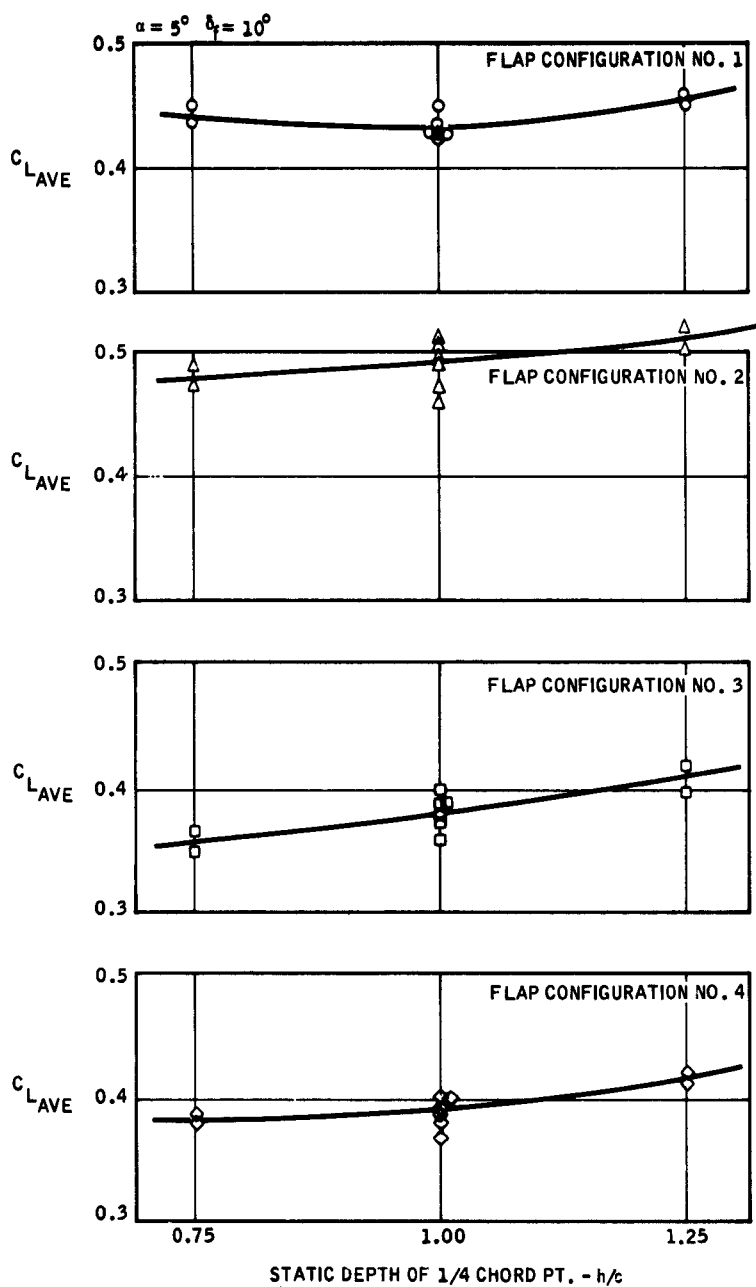
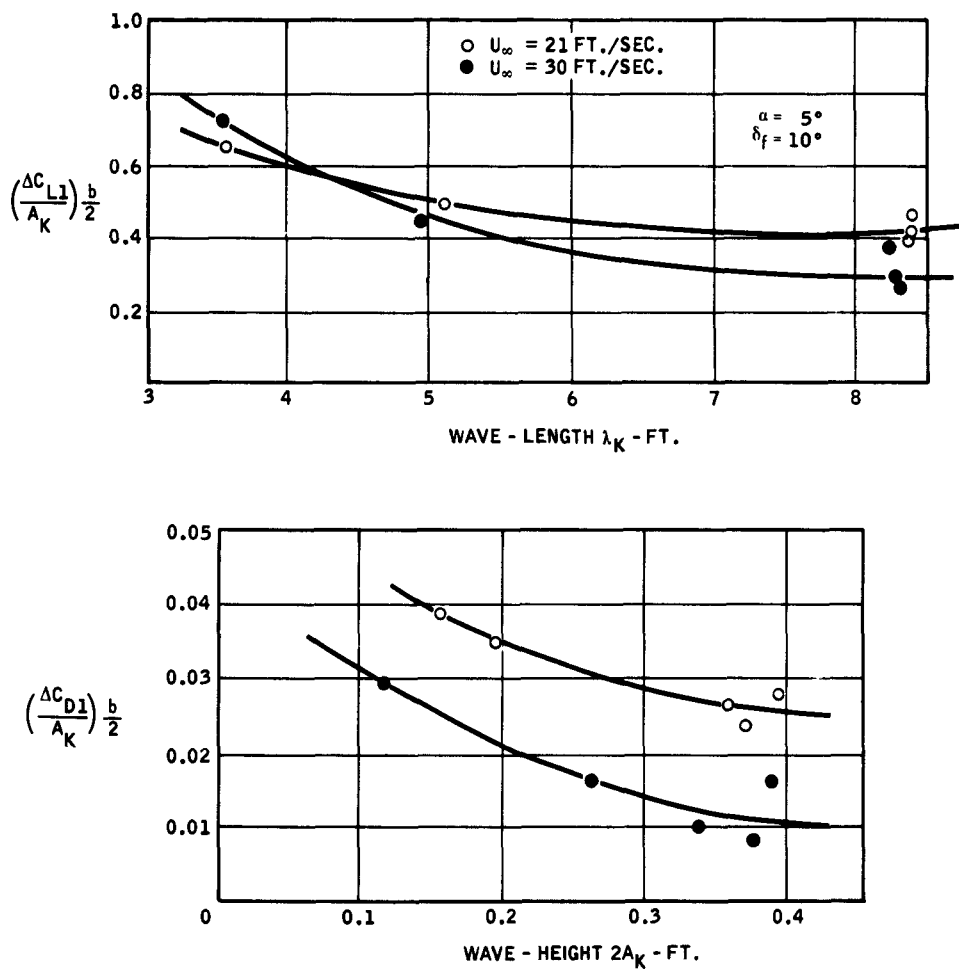


Figure 60. Effect of Depth on Average  $C_L$ , Flaps Fixed in Waves, Following Sea



**Figure 61. Flap Configuration 1 — Oscillatory Lift and Drag Parameters, Flaps Fixed in Waves, Following Sea**

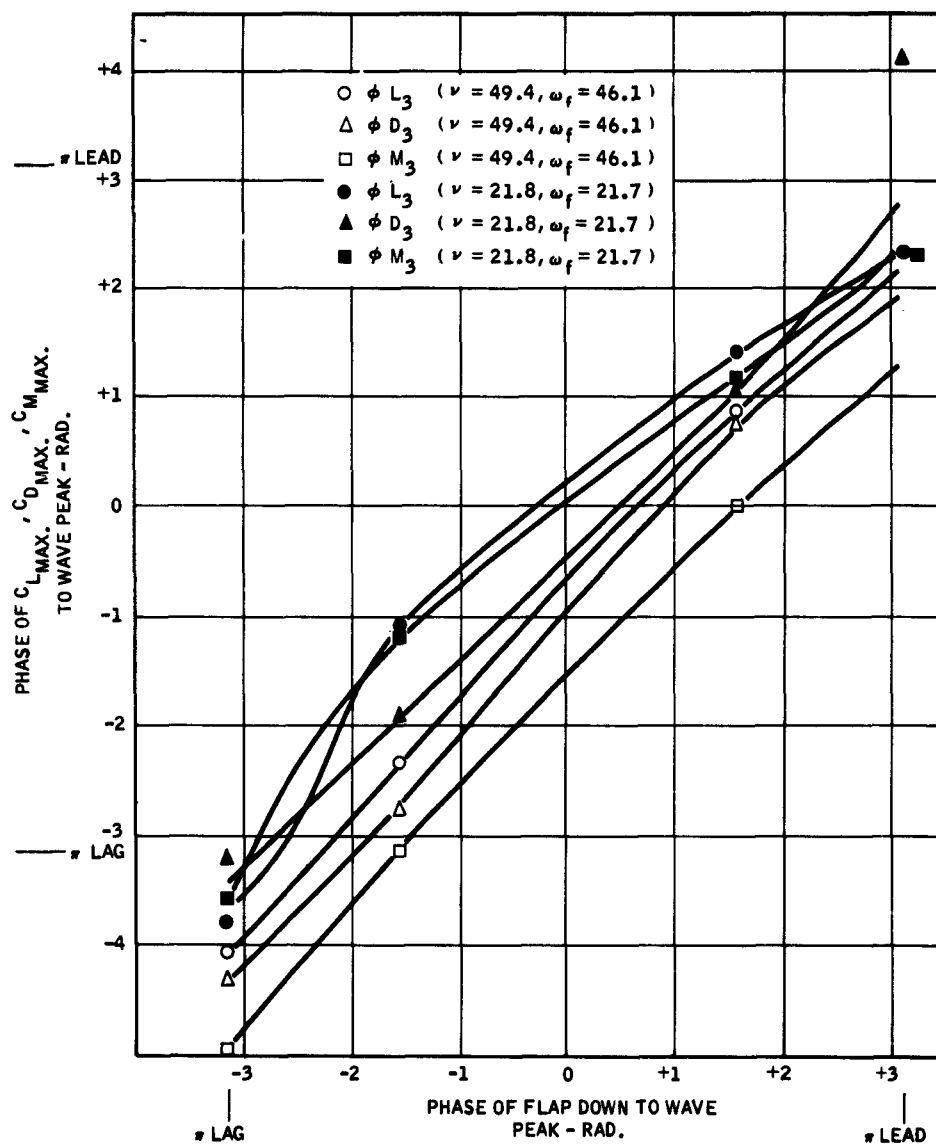


Figure 62. Flap Configuration 1 — Phase Relationships — Flaps Cycling in Waves, Head Sea

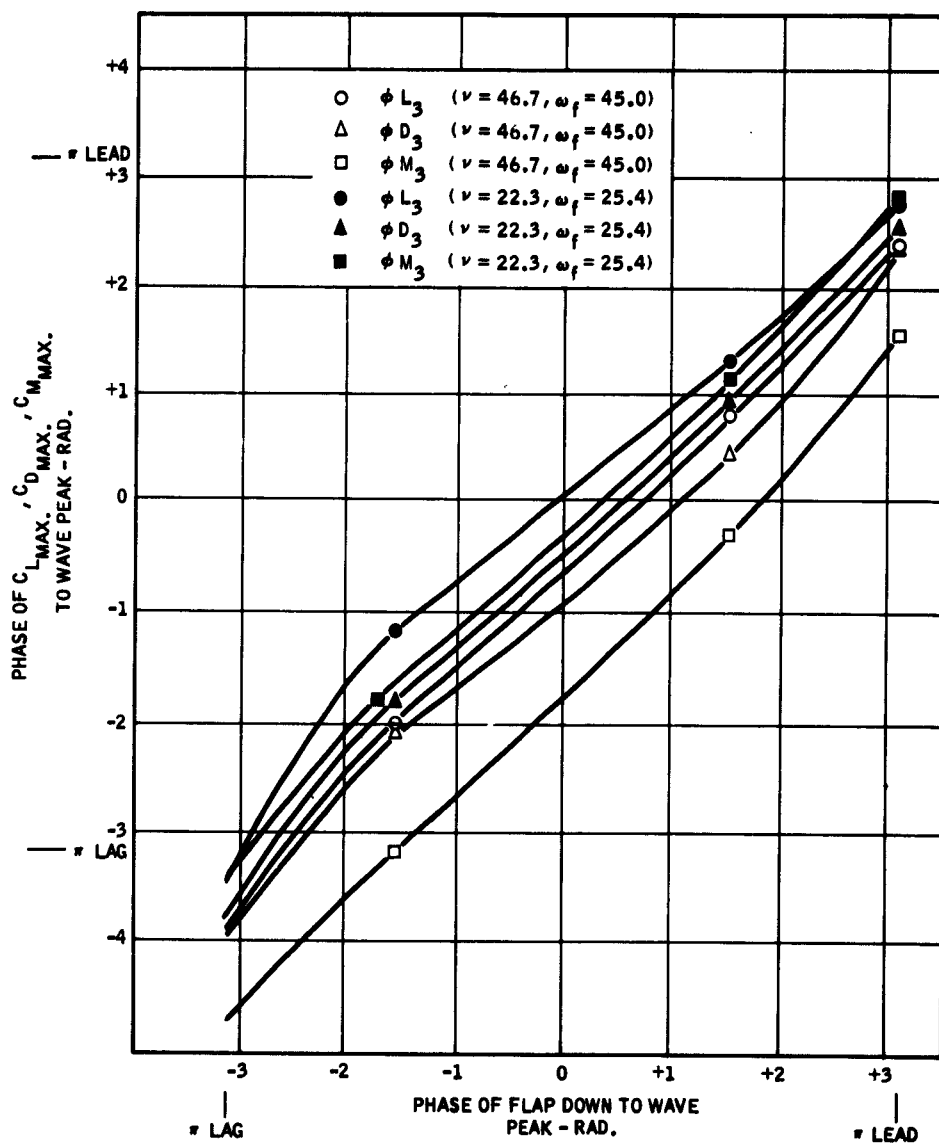


Figure 63. Flap Configuration 2, Phase Relationships — Flaps Cycling in Waves, Head Sea

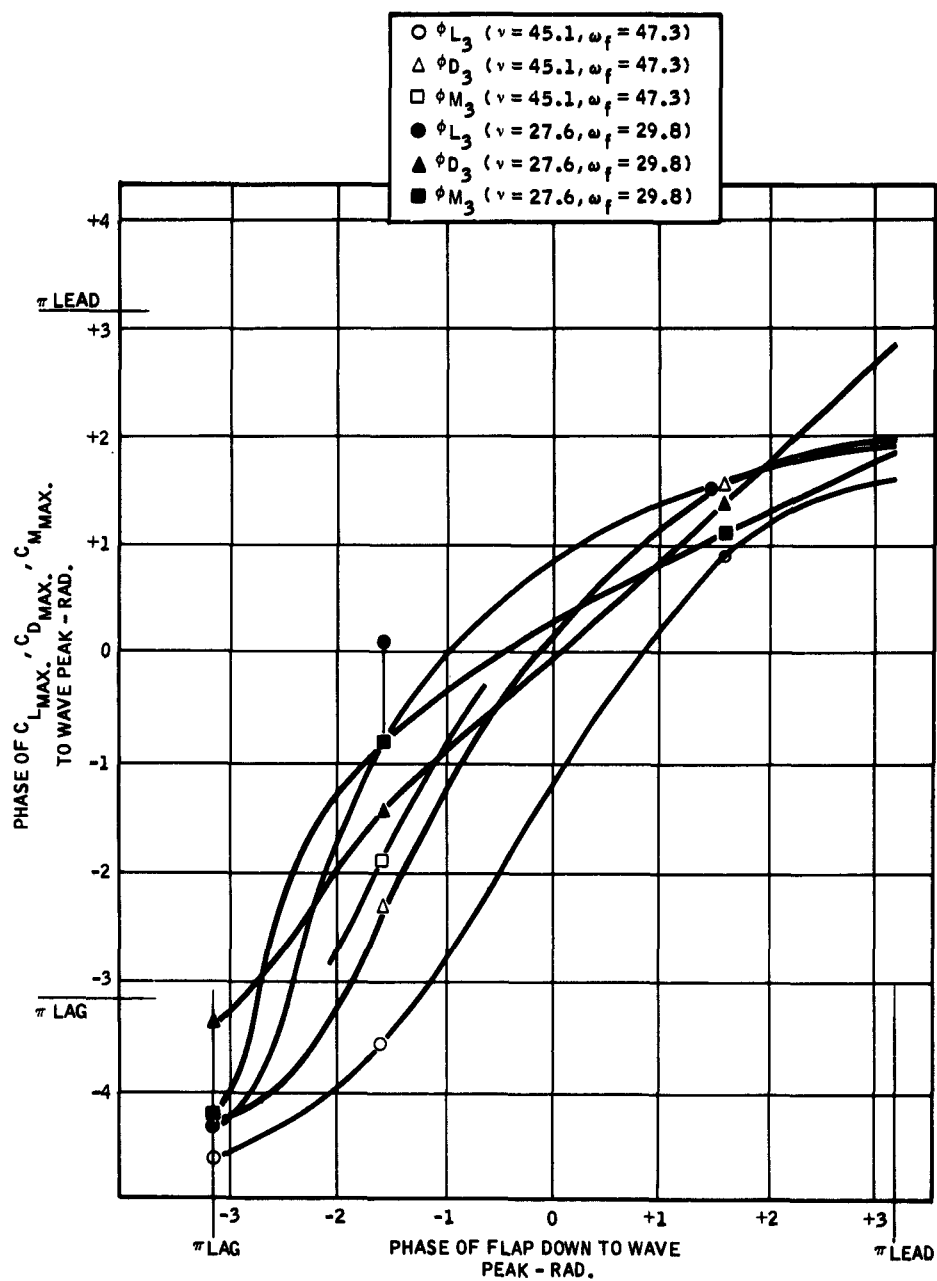


Figure 64. Flap Configuration 3, Phase Relationships — Flaps Cycling in Waves, Head Sea

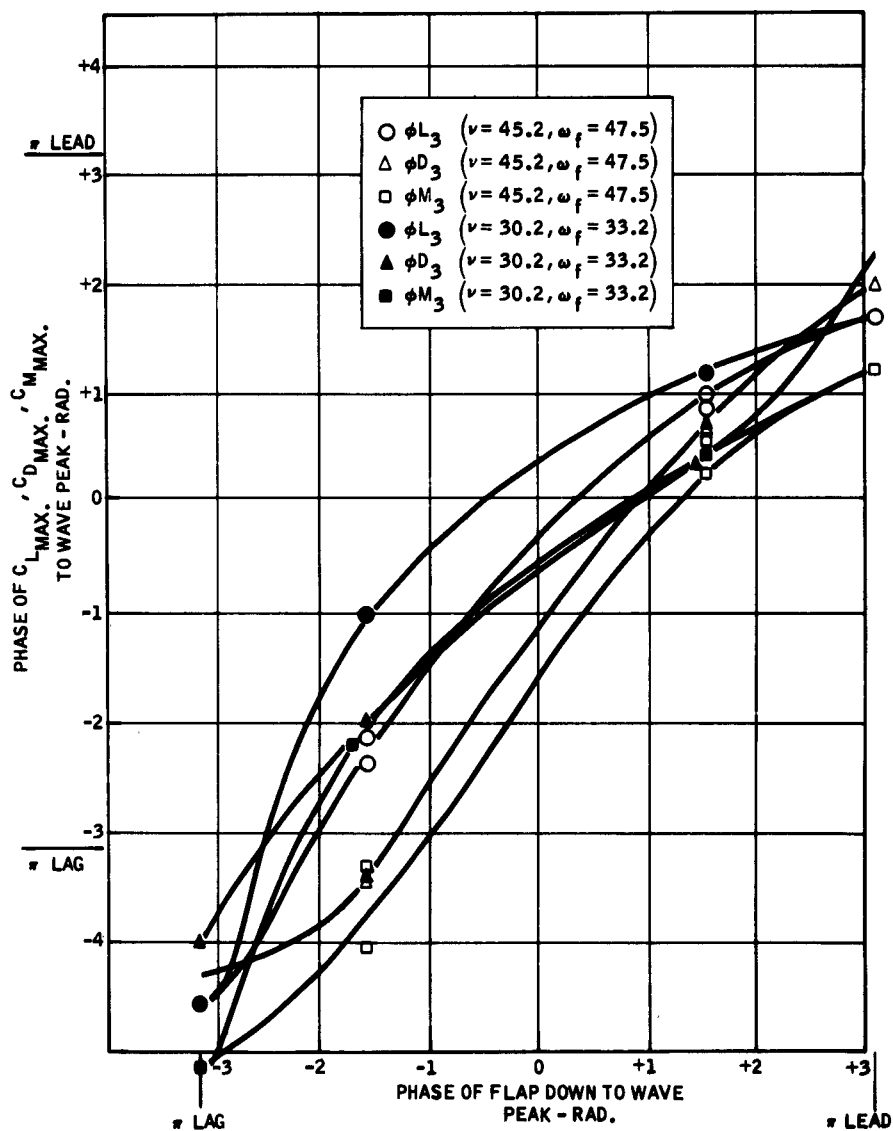


Figure 65. Flap Configuration 4, Phase Relationships — Flaps Cycling in Waves, Following Sea

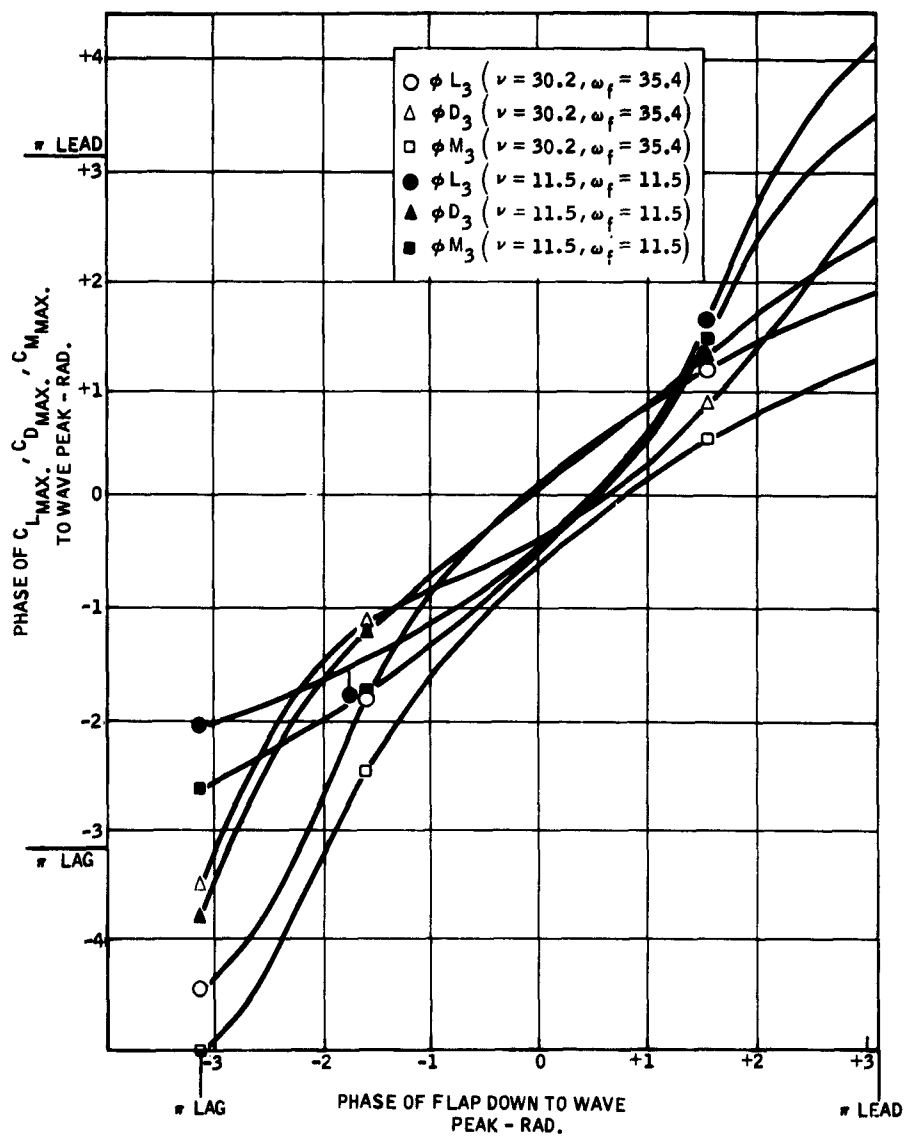


Figure 66. Flap Configuration 2, Phase Relationships — Flaps Cycling in Waves, Following Sea

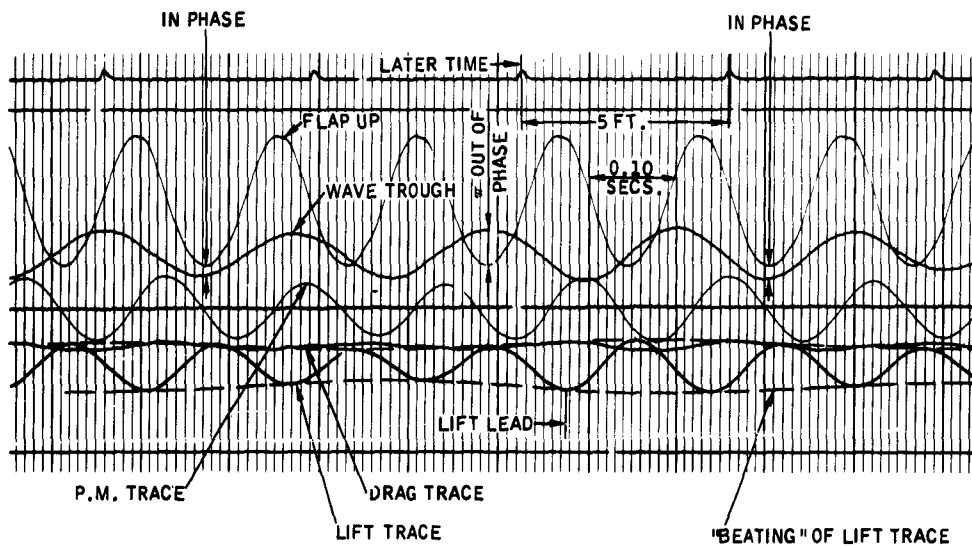


Figure 67. Typical Oscillograph Record, Flaps Cycling in Waves, Following Sea, Run 13191

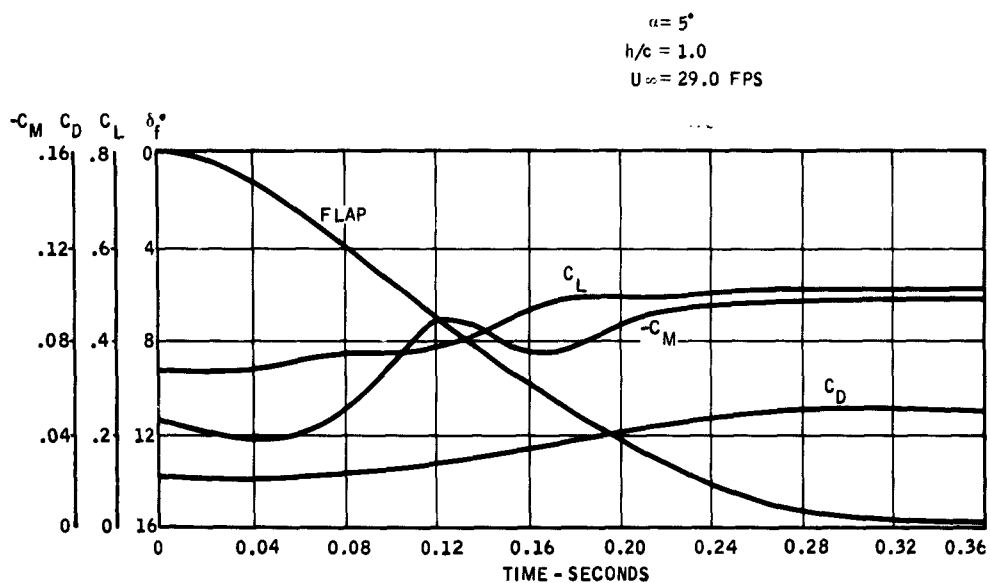


Figure 68. Sudden Flap Deflection, Time History of Force and Moment Build-up — Flap Configuration 1, Run 13125, 16 CPS Flap Cycling Rate

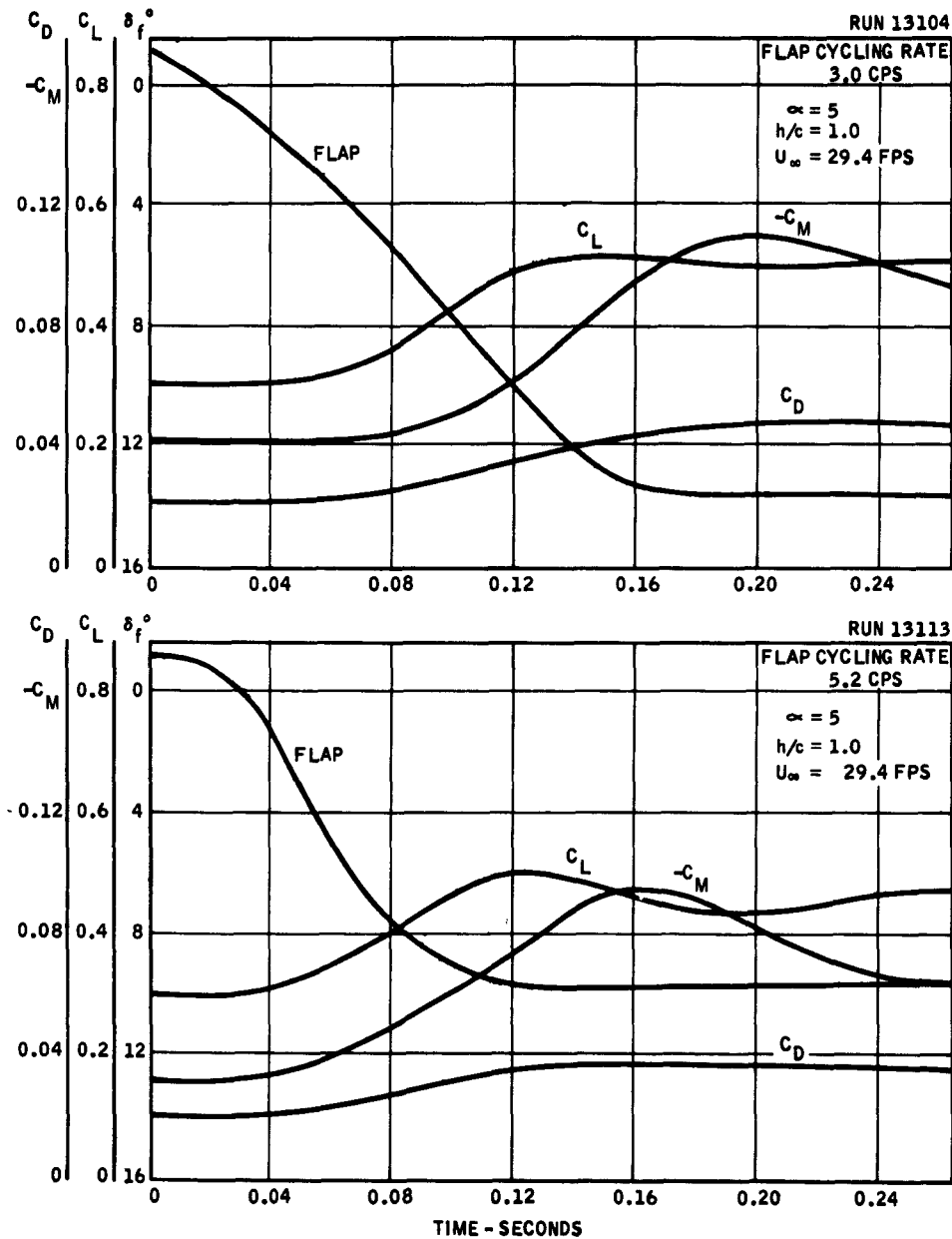


Figure 69. Sudden Flap Deflection, Time History of Force and Moment Build-up — Flap Configuration 1

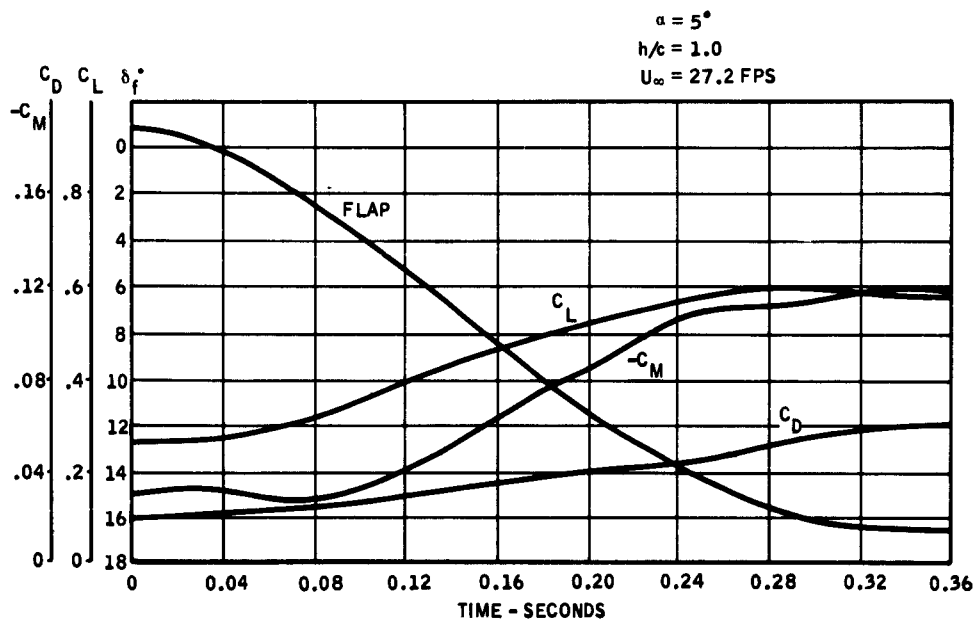
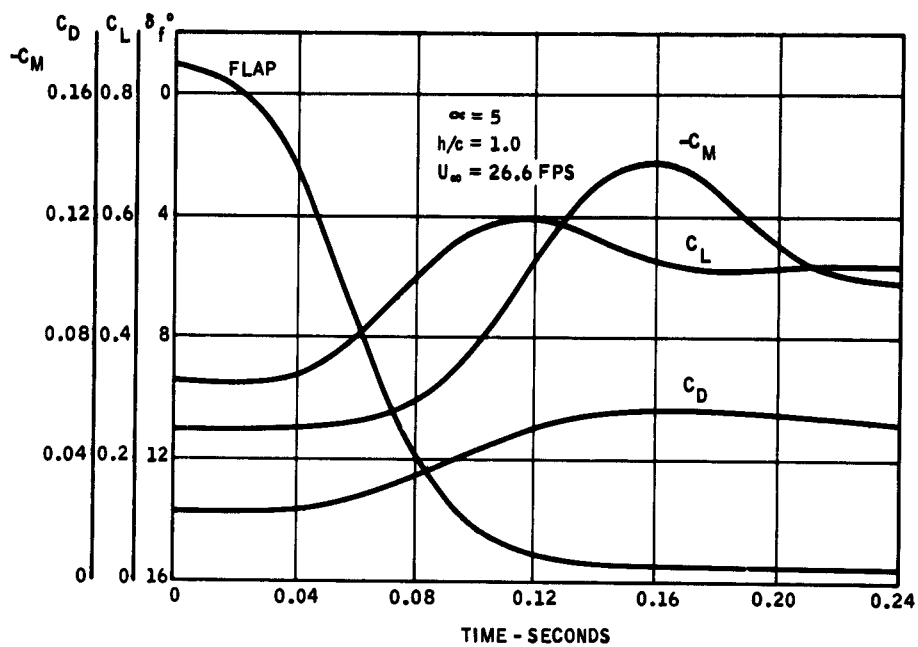
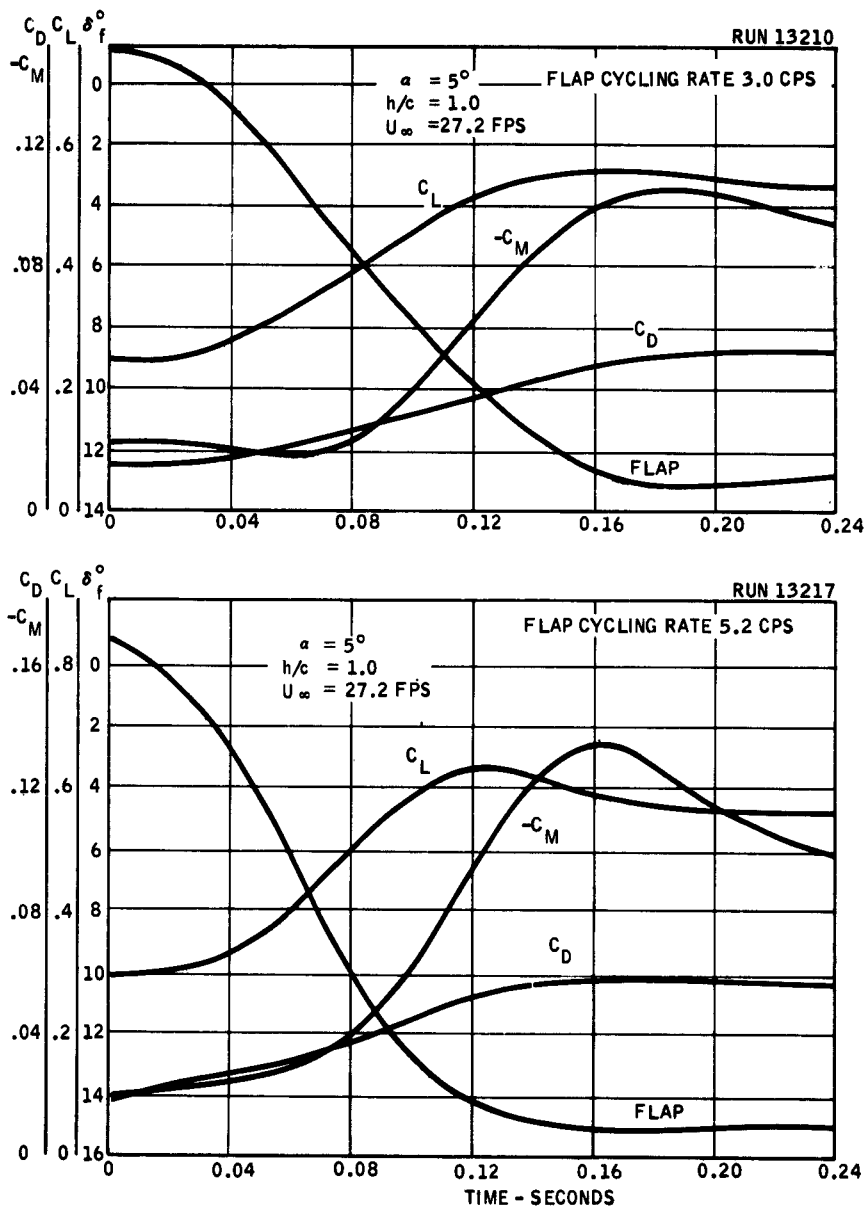
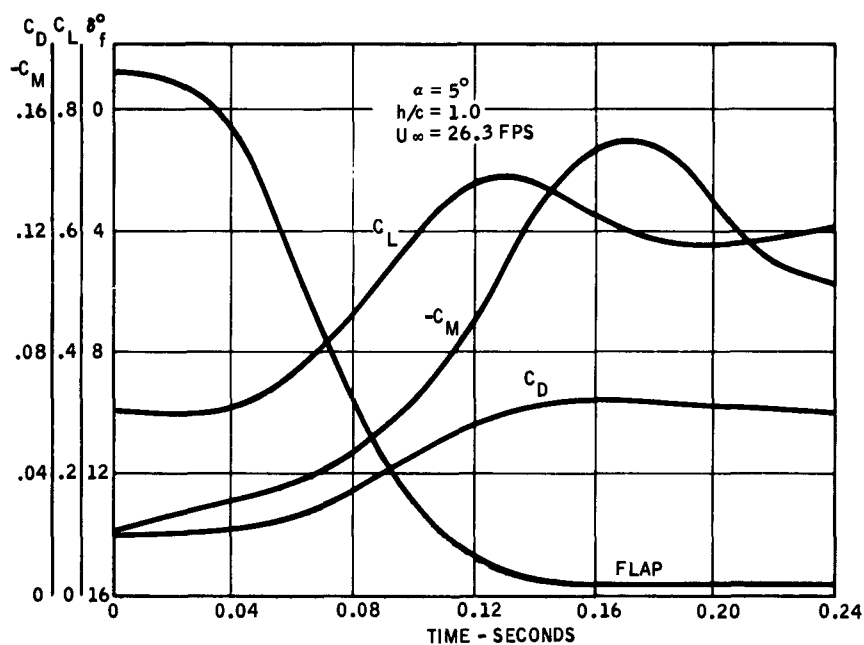


Figure 71. Sudden Flap Deflection, Time History of Force and Moment Build-up  
 - Flap Configuration 2, Run 13230, 1.6 CPS Flap Cycling Rate



**Figure 72. Sudden Flap Deflection, Time History of Force and Moment Build-Up — Flap Configuration 2, Run 13210**



**Figure 73. Sudden Flap Deflection, Time History of Force and Moment Build-Up**  
**- Flap Configuration 2, Run 13219, 6.5 CPS Flap Cycling Rate**

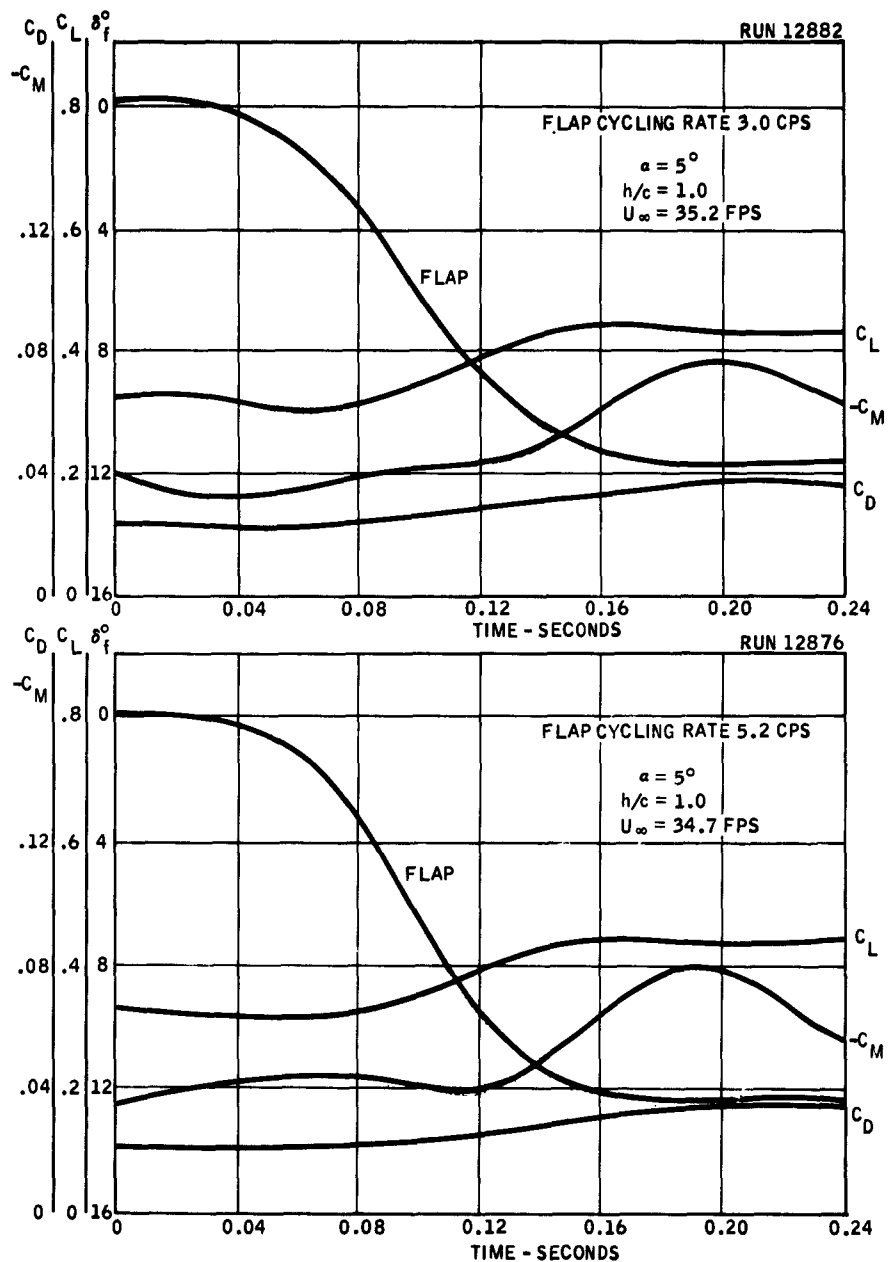


**Figure 74. Sudden Flap Deflection, Time History of Force and Moment Build-Up — Flap Configuration 3**

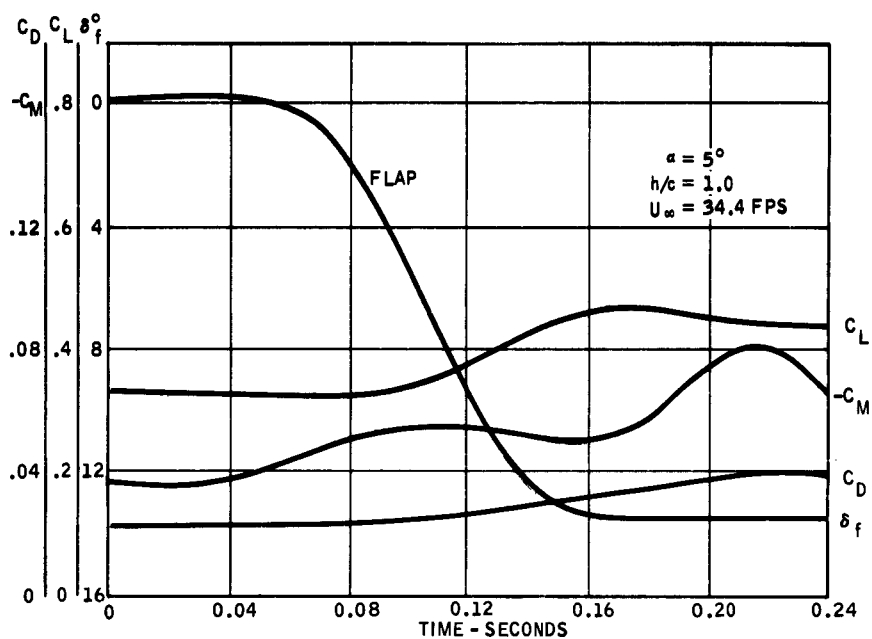
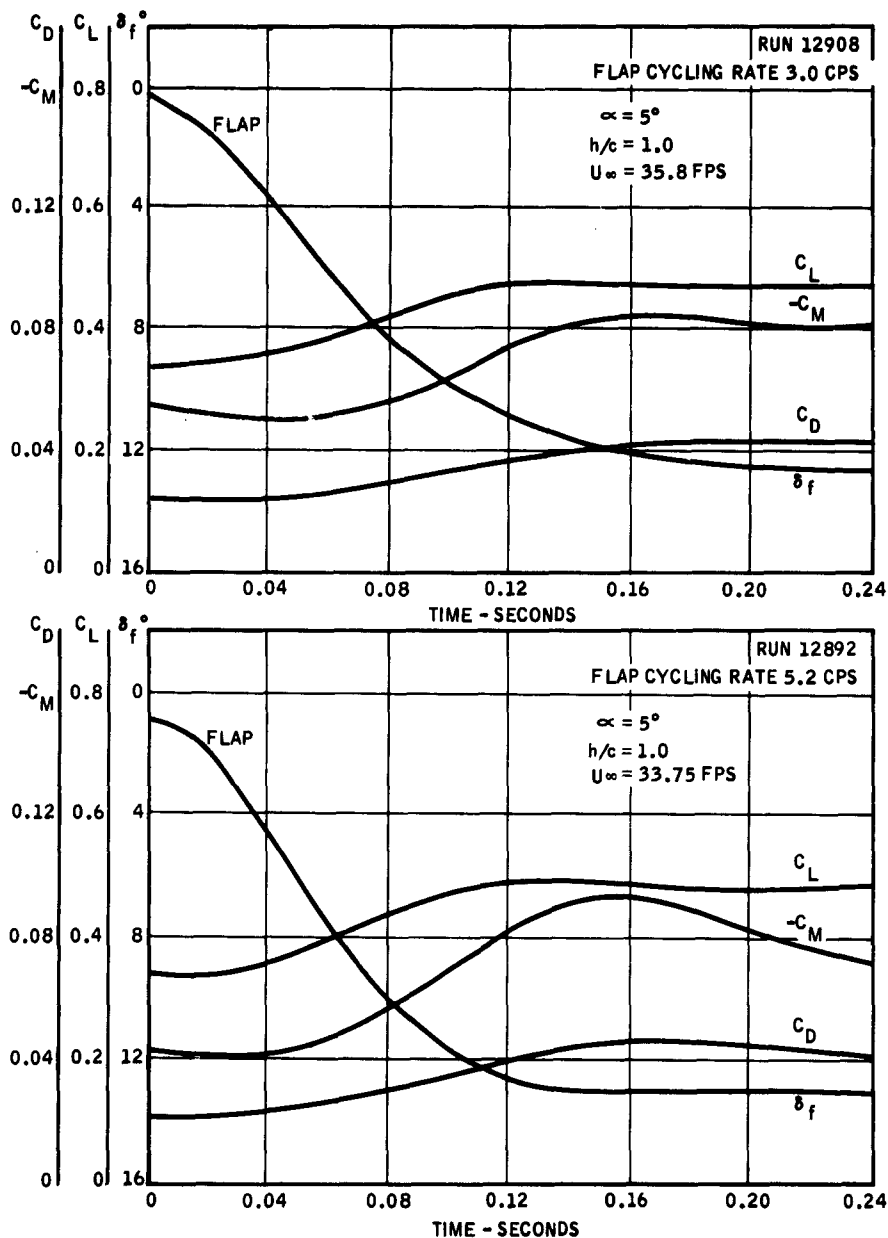
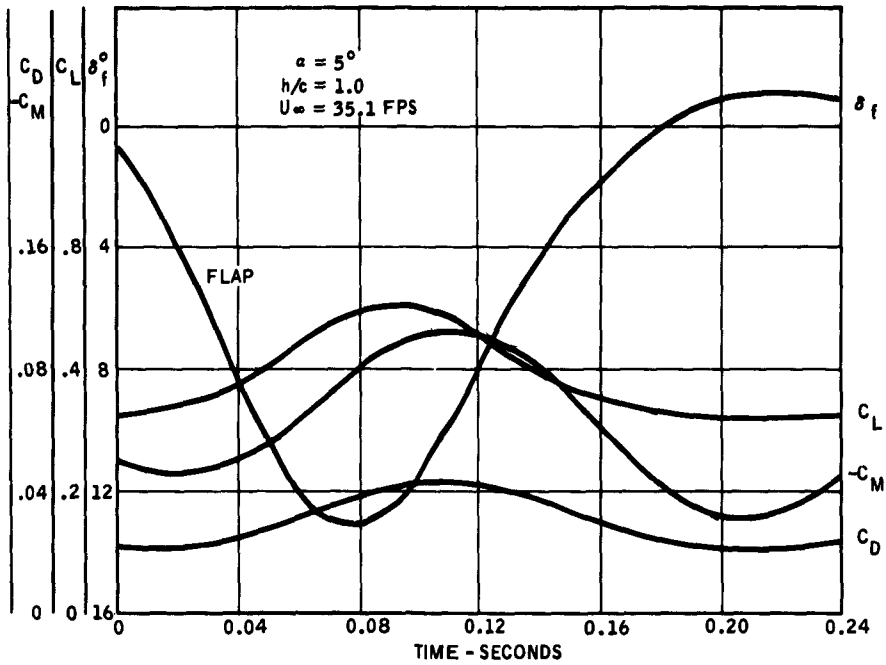


Figure 75. Sudden Flap Deflection, Time History of Force and Moment Build-up  
 — Flap Configuration 3, Run 12878, 6.3 CPS Flap Cycling Rate



**Figure 76. Sudden Flap Deflection, Time History of Force and Moment Build-up — Flap Configuration 4**



**Figure 77. Sudden Flap Deflection, Time History of Force and Moment Build-up — Flap Configuration 4, Run 12895, 6.3 CPS Flap Cycling Rate**

## DISTRIBUTION LIST

### Copies

3 Chief of Naval Research  
Department of the Navy  
Washington 25, D.C.  
Attn: Code 438  
1 Code 461

1 Commanding Officer  
Office of Naval Research  
Branch Office  
495 Summer Street  
Boston 10, Massachusetts

1 Commanding Officer  
Office of Naval Research  
Branch Office  
207 West 24th St.  
New York 11, New York

1 Commanding Officer  
Office of Naval Research  
Branch Office  
1030 East Green Street  
Pasadena, California

1 Commanding Officer  
Office of Naval Research  
Branch Office  
1000 Geary Street  
San Francisco 9, California

25 Commanding Officer  
Office of Naval Research  
Branch Office  
Box 39, Navy No. 100  
Fleet Post Office  
New York, New York

### Copies

6 Director  
Naval Research Laboratory  
Washington 25, D.C.  
Attn: Code 2027

Chief, Bureau of Naval Weapons  
Department of the Navy  
Washington 25, D.C.  
1 Attn: Code RUAW-4  
1 RRRE  
1 RAAD  
1 DIS-42

Chief, Bureau of Ships  
Department of the Navy  
Washington 25, D.C.  
1 Attn: Codes 106  
310  
1 312  
1 420  
1 421  
1 440  
1 442  
1 449

1 Chief, Bureau of Yards and Docks  
Department of the Navy  
Washington 25, D.C.  
Attn: Code D-400

1 Commanding Officer and Director  
David Taylor Model Basin  
Washington 7, D.C.  
1 Attn: Codes 142  
1 500

1 Commanding Officer and Director David Taylor Model Basin Washington 7, D.C.	1 Commander Planning Department San Francisco Naval Shipyard San Francisco 24, California
1 Attn: Codes 513	
1 520	
1 526A	1 Commander Planning Department Mare Island Naval Shipyard Vallejo, California
1 530	
1 533	
1 580	
1 585	
1 591	1 Commander Planning Department New York Naval Shipyard Brooklyn 1, New York
1 591A	
1 Commander U.S. Naval Ordnance Test Station Pasadena Annex 3202 E. Foothill Blvd Pasadena 8, California	1 Commander Planning Department Puget Sound Naval Shipyard Bremerton, Washington
1 Commander U.S. Naval Ordnance Test Station China Lake, California Attn: Code 753	1 Commander Planning Department Philadelphia Naval Shipyard U.S. Naval Base Philadelphia 12, Pennsylvania
1 Commander Planning Department Portsmouth Naval Shipyard Portsmouth, New Hampshire	1 Commander Planning Department Norfolk Naval Shipyard Portsmouth, Virginia
1 Commander Planning Department Boston Naval Shipyard Boston 29, Massachusetts	1 Commander Planning Department Charleston Naval Shipyard U.S. Naval Base Charleston, South Carolina
1 Commander Planning Department Pearl Harbor Naval Shipyard Navy 128, Fleet Post Office San Francisco, California	1 Commander Planning Department Long Beach Naval Shipyard Long Beach 2, California

- |  |  |
|--|--|
| <p>1 Commander<br/>Planning Department<br/>U.S. Naval Weapons Laboratory<br/>Dahlgren, Virginia</p>  | <p>1 Superintendent<br/>U.S. Merchant Marine Academy<br/>Kings Point, Long Island, New York<br/>Attn: Capt. L.S. McCready (Dept<br/>of Engineering)</p>      |
| <p>1 Dr. A. V. Hershey<br/>Computation &amp; Exterior Ballistics<br/>Laboratory<br/>U.S. Naval Weapons Laboratory<br/>Dahlgren, Virginia</p> | <p>2 U.S. Army Transportation Research<br/>&amp; Development Command<br/>Fort Eustis, Virginia<br/>Attn: Marine Transport Division</p>                       |
| <p>1 Superintendent<br/>U.S. Naval Academy<br/>Annapolis, Maryland<br/>Attn: Library</p>   | <p>1 Director of Research<br/>National Aeronautics and Space<br/>Administration<br/>1512 H Street, N.W.<br/>Washington 25, D.C.</p>                          |
| <p>1 Superintendent<br/>U.S. Naval Postgraduate School<br/>Monterey, California</p>  | <p>2 J. B. Parkinson<br/>National Aeronautics &amp; Space<br/>Administration<br/>Langley Aeronautical Laboratory<br/>Langley Field, Virginia</p>             |
| <p>1 Commandant<br/>U.S. Coast Guard<br/>1300 E Street, N.W.<br/>Washington, D.C.</p>  | <p>1 Director<br/>Engineering Sciences Division<br/>National Science Foundation<br/>1951 Constitution Avenue, N.W.<br/>Washington 25, D.C.</p>               |
| <p>1 Secretary Ship Structure Committee<br/>U.S. Coast Guard Headquarters<br/>1300 E Street, N.W.<br/>Washington, D.C.</p>                   | <p>Director<br/>National Bureau of Standards<br/>Washington 25, D.C.<br/>Attn: Fluid Mechanics Division<br/>(Dr. G. B. Schubauer)<br/>Dr. G. H. Keulegan</p> |
| <p>1 Commander<br/>Military Sea Transportation Service<br/>Department of the Navy<br/>Washington 25, D.C.</p>                                | <p>10 Armed Services Technical<br/>Information Agency<br/>Arlington Hall Station<br/>Arlington 12, Virginia</p>  |
| <p>U.S. Maritime Administration<br/>GAO Building<br/>441 G Street, N.W.<br/>Washington, D. C.</p>  |  |
| <p>1 Attn: Division of Ship Design</p>   |  |
| <p>1 Division of Research</p>  |  |

- |  |  |
|--|--|
| 1 Office of Technical Services<br>Department of Commerce<br>Washington 25, D.C.                                    | 3 State University of Iowa<br>Iowa Institute of Hydraulic Research<br>Iowa City, Iowa  |
| California Institute of Technology<br>Pasadena 4, California   | Harvard University<br>Cambridge 38, Massachusetts  |
| 1 Attn: Professor M. S. Plesset  | 1 Attn: Prof. G. Birkhoff (Dept of Mathematics)  |
| 1 Prof. T. Y. Wu   | 1 Prof. G. F. Carrier (Dept of Mathematics)  |
| 1 Prof. A. J. Acosta   |  |
| 3 University of California<br>Berkeley 4, California<br>Attn: Division of Engineering                              | Massachusetts Institute of Technology<br>Cambridge 39, Massachusetts   |
| 1 University of California<br>Department of Engineering<br>Los Angeles 24, California<br>Attn: Dr. A. Powell       | 1 Attn: Department of Naval Architecture and Marine Engineering  |
|  | 1 Prof. A. T. Ippen  |
| 1 Director<br>Scripps Institute of Oceanography<br>University of California<br>La Jolla, California                | University of Michigan<br>Ann Arbor, Michigan  |
| 1 Professor M. L. Albertson<br>Department of Civil Engineering<br>Colorado A&M College<br>Fort Collins, Colorado   | 2 Attn: Prof. R. B. Couch (Dept of Naval Architecture)   |
|  | 1 Prof. W. W. Willmarth (Aero Engr Department)   |
|  | 1 Prof. M. S. Uberoi (Aero Engr Department)  |
| 1 Professor J. E. Cermak<br>Department of Civil Engineering<br>Colorado State University<br>Fort Collins, Colorado | 1 Dr. L. G. Straub, Director<br>St. Anthony Falls Hydraulic Laboratory<br>University of Minnesota<br>Minneapolis 14, Minnesota |
| 1 Professor W. R. Sears<br>Graduate School of Aeronautical Engineering<br>Cornell University<br>Ithaca, New York   | 1 Professor J. J. Foody<br>Engineering Department<br>New York State University<br>Maritime College<br>Fort Schuyler, New York  |

- New York University  
Institute of Mathematical Sciences  
25 Waverly Place  
New York 3, New York
- 1 Attn: Prof. J. Keller  
1 Prof. J. J. Stoker  
1 Prof. R. Kraichnan
- The Johns Hopkins University  
Department of Mechanical  
Engineering  
Baltimore 18, Maryland
- 1 Attn: Prof. S. Corrsin  
2 Prof. O. M. Phillips
- 1 Massachusetts Institute of  
Technology  
Department of Naval Architecture  
and Marine Engineering  
Cambridge 39, Massachusetts  
Attn: Prof. M. A. Abkowitz, Head
- 1 Dr. G. F. Wislicenus  
Ordnance Research Laboratory  
Pennsylvania State University  
University Park, Pennsylvania
- 1 Professor R. C. DiPrima  
Department of Mathematics  
Rensselaer Polytechnic Institute  
Troy, New York
- Stevens Institute of Technology  
Davidson Laboratory  
Castle Point Station  
Hoboken, New Jersey
- 1 Attn: Mr. J. P. Breslin  
1 Mr. D. Savitsky
- 1 Webb Institute of Naval  
Architecture  
Crescent Beach Road  
Glen Cove, New York  
Attn: Technical Library
- 1 Director  
Woods Hole Oceanographic Institute  
Woods Hole, Massachusetts
- Hamburgische Schiffbau-  
Versuchsanstalt  
Bramfelder Strasse 164  
Hamburg 33, Germany
- 1 Attn: Dr. O. Grim  
1 Dr. H. W. Lerbs
- 1 Institut für Schiffbau der  
Universität Hamburg  
Berliner Tor 21  
Hamburg 1, Germany  
Attn: Prof. G. P. Weinblum,  
Director
- 1 Max-Planck Institut für  
Strömungsforschung  
Bottingerstrasse 6/8  
Göttingen, Germany
- 1 Hydro-og Aerodynamisk  
Laboratorium  
Lyngby, Denmark  
Attn: Prof. Carl Prohaska
- 1 Skipsmodelltanken  
Trondheim, Norway  
Attn: Prof. J. K. Lunde
- 1 Versuchsanstalt für Wasserbau  
and Schiffbau  
Schleuseninsel im Tiergarten  
Berlin, Germany

- 1 Technische Hogeschool  
Institut voor Toegepaste Wiskunde  
Julianalaan 132  
Delft, Netherlands  
Attn: Prof. R. Timman
- 1 Bureau D'Analyse et de Recherche  
Appliquees  
2 Rue Joseph Sansboeuf  
Paris 8, France  
Attn: Prof. L. Malavard
- 1 Netherlands Ship Model Basin  
Wageningen, Netherlands  
Attn: Dr. Ir. J. D. van Manen
- 1 Allied Research Associates, Inc.  
43 Leon Street  
Boston 15, Massachusetts  
Attn: Dr. T. R. Goodman
- 1 General Dynamics/Convair  
San Diego 12, California  
Attn: R. H. Oversmith
- 1 Dynamic Developments Inc.  
Midway Avenue  
Babylon, New York  
Attn: W. P. Carl
- 1 Dr. S. F. Hoerner  
148 Busted Drive  
Midland Park, New Jersey
- 1 Hydronautics, Incorporated  
200 Monroe Street  
Rockville, Maryland  
Attn: Phillip Eisenberg
- 1 Rand Development Corporation  
13600 Deise Avenue  
Cleveland 10, Ohio  
Attn: Dr. A. S. Iberall
- 1 U.S. Rubber Company  
Research and Development  
Department  
Wayne, New Jersey  
Attn: L. M. White  
  
Technical Research Group, Inc.  
2 Aerial Way  
Syosset, Long Island, New York  
1 Attn: Jack Kotik  
Dr. Paul Kaplan
- 1 C. Wigley  
Flat 102  
6-9 Charterhouse Square  
London, E.C.1, England
- 1 AVCO Corporation  
Lycoming Division  
1701 K Street, N.W.  
Apt. 904  
Washington, D. C.  
Attn: T. A. Duncan
- 1 Mr. J. G. Baker  
Baker Manufacturing Company  
Evansville, Wisconsin
- 1 Curtiss-Wright Corporation  
Research Division  
Turbomachinery Division  
Quehanna, Pennsylvania  
Attn: George H. Pedersen

- 1 Hughes Tool Company  
Aircraft Division  
Culver City, California  
Attn: M. S. Harned
- 2 National Research Council  
Montreal Road  
Ottawa 2, Canada  
Attn: E. S. Turner
- 1 The RAND Corporation  
1700 Main Street  
Santa Monica, California  
Attn: Blaine Parkin
- 1 Stanford University  
Department of Civil Engineering  
Stanford, California  
Attn: Dr. Byrne Perry
- 1 Waste King Corporation  
5550 Harbor Street  
Los Angeles 22, California  
Attn: Dr. A. Schneider
- 1 Lockheed Aircraft Corporation  
California Division  
Hydrodynamics Research  
Burbank, California  
Attn: Mr. Bill East